National and Kapodistrian
UNIVERSITY OF ATHENS

School of Health Sciences, Department of Medicine, Laboratory of Anatomy

2020

Dissertation for Doctor of Philosophy (PhD)

« Examination of the death promoting effects of Natural extracted compounds against cancer: Pathway and morphological changes Identification in respect to cellular stress »

PhD candidate: Andreas Yiallouris

Three Member committee

Johnson E. (Professor -Supervisor)

Patrikios I. (Professor, European University Cyprus)

Stephanou A. (Professor, European University Cyprus)

Εθνικό και Καποδιστριακό Πανεπιστήμιο
Ιατρική Σχολή Αθηνών
Εργαστήριο Ανατομίας και Χειρουργικής Ανατομίας - «Ανατομείο»

2020

Dissertation for Doctor of Philosophy (PhD)

Ημερομηνία	Τύπος Αρχείου	Αριθμός Πρωτοκόλλου
22/02/17	Πρόταση	1617018856
28/04/17	Ορισμός Τριμελούς Επιτροπής	1617025257
26/07/17	Ετήσια Πρόοδος Ι	1617035085
27/06/18	Ετήσια Πρόοδος ΙΙ	1718033228
22/02/19	Ετήσια Πρόοδος ΙΙΙ	1819023158
29/04/20	Σύσταση Επταμελής Επιτροπής	1920026184/29-04-2020.

Μέλη Εξεταστικής Επταμελής Επιτροπής

1. Θ. Τρουπής Αναπληρωτής Καθηγητής Ανατομίας
2. Β. Πρωτογέρου Αναπληρωτής Καθηγητής Ανατομίας
3. Α. Μαζαρακης Αναπληρωτής Καθηγητής Ανατομίας
4. Μ. Πιαγκου. Επίκουρη Καθηγήτρια Ανατομίας

1

ΙΠΠΟΚΡΑΤΟΥΣ ΟΡΚΟΣ

HIPPOCRATIS IVSIVRANDVM

04/16 –to date	• National and Kapodestrian University Athens, School of Medicine Phd Candidate.
22nd -25th June 2015	• Operators Training Course for Thermo Scientific Dionex ULTIMATE 3000 HPLC system and Chromeleon software.
22nd April	• Gaumard Simulators for Health Care Education training on 22nd April 2015 at Scientronics.
2011-2012	• University of Essex, Colchester, United Kingdom, MSc Molecular Medicine, Department of Biological Sciences.
2006-2011	• University of Cyprus, Nicosia, Cyprus, Bachelor of Science, Department of Chemistry.
2001-2004	• Pancyprian High School, Nicosia, Cyprus

24/09/2018 -To Date	Teaching Medical Biochemistry and Human Metabolism (DEN120, DEN155) to Dentistry Students Business European University Cyprus
01/05/2014 -To date	Equipment Specialist. I am responsible for technology, all dry and wed labs at the Medical School. Business European University Cyprus
02/10/2013 - 02-04/2014	Chemist at the chemical laboratory of the Geological Survey Department (ISO 17025) Sector Geological Survey Department

PERSONAL SKILLS	
MOTHER TONGUE(S)	Greek
OTHER LANGUAGE(S)	English (IELTS 7.0), ESOL international Level-2 Anglia Proficiency (C1)

PROJECTS 2014-UNTIL NOW SELECTED PUPLICATIONS	Research in Cancer treatment using natural extracts. https://www.researchgate.net/profile/Andreas_Yiallouris 1. Ioannis, Patrikios, Stephanou Anastasis, and Yiallouris Andreas. ANTICANCER PROPERTIES OF Na+/K+-ATPase: A MINI REVIEW. *Asian Journal of Science and Technology Vol.07, Issue, 05, 2016 pp.2864-2868.* 2. Patrikios Ioannis, Stephanou Anastasis, Yiallouris Andreas. Graviola: A Systematic Review on Its Anticancer Properties. American Journal of Cancer Prevention. Vol. 3, No. 6, 128-131, 2015. 3. Patrikios Ioannis[1], Stephanou Anastasis[1], and Yiallouris Andreas[1]: "Tripterygium wilfordii and Amydalin Promotes cell death in Cancer Cells: True or a Myth". *American Journal of Educational Research* Vol. 3, No. 4, 2015. 4. Adrenal Aging and Its Implications on Stress Responsiveness in Humans. Andreas Yiallouris, Constantinos Tsioutis,Eirini Agapidaki, Maria Zafeiri, Aris P. Agouridis,Dimitrios Ntourakis,and Elizabeth O. Johnson. Front. Endocrinol., 07 February 2019 https://doi.org/10.3389/fendo.2019.00054

No one who archives success does so without acknowledging the help of others.

Acknowledgements

I would like to thank the department of anatomy and the National

…….

Table of Contents

Περίληψη

Ο καρκίνος συγκαταλέγεται στις σημαντικότερες αιτίες θανάτου παγκοσμίως. Υπολογίζεται ότι μέχρι το 2030 ο αριθμός των νέων περιστατικών θα ανέλθει στα 23.6 εκατομμύρια παγκοσμίως. Μέχρι σήμερα οι τρόποι αντιμετώπισής περιλαμβάνουν τη χορήγηση χημειοθεραπείας, μεταξύ άλλων. Οι ασθενείς μετά τη χορήγηση της χημειοθεραπείας εμφανίζουν διαφόρων ειδών παρενέργειες. Η παρούσα διδακτορική διατριβή διερευνά την αντιμετώπιση της νόσου με τη χρήση φυσικών/φυτικών ενώσεων που απαντώνται στο φυτό Γκραβιόλα. Ένα από τα πολλά μόρια που απαντώνται στο φυτό αυτό, είναι η ανονακίνη. Το συγκεκριμένο αυτό μόριο φαίνεται να έχει περιορισμένη τοξικότητα σε φυσιολογικές κυτταρικές σειρές ενώ οδηγεί το καρκινικό κύτταρο σε απόπτωση, μέσω αναστολής των αντλιών νατρίου/καλίου και ασβεστίου. Χρησιμοποιήθηκε προσέγγιση *in silico* για την αναγνώριση του κυτταρικού και του μοριακού στόχου της ανονακίνης. Αυτή η μελέτη αποκάλυψε ότι η ανονακίνη φαίνεται να στοχεύει στην οικογένεια του τύπου P της αντλίας της ATPάσης, η οποία περιλαμβάνει την Νάτριο/Κάλιο ATPάση (NKA) και την σαρκοπλασματική/δικτυοενδοθηλιακή ATPάση (SERCA). Επιπρόσθετα τα δεδομένα της *in silico* μελέτης έδειξαν ότι η ανονακίνη είναι όντως ένας ισχυρός αναστολέας των αντλιών NKA και SERCA. Επιπλέον, η ανονακίνη μείωσε το μέγεθος του όγκου σε ζωικό μοντέλο καρκίνου. Τέλος η βιοπληροφορική ανάλυση έδειξε ισχυρή συσχέτιση μεταξύ της έκφρασης NKA ή SERCA στην επιβίωση ασθενών με καρκίνο. Ως συμπέρασμα, η μελέτη αποδεικνύει ότι η ανονακίνη στοχεύει και τις δύο αντλίες (NKA και SERCA) και αναδεικνύει νέα θεραπευτικά μονοπάτια για τη θεραπεία του καρκίνου.

Abstract

Cancer is a leading cause of death and mortality in the world and by 2030 the numbers of new cancer cases is expected to rise 23.6 million. Although conventional chemotherapy is still the first choice of treatment, such procedures is associated with major cytotoxic side effects. In the present study it was shown that the phyto-compound *annonacin* (found in the fruit Graviola / *Annona muricata*) promotes anti-cancer activity in cancer cell lines. In contrast, *annoancin* showed limited toxicity in normal and non-transformed cells. In order to identify the cellular and molecular target of *annonacin an in silico* approach was undertaken. Such study revealed that *annonacin*, seem to target P-type ATPase pump family, that include the sodium potassium ATPase (NKA) and Sarco/endoplasmic reticulum calcium ATPase (SERCA) family members. Furthermore, the *in silico* data was validated by showing that *annonacin* is indeed a potent inhibitor of NKA and SERCA pumps. Moreover, *annonacin* also reduced tumor growth in a xenograft cancer model. Finally, bioinformatics analysis showed strong correlation between NKA or SERCA expressions in cancer patient's survival. Overall, this study strongly suggests that *annonacin* targets both the NKA and SERCA pumps as novel pathways for cancer treatment

Abbreviations

AMOG	Adhesion Molecule on Glia
AMPK	AMPK AMP-activated Protein Kinase
ATP	Adenosine Triphosphate
Bcl-2	B-cell lymphoma 2
CaMKKβ	Ca2+/calmodulin-dependent Kinase Kinase-β
CG	Cardiac Glycosides
ERK	Extracellular Signal-Regulated Kinases
HKA	Hydrogen Potassium ATPase
IL-8	Interleukin 8
JNK	c-Jun N-terminal kinases
MAPK	Mitogen-Activated Protein Kinase
mTOR	Mammalian Target of Rapamycin
NF- κB	Nuclear Factor Kappa-light-chain-Enhancer of Activated B cells
NKA	Sodium Potassium ATPase
OCCC	Ovarian Clear Cell Carcinoma
PPI	Proton Pump Inhıbıtor
TAB	Trametenolıc Acıd B
TNF	Tumor necrosis factor
ROS	Reactive Oxygen Species
EGFR	Epidermal growth factor receptor
BC	Breast Cancer
PIK3	Phosphoinositide 3-kinase
PARP	Poly (ADP-ribose) polymerase
ER	Endoplasmic reticulum
WHO	World health organization
RA	Rheumatoid arthritis
CASP	Caspase
PBMC	Peripheral blood mononuclear cells

NKA	Sodium/potassium ATPase
SERCA	Sarco/endoplasmic reticulum calcium ATPase
HKA	Hydrogen ATPase
GC	Gas Chromatography
HPLC	High performance liquid chromatography
TLC	Thin layer chromatography
CS	Cardiac Glycosides

Background Information

Cancer was described by ancient Greeks centuries ago with reports of tumors and fruitless efforts to treat them. As early as 460 BC, Hippocrates described cancer as *carcinos* (Greek *meaning crab or crayfish*). The name is related to the shape (cut surface) of solid tumors, which were described as similar to crab's feet. The translation into the Latin name *cancer* introduced by Celsus 25 BC – 50 AD were Galen, 2nd century AD, referred *oncos* to the initial tumor formation and later added the suffix *-oma*, Greek for swelling, giving the full name *carcinoma*[1].

According to National Cancer Institute (NCI) cancer is described as abnormal and un-controlled cell growth which can invade nearby tissues[2]. There are several main types of cancer, such as Carcinoma, which begins in the skin or in tissues that line or cover internal organs[2]. Sarcoma is a cancer that begins in bone, cartilage, fat, muscle, blood vessels, or other connective or supportive tissue. Leukemia is a cancer that starts in blood-forming tissue, such as the bone marrow, and causes large numbers of abnormal blood cells to be produced and enter the . Lymphoma and multiple myeloma are cancers that begin in the cells of the immune system. Central nervous system cancers are cancers that begin in the tissues of the brain and spinal cord. Also called malignancy[3].

There are different grades and stages of tumors, based on the cancer cells abnormality (size, shape location etc.), as well as according to the visible characteristics observed under microscope. Grading system is numerical and vary according to the specific type of cancer.

Generally, tumors are graded as 1, 2, 3, and 4 were severance, invasion and abnormality increases with increase grade number[4].

1.1 Cancer Metrics

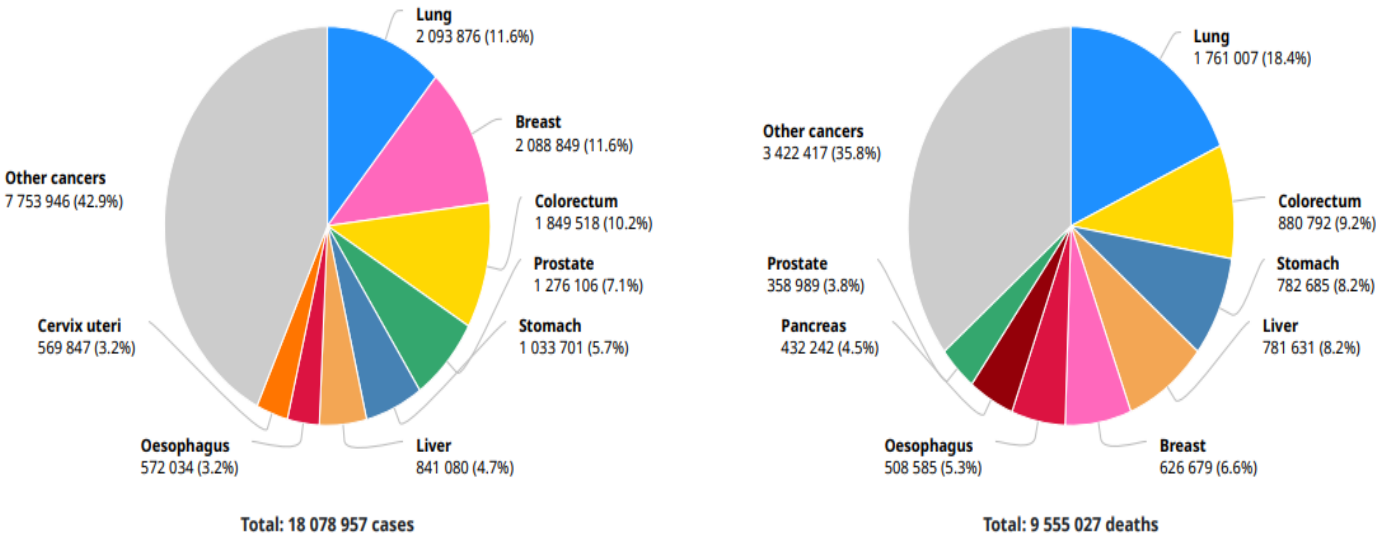

	Both sexes		Males		Females		Both sexes		Males		Females	
	New cases	Cum. risk 0-74 (%)	New cases	Cum. risk 0-74 (%)	New cases	Cum. risk 0-74 (%)	Deaths	Cum. risk 0-74 (%)	Deaths	Cum. risk 0-74 (%)	Deaths	Cum. risk 0-74 (%)
Eastern Africa	332 177	13.47	129 476	11.56	202 701	15.20	230 968	10.21	94 731	8.89	136 237	11.40
Middle Africa	95 735	10.86	41 407	10.62	54 328	11.23	68 763	8.30	30 852	8.01	37 911	8.66
Northern Africa	283 219	14.27	134 627	14.69	148 592	13.94	178 754	9.39	96 874	10.64	81 880	8.22
Southern Africa	114 582	19.93	50 814	22.35	63 768	18.54	61 670	11.33	30 106	13.54	31 564	9.84
Western Africa	229 459	11.42	90 232	10.10	139 227	12.72	153 332	8.26	63 968	7.36	89 364	9.14
Caribbean	111 933	20.23	57 728	22.41	54 205	18.28	63 075	10.42	34 354	11.69	28 721	9.29
Central America	256 782	14.70	115 751	14.53	141 031	14.90	119 168	6.86	57 609	6.83	61 559	6.89
South America	1 044 017	20.56	509 014	22.40	535 003	19.12	490 515	9.51	253 762	10.79	236 753	8.43
North America	2 378 785	33.13	1 274 306	36.25	1 104 479	30.31	698 266	9.64	367 738	10.82	330 528	8.58
Eastern Asia	5 622 367	21.54	3 108 655	24.23	2 513 712	18.91	3 456 734	12.88	2 136 217	16.36	1 320 517	9.35
South-Eastern Asia	989 191	15.29	478 093	16.33	511 098	14.52	631 190	10.14	345 482	11.95	285 708	8.57
South-Central Asia	1 739 497	10.26	859 799	10.57	879 698	10.02	1 167 183	7.22	619 488	7.84	547 695	6.62
Western Asia	399 877	17.51	210 004	19.94	189 873	15.55	221 957	10.17	130 276	12.75	91 681	7.81
Central and Eastern Europe	1 240 057	24.95	612 026	29.43	628 031	21.98	699 446	13.84	385 301	18.83	314 145	10.16
Western Europe	1 370 332	31.24	752 802	34.94	617 530	27.73	548 355	10.99	307 423	13.28	240 932	8.82
Southern Europe	933 181	27.55	516 339	31.78	416 842	23.72	422 054	10.60	246 579	13.53	175 475	7.91
Northern Europe	686 092	30.44	366 351	33.07	319 741	28.01	273 623	10.32	146 289	11.58	127 334	9.14
Australia and New Zealand	233 773	41.53	140 821	49.06	92 952	33.28	59 247	9.39	33 374	10.75	25 873	8.07
Melanesia	15 379	20.05	6 840	20.76	8 539	19.78	9 257	13.07	4 375	13.94	4 882	12.48
Polynesia	1 539	23.68	805	26.56	734	21.05	838	13.08	472	15.52	366	10.77
Micronesia	983	18.93	528	21.29	455	16.48	632	11.99	370	14.56	262	9.44
Low HDI	672 218	11.79	270 241	10.52	401 977	13.02	464 569	8.80	196 682	7.92	267 887	9.66
Medium HDI	2 828 475	11.94	1 364 853	12.30	1 463 622	11.67	1 861 723	8.21	984 221	9.08	877 502	7.42
High HDI	6 515 063	19.97	3 476 436	22.24	3 038 627	17.88	4 020 422	12.36	2 425 680	15.46	1 594 742	9.34
Very high HDI	8 054 578	29.05	4 340 394	32.72	3 714 184	25.88	3 204 212	10.52	1 776 814	12.81	1 427 398	8.47
World	18 078 957	20.20	9 456 418	22.41	8 622 539	18.25	9 555 027	10.63	5 385 640	12.71	4 169 387	8.70

Figure 1. Cancer metrics, Adopted from WHO (NCI) website last update May, 2019.

The cancer significance and its affliction can easily be projected by the statistics published from National Cancer Institute. The number of new cancer cases per year expected to rise to 23.6 million by 2030 [5].

The data from NCI shows that this multifactorial disease is expanding rapidly, which strongly indicate the need to discover new or alternative methods of treatment. Among the possible options for treatment are the repurposing drugs as well as natural extracts as single agents or in combination with known anticancer drugs.

1.2 Repurposing Drugs

Given the high attrition rates, substantial costs and slow pace of new drug discovery and development, repurposing of 'old' drugs to treat both common and rare diseases is increasingly becoming attractive, this is because it involves the use of de-risked compounds, with potentially lower overall development costs and shorter development timelines [6]. Various data-driven and experimental approaches have been suggested for the identification of repurposable drug candidates; however, there are also major technological and regulatory challenges that still need to be addressed [6,7].

Drug repurposing (also called drug repositioning, reprofiling or re-tasking) is a strategy for identifying new uses for approved or investigational drugs that are outside the scope of the original medical indication. This strategy offers various advantages over developing an entirely new drug for a given indication [8]. First, and perhaps most importantly, the risk of failure is lower; because the repurposed drug has already been found to be

sufficiently safe in preclinical models and humans, if early-stage trials have been completed and it is less likely to fail, at least from a safety point of view, in subsequent efficacy trials. Second, the time frame for drug development can be reduced, because most of the preclinical testing, safety assessment and, in some cases, formulation development will already have been completed [9]. Third, less investment is needed, although this will vary greatly depending on the stage and process of development of the repurposing candidate [10]. The regulatory and Phase III costs may remain more or less the same for a repurposed drug as for a new drug in the same indication, but there could still be substantial savings in preclinical and Phase I and II costs [10]. Together, these advantages have the potential to result in a less risky and more rapid return on investment in the development of repurposed drugs, with lower average associated costs once failures have been accounted for, (The costs, of bringing a repurposed drug to market have been estimated to be US$300 million on average, compared with an estimated $2–3 billion for a new chemical entity). Finally, repurposed drugs may reveal new targets and pathways that can be further exploited [11,12].

1.3 Natural extracts

Natural extracts from various sources, such as plants, marine and animals have been used for centuries in traditional medicine. Their involvement in the treatment of a number of diseases is, without doubt, invaluable. It is estimated that over 60% of the approved drugs and new drug developments for cancer and infectious diseases are from natural origin [13].

New techniques, as well as analytical advances have paved the way for the characterization and synthesis of millions of new drug candidates. The use of computational

libraries and *in silico* approaches were designed according to molecular scaffold or leads allow the new drug development for a number of diseases including cancer. In addition, the shift from "monotherapy" "one drug-one target", also paved the way for new strategical thinking. Today, although synergy and combinational treatment is challenging and difficult, the needs for multitargeting are more than the traditional treatments, as well as more effective.

Natural compounds are following an evolutions for years, they have been selected as complex sources of medicinal agents. This is the basis of xenohormesis hypothesis [14,15]. They present very diverse chemical structures, from the simplest phenolic acids in plants to the most complex marine compounds [16–18]. Glycosylation, methylation and other esterifications and the presence of other moieties, increase the number and diversity of natural compounds. This constituting a countless and invaluable source of new drugs. From a biomedical point of view, hormesis is an adaptive response, in which the exposure to a low dose of an environmental factor or chemical compound, that is harmful at high concentrations, has a beneficial and/or adaptive effect on a cell or organism. Sometimes this response is mediated by some compounds that, when incorporated in the heterotroph diet, induce biological responses leading to pharmacological effects[19]. This final effect is called xenohormesis, as the final benefit is obtained by the heterotroph organism, not for the plant that originally adapted to the stressful condition[14]. Xenohormesis is a way of cross-species interaction and communication.

Although hormesis is an essential concept in evolution, xenohormesis has also allowed the expansion and fixation of evolutionary advances in non-autotroph organisms. Today, xenohormesis gives us a chance to obtain benefits from natural compounds and obtain new drugs selected by nature through the normal evolutional process. These compounds can be

used directly for anticancer drug discovery, and also as new leads in novel developments, using the classical structurally guided or *in silico* approaches [20,21]. This is one of the main advantages of natural extracts and their compounds. They can be used as any other drugs, but with the benefit of being selected by natural evolution.

Natural plant extracts have been used for centuries by many cultures and civilizations as a basis for treating various diseases. More than 80% of the global population now depends on natural plant extracts through traditional therapies [20]. Recent investigators have focused on the progression, treatment and prevention of cancer with such compounds, but room for improvement still remains [23].

To date, the use of conventional synthetic chemotherapeutic drugs lack the properties to be considered as effective therapeutic agents, with most of those associated with severe side effects and toxicity of the normal host cells. Whereas an alternative therapeutic approach that uses natural plant extracts is advantageous vs conventional therapy with limited side effects.

One of the first systematic approaches was carried out in 1950 with the vinca alkaloids (vinblastin and vincristine) discovery, isolated from the *Catharanthus roseus* G. Don. (Apocynaceae), followed by a number of effective extracts, such as Triptolide (Tripterigium wilfordii), Amygdalin (B12), *Achyranthes aspera* Linn and Annonacin from Graviola.

The plants selected to be examined is Gaviola

1.4 Graviola/Annonacin

Graviola belongs to *Annonaceae* family, *Annona* genus and *muricata* species[24,25]. Graviola is a fruit tree with many uses in traditional and alternative medicine. Graviola, soursop, guanábana, guanábano, guanavana, guanaba, corossol épineux, huanaba, toge-banreisi, durian benggala, nangka blanda, cachiman épineux are altering names for this evergreen plant that is mostly distributed in tropical and subtropical regions of the world [26]. Graviola is a heart shaped edible fruit and together with its leaves, root and seeds is known to have beneficial properties in alternative medicine [23,27]. The fruits of Graviola are extensively used to make candies, syrups, ice creams, shakes and beverages. A wide range of ethno-medicinal activities in Africa and South America extensively use this plant in their conventional medicine.[28] A number of laboratories have reported Graviola for its benifical actions against anticonvulsant, antiparasitic, anti-arthritic, antimalarial, antidiabetic hepatoprotective and anti-cancer activities [23,27]. Biological and chemical characterization studies indicate that annonaceous acetogenins are the main ingredients of Graviola [29].

Nowadays more than 100 annonaceous acetogenins that are generally characterized as a family of natural products with antitumor activities, from roots, leaves, barks, fruits and seeds of Graviola have been widely used in alternative medicine for many purposes [24,28]. In the Peruvian Andes for example, the Graviola leaves are used to combat parasites and treat diabetes. In the Brazilian Amazon the leaves were used to treat liver problems and the leave –oil is believed to help with rheumatism, neuralgia and arthritis. In the Eastern Andes and Jamaica, Haiti the juice of Graviola was used to stop diarrhea, used as muscle relaxant and lower the intestinal acidity[30,31].

Other reports have demonstrated that Graviola has a number of biological activities, such as antifungal, anti-bacterial, anti-malarial and antioxidant [32–34]. Furthermore, it has been shown to have anti-cancer properties on multi-drug resistant cancer cell lines. The ability of Graviola to have selective growth inhibition against a variety of cancer cells, including lung carcinoma cell lines, breast solid tumor lines, prostate adenocarcinoma, pancreatic carcinoma cell lines, colon adenocarcinoma cell lines, liver cancer cell lines, human lymphoma cell lines, and multi-drug resistant human breast adenocarcinoma [35–37].

Graviola's fruit flesh consists of 80% water, 1% protein, 18% carbohydrates and small amount of vitamins B, B2, C, potassium and dietary fiber [38]. The main group, annonaceous acetogenin, is a unique set of derivatives of C35 or C37 long chain fatty acids derived from the polyketide pathway (Figure 2)[39]. The annonaceous acetogenins found in Graviola include Annocatalin, annohexocin, annomonicin, annomontacin, annomuricatin A and B, annomuricin A through E, annomutacin, annonacin, annonacinone, annopentocin A thru C, cis-annonacin, cis-corossolone,cohibin A through D, corepoxylone, coronin, corossolin, corossolone, donhexocin, epomuricenin A and B,gigantetrocin, gigantetrocin A and B, gigantetrocinone, gigantetronenin, goniothalamicin, iso-annonacin, javoricin, montanacin, montecristin, muracin A through G, muricapentocin, muricatalicin, muricatalin, muri-catenol, uricatetrocin A and B muricatin D, muricatocin A through C muricin H, muricin I, muricoreacin, murihexocin 3, murihexocin A thru C, murihexol, murisolin, robustocin, rolliniastatin 1 and 2, saba-delin, solamin, uvariamicin I & IV, xylomaticin isolated from the leaves, root and stem barks of Graviola [40].

The essential oil of the fresh fruit pulp contains 2-hexenoic acid methyl ester (23.9%), 2-hexenoic acid ethyl ester (8.6%), 2-octenoic acid methyl ester (5.4%), 2-butenoic acid methyl ester (2.4%), β-caryophyllene (12.7%), 1,8- cineole (9.9%), linalool (7.8%), α-terpineol (2.8%), lialyl propionate (2.2%) and calarence (2.2%) [28,38].

Limited number of published data are found in literature for the anti-carcinogenic potential of Graviola natural extracts. Recent studies have suggested that Graviola also expresses analgestic and anti-inflammatory effects, promotes apoptosis (programmed cell death) and cytotoxicity on cancer cells that may result from the presence of alkaloids, essential oils and acetogenins [28,29,31,41]. These acetogenins demonstrated to be selective and toxic against various types of cancer cells without harming normal and healthy host cells [42–44].

It has been previously reported that the Graviola extracts have significant anti-cancer effects in a number of cancer cell lines both *in vitro* and *in vivo* [26]. Studies revealed the Graviola extracts as having selective inhibition of breast cancer cells via epidermal growth factor receptor (EGFR) downregulation. The EGFR is an oncogene frequently overexpressed in breast cancer (BC), and its overexpression has been associated with poor prognosis and drug resistance [25]. EGFR is therefore a rational target for BC therapy development. In addition, experiments showed that Graviola fruit extract (GFE) inhibit the growth of BC cells using xenografts mouse model studies [35]. Moreover, GFE selectively inhibited the growth of EGFR-overexpressing human BC (MDA-MB-468) cells but not in non-tumorigenic human breast epithelial cells (MCF-10A). These studies strengthen the evidence that Graviola has selective anti-growth effects between cancer and non-cancer cells.

Another study on breast cancer cells supported that Graviola promotes apoptosis in ER-related pathways. Moreover, Graviola decreased MCF-7 tumor growth while inhibiting ER-cyclin D1 and Bcl-2 protein expressions in nude mice [45]. In colon cancer cells, Graviola leaves also has significant effects on cell survival potential via mitochondrial-mediated apoptosis associated with the G1 cell cycle arrest. Graviola induces apoptosis by generating reactive oxygen species ROS and down-regulating the anti-apoptotic Bcl-2 protein, while up-regulating pro-apoptotic Bax protein. These processes subsequently lead to attenuation of mitochondrial membrane potential (MMP) and cytochrome c release. Release of cytochrome c activates apotosome and the intrinsic caspase cascade that triggers execution of apoptosis through DNA fragmentation [40,46]. Graviola has also been reported to have anti-proliferative effects of HL-60 cells via loss of cell viability, loss of MMP, G0/G1 phase cell arrest and morphological apoptotic changes. These results substantiate and confirm that Graviola does indeed have anti-proliferative and cytostatic activity in HL-60 cells [46].

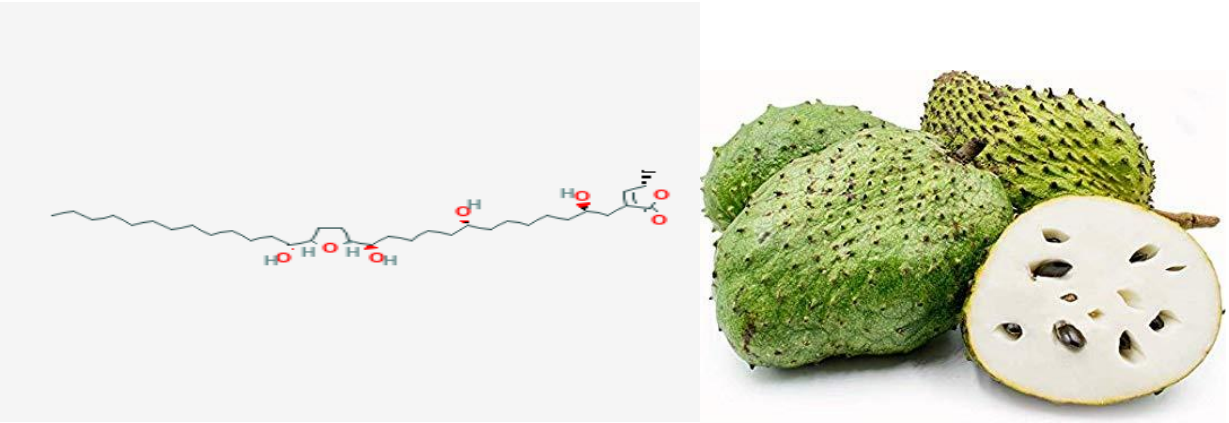

Figure 2. Chemical structure of *annonacin* and photo of graviola plant

1.5 Cell Death

As Noted above, natural extracted phytocompounds have the ability to lead the cell to death/survival pathways[47]. Cell death and cell division are the most crucial pathways found in all living organisms [48]. These two pathways have to be in a perfect balance in order to generate the proper numbers and types of cells for the needs of the organism. The view that some cells die as a normal part of both development and homeostasis was established fifty years ago we re the exact function of regulation and mechanism is still a subject of many researchers [49].

Cell death can be classified according to immunological, morphological, enzymatic and functional criteria [50]. The most common cell death types (Figure 3) are apoptosis, necrosis, autophagy and necroptosis. However over the course of the decade new atypical cell death pathways are descripted such as, pyroptosis, feroptosis and the breakthrough discovery of "Anastasis", which is the return from a death pathway [51].

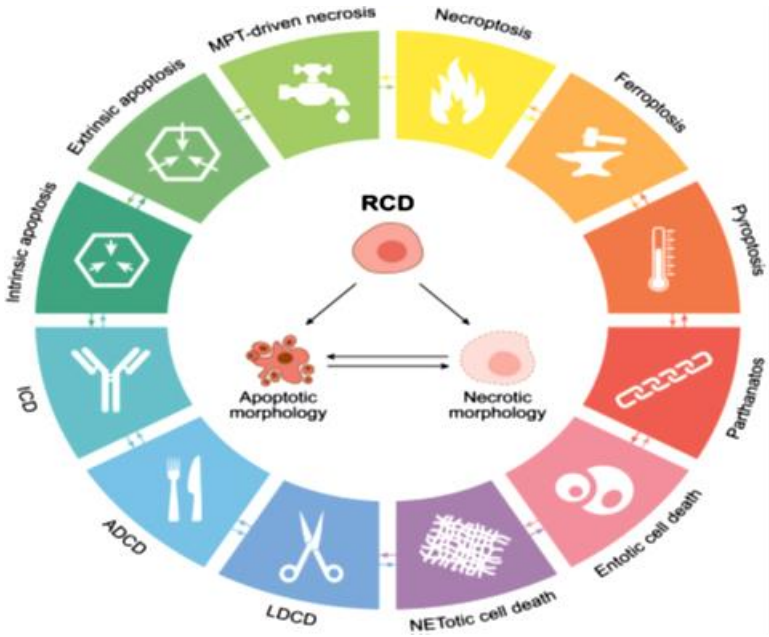

Figure 3. Schematic illustration of Cell Death types

1.5.1 Apoptosis

Apoptosis as the oldest cell death pathway, descripted in 1842, is characterized by cellular volume reduction (pyknosis), cell round-up conformation, retraction of pseudopodes, chromatin condensation, nuclear fragmentation (karyorrhexis) and plasma membrane bleeding [52,53]. The cells commits suicide by activating an intracellular death program via regulators called caspases. Belonging to the cysteine proteases family, caspases are key regulators of apoptosis and subdivided into initiator and effector caspases. caspases-2, -8, -9, -10, -11, and -12 belong initiators and coupled to pro-apoptotic signals [53]. Whilst caspases 3, -6, and -7 belong to effector caspases and execute apoptosis by cleaving cellular proteins. According to a specific signal, there are two possible apoptotic pathways, Intrinsic and extrinsic (Figure 4). As a regulated cell death pathway, intrinsic apoptosis is mediated by a variety of micro-environmental perturbations including growth factor withdrawal, DNA damage, endoplasmic reticulum (ER) stress, reactive oxygen species (ROS) mitotic defects [54]. The irreversible and critical step in intrinsic apoptosis is regulated by pro-apoptotic and anti-apoptotic members of the BCL2, apoptosis regulator (BCL2) protein family, a group of proteins sharing one to four BCL2 homology (BH) domains (i.e., BH1, BH2, BH3, and BH4) [55]. These pro-apoptotic members of the BCL2 protein family are activated transcriptionally or post-translationally as specific organelles or cellular compartments experience perturbations of homeostasis, de facto operating as cellular transducers of stress signaling, which activates initiator caspase-9 then cleaves and activates the executioner caspases-3/6/7, resulting in cell apoptosis[56].

Extrinsic apoptotic pathway is also a regulated cell death is initiated by extracellular alarms. This death pathway is driven by two membrane receptors, the death receptors were

activated by the cognate ligand biding and the dependence receptors were activated by their low ligands concentrations. The death ligands are surface receptors belonging to FAS and TNF receptor family. In general, the death receptor ligation allows the formation of the multiprotein complex at the intracellular tail of the receptor, such as so-called “death-inducing signaling complex” (DISC), “complex I”, and “complex II”, which operate as molecular platforms to regulate the activation and functions of CASP8 and CASP10)[57].

Dysregulation of the apoptotic pathway is a major hallmark in cancer.

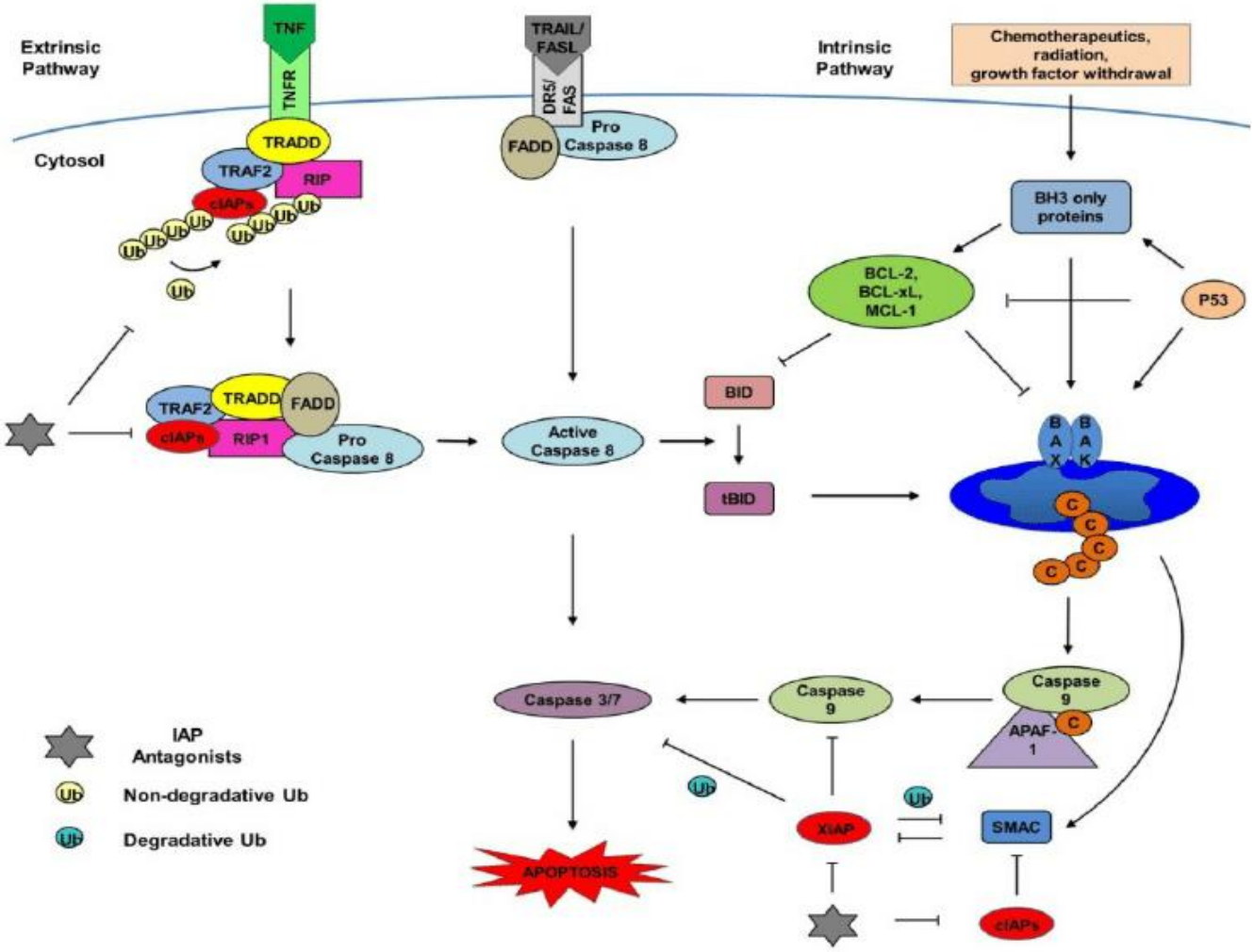

Figure 4. Extrinsic and intrinsic apoptotic pathways

1.5.2 Autophagy

Autophagy comes from the Greek to eat" ("phagy") oneself ("auto"), used for lysosomal-derived vesicles containing cytoplasmic particles, including organelles, in various stages of disintegration captured under electron microscopy [58]. To date, autophagy is a key process in order to recycle damaged or nonessential organelles and various cell components. Autophagy is an adaptive response to stress such as nutrient deficiency. It is also involved in tumor suppression, antigen presentation, toxic misfolded proteins and elimination of intracellular microorganisms. There are three autophagy forms defined from the degradation approach via lysosomes. In macroautophagy, the "auto killer" called autophagosome encapsulates the cargo and finally fuses with lysosomes [59]. In microautophagy, an invagination of the lysosomal membrane engulfs the cargo. In chaperone-mediated autophagy, heat-shock cognate proteins deliver substrates to lysosomes. Post fusion of autophagosome, the material is ingested into metabolic substrates [60]. The typical whorls in autophagic vacuoles are remnants of membranes. A complex set of autophagyrelated proteins regulates the formation of autophagosomes. Among these is a complex consisting of class III phosphatidylinositol-3-kinase (PI3K) and beclin-1 (BECN1), a member of the BCL2 family with a BH3-only domain. There is additional control by mTOR (the mammalian target of rapamycin [now known as sirolimus]), a serine– threonine protein kinase that integrates input from cellular nutrients, growth factors, and cellular redox state to inhibit autophagosome formation [61].

1.5.3 Necrosis

Necrosis comes from the Greek “nekros,” for corpse, and is described as a non-programmed cell death pathway and occurs in response to hypoxic or acute injury as well as in super physiological conditions such as cold, heat mechanical force and etc. [62]. Necrosis is also mediated via ROS, calcium ions, poly–ADP– ribose polymerase (PARP), calcium-activated nonlysosomal proteases (calpains), and cathepsins [63]. As soon as cells die from necrosis, damage-associated molecular- pattern (DAMP) molecules, enter the circulation and activate innate immune cells. Thus, the first cells that die from trauma or infection may function as sentinels, alerting the host to the need for defensive or reparative responses. In addition, necrosis can be initiated by the activation of selected cell-surface receptors [63]. As a result, necrosis in a pro-infamatory response that leads to the major injury at sites of necrosis.

1.5.4 Necroptosis

Necroptosis is a programmed form of necrosis also called inflammatory cell death [64]. This form of necrosis works against pathogen-mediated infections, morphologically characterized by cell swelling followed by rupturing of plasma membrane [65]. It is well known that involvement of receptor like Fas, TNF, and TRAIL can lead to cell death through the recruitment of caspase-8 leading to initiation of extrinsic apoptotic pathway. A plethora of evidences has shown that inhibition of caspase-8 molecule shift extrinsic apoptosis to necrosis mode of cell death due to activation of RIPK3 and MLKL[66]. Hence, it is an alternative mode of cell death when caspase-8-dependent apoptotic pathway is blocked. Initiation of necroptosis is mediated by immune ligands including Fas, TNF, and LPS leading to activation of RIPK3 which further activates the MLKL by phosphorylation [66].

1.5.5 Ferroptosis

Ferroptosis is a recently recognized form of regulated cell death. It is characterized morphologically by the presence of smaller than normal mitochondria with condensed mitochondrial membrane densities, reduction or vanishing of mitochondria crista, and outer mitochondrial membrane rupture [67]. It can be induced by experimental compounds (e.g., erastin, Ras-selective lethal small molecule 3, and buthionine sulfoximine) or clinical drugs (e.g., sulfasalazine, sorafenib, and artesunate) in cancer cells and certain normal cells (e.g., kidney tubule cells, neurons, fibroblasts, and T cells) [68]. Activation of mitochondrial voltage-dependent anion channels and mitogen-activated protein kinases, upregulation of endoplasmic reticulum stress, and inhibition of cystine/glutamate antiporter is involved in the induction of ferroptosis. This process is characterized by the accumulation of lipid peroxidation products and lethal reactive oxygen species (ROS) derived from iron metabolism and can be pharmacologically inhibited by iron chelators (e.g., deferoxamine and desferrioxamine mesylate) and lipid peroxidation inhibitors (e.g., ferrostatin, liproxstatin, and zileuton). Glutathione peroxidase 4, heat shock protein beta-1, and nuclear factor erythroid 2-related factor 2 function as negative regulators of ferroptosis by limiting ROS production and reducing cellular iron uptake, respectively[69]. In contrast, NADPH oxidase and p53 (especially acetylation-defective mutant p53) act as positive regulators of ferroptosis by promotion of ROS production and inhibition of expression of SLC7A11 (a specific light-chain subunit of the cystine/glutamate antiporter), respectively. Misregulated ferroptosis has been implicated in multiple physiological and pathological processes, including cancer cell death,

neurotoxicity, neurodegenerative diseases, acute renal failure, drug-induced hepatotoxicity, hepatic and heart ischemia/reperfusion injury, and T-cell immunity [68,69].

1.5.6 Pyroptosis

Pyroptosis is morphologically and mechanistically distinct from other forms of cell death. Caspase 1 dependence is a defining feature of pyroptosis, and caspase 1 is the enzyme that mediates this process of cell death [70]. Caspase 1 is not involved in apoptosis. Pyroptosis features rapid plasma-membrane rupture and release of proinflammatory intracellular contents. This is in marked contrast to the packaging of cellular contents and non-inflammatory phagocytic uptake of membrane-bound apoptotic bodies that characterizes apoptosis. Cell lysis during pyroptosis results from caspase 1-mediated processes [71].

1.5.7 Cell "Anastasis"

The ability of cells to survive caspase 3 activity has implications for normal development, cancer, and degenerative and ischemic diseases. Anastasis is the most recent cell death pathway that has been characterized. However, Anastasis is a cell survival pathway that initiates signaling event that lead to the reversal of a dying cell to one that begins to survive. Anastasis proceeds in two clearly defined stages that are characterized by distinct repertoires of genes. In the early stage, cells transcribe mRNAs encoding many transcription factors and reenter the cell cycle. In the late stage, cells pause in proliferation while increasing migration. Whereas the proliferation and migration responses were transient, others were longer lasting [72].

In order to end up with cell death there are many factors that are involved. Apart from external factors, stress and various other, the pumps are key players in signaling and signal transduction as well as Survival [73].

1.6 P-type ATPase's

The movement of ions across a biological membrane is a crucial physiological process necessary for maintaining cellular homeostasis. The process involves channels that allow ions to cross the membrane down their concentration gradient and pumps that transport ions against their concentration gradient. The latter is considered an active transport mechanism that is achieved by harnessing Adenosine Triphosphate (ATP)[74]. This family of active transporters includes the P-type, the V-ATP and the ABC transporter [74]. These ion pumps are regulated by various means, including phosphorylation, allosteric inhibition or activation, and ion sensitivity.

The p-class pumps belong to the primary active transport family present in all eukaryotic cells, as well as in bacteria [74]. These proteins consist of a conserved amino acid region, an acid-stable aspartyl phosphate intermediate and a number of conserved motifs that are associated with their catalytic mechanism [75]. Three members of this family have been extensively studied *in vitro, in vivo* and in clinical studies: sodium (Na+)/potassium (K+)-ATPase (NKA), sarcoendoplasmic reticulum calcium (Ca2+) ATPase (SERCA), and proton (H+) / K+ ATPase (HKA) (Figure 5) [75]. P-type ATPase family is divided into five subfamilies (P1–P5), which are classified further into subgroups A, B, C, D [76].

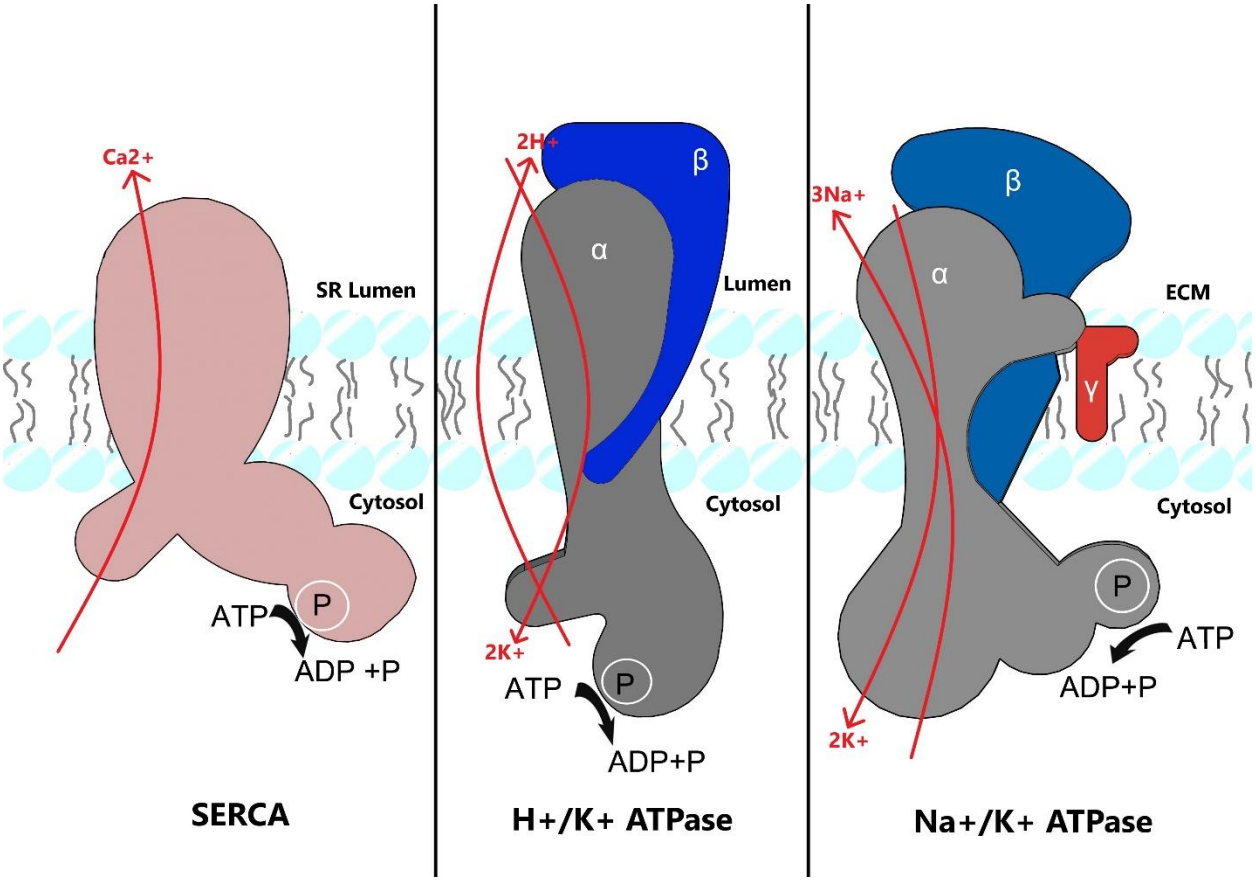

Figure 5. Illustration of the structure and function of P-class pumps.

Cancer cells create an acidic extracellular environment, due to systems such as aerobic and anaerobic glycolysis, build-up of H+ extracellularly and production of lactic acid [77]. These properties allow cancer cells to resist the effects of chemotherapeutic drugs and affect patterns of both metastasis and proliferation [78]. Provided the ability of P-type pumps to alter pH of cells and manipulate other cellular functions their influence as antineoplastic or antitumor targets/biomarkers is being widely evaluated.

1.6.1 Na/K ATPase (NKA)

NKA pumps potassium into the cytosol, while simultaneously transporting sodium to the extracellular environment, both movements taking place actively against their concentration gradients. For every ATP molecule that the pump uses, two potassium ions are imported and three sodium ions are exported, resulting in a net export of a positive charge per pumping cycle [79]. The NKA transmembrane proteins consisted of two subunits, α and β, which subdivided into four and three isoforms, respectively. The α subunit is a large polypeptide comprised of 1,000 amino acid residues that spans the membrane ten times, but which is found principally in the cytoplasm. The β subunit consists of a smaller polypeptide of approximately 300 residues which spans the membrane only once, with the remaining portion resting in the extracellular domain [79–81].

Each of the two units of NKA divided into three structural subunits that seem to serve different roles and are present in different tissues. The α1 subunit of NKA seems to be more than just a pump as it appears in most tissues and it plays a key role in signal transduction, cell/cell adhesion and tight junctions [82]. The α2 subunit is highly expressed in cardiac T-tubules, skeletal and smooth muscle, lung, astrocytes and adipose tissue [83–85]. The α3 subunit is mostly expressed in the heart (myocardial cells) and neurons, while the α4 in the testes. The β1 subunit is mostly present in brain tissue and skeletal muscle, [86]. The β2 subunit is more commonly expressed in glial cells but is also expressed in other tissues, such as myocardial cells [87,88]. Finally, the β3 subunit is expressed predominately in the testes, although it has also been detected in neurons [89,90].

1.6.2 Na/K ATPase significance in cancer

NKA is crucial for cell function, serving as a signal transducer involved in cell adhesion [91]. The role of NKA in cancer has also been supported by a growing number of studies, including *in vivo*, *in vitro* and genetic studies that evaluated either differential expression of NKA subunits, or the effects of different NKA modulators in malignancy[91–94]. In particular, abnormal NKA expression/mutation was reported, which results in expression differences in α- and β-subunit levels in cancer compared to healthy cells[91,92]. This suggests that NKA may play a key role in cancer. In this regard, the α3β1 subunit (isozymes) was found to be abundant in colon cancer cells that metastasized to the liver, but tended to be absent in healthy liver tissue, suggesting that the α3β1 isozyme could potentially serve as a marker for detecting colorectal cancer metastasis to the liver [93].

Changes in metabolic pathways result in a downregulation of NKA in prostate cancer cell lines and appears to be accompanied by the increase in voltage-gated sodium ions, where sodium increases intracellularly leading to loss of homeostasis followed by excitation of prostate cells [95]. A receptor complex was identified linking Src (a protein kinase that promotes cell proliferation and invasion) with α1, which renders Src inactive [82]. An *in vivo* study illustrated that administration of pNaktide (a NKA α1 mimetic peptide) inhibits Src expression, which further decreases proliferation, migration and/or invasion (Table 1) [82].

Table 1 Listing of clinical effects of P-class pumps in cancer.

Drug	Cancer	Pump Outcome (PETD)	Cellular Alterations (PETD)	References
Oleandrin	Human Colorectal Cancer (*in vitro)*	↓NKA (α3)	↑K^+ intracellularly ↓Ca^{2+}intracellularly	[96]
Oleandrin	Prostate Cancer (*in vitro, in vivo*)	↓NKA	↑K^+ intracellularly ↓Ca^{2+}intracellularly	[97]
Oleandrin	Pancreatic Cancer (*in vitro*)	↓NKA	↓pAkt ↑pERK ↓G2/M cell	[98]
pNaktide (peptide)	Prostate Cancer (*in vivo*)	↑NKA (α1)	↑K^+ intracellularly ↓Ca^{2+}intracellularly ↓Src	[99]
Perillyl alcohol	Glioblastoma *(in vitro*)	↓NKA(α1)	↑K^+ intracellularly ↓Ca^{2+}intracellularly ↓JNK	[100]
Istaroxime	Prostate Cancer (*in vitro, in vivo*)	↓NKA	↑K^+ intracellularly ↓Ca^{2+}intracellularly Caspase -3	[101]

			↓c-Myc expression	
Bufalin (CG)	Hepatocallular Carcinoma (*in vitro*)	↓NKA (α3)	↑Akt ↓F0x03a ↑ERK ↑K^+ intracellularly ↓Ca^{2+}intracellularly	[102]
Bufalin (CG)	Leukaemia (*in vitro*)	↓NKA (α3)	↑K^+ intracellularly ↓Ca^{2+}intracellularly	[103]
Bufalin (CG)	Colorectal Cancer (*in vitro*)	↓NKA (α3)	↑K^+ intracellularly ↓Ca^{2+}intracellularly ↓(N_F)- κB ↓(HIF)-1α ↓Cell cycle G2/M	[104]
Cinobufagin (CG)	Prostate Cancer (*in vitro*)	↓NKA	↑K^+ intracellularly ↓Ca^{2+}intracellularly ↑ Caspase-3 cytochrome c release	[105]
Digoxin (CG)	Leukemia (*in vitro*)	↓NKA	↑K^+ intracellularly ↓Ca^{2+}intracellularly ↑FasL	[106]

Digitoxin (CG)	Pancreatic Cancer (*in vitro*)	↓NKA	↑Src ↑ MAPK signalling ↑K^+ intracellularly ↓Ca^{2+}intracellularly	[107]
Digoxin (CG)	Ovarian Clear-cell Carcinoma (*in vitro, in vivo*)	↓NKA	↓FXYD2 ↑K^+ intracellularly ↓Ca^{2+}intracellularly	[108]
Latonoside C (CG)	Colorectal Cancer (*in vitro*)	↓NKA	↑K^+ intracellularly ↓Ca^{2+}intracellularly Repair mitochondrial membrane potential	[109]
Ouabain (CG)	Lung cancer (*in vitro*)	↓NKA	↑K^+ intracellularly ↓Ca^{2+}intracellularly	[110]
Ouabain (CG)	Prostate Cancer (*in vitro*)	↓NKA (α)	↑K^+ intracellularly ↓Ca^{2+}intracellularly Restore mitochondrial membrane potential	[111]

Ouabain (CG)	Brain Glioblastoma (*in vivo*)	↓NKA (α)	↑K^+ intracellularly ↓Ca^{2+}intracellularly	[112]
Digoxin (CG)	Glioblastoma (*in vitro, in vivo*)	↓NKA (β2)	↑K^+ intracellularly ↓Ca^{2+}intracellularly Cell cycle arrest at G2/M phase	[113]
21-benzylidene digoxin (CG)	Cervical Cancer & Colon Carcinoma (*In vitro*)	↓NKA (α1)	DNA damage ↑p21 ↓Cyclin A, Bcl-2 and Bcl-XL	[114]
Thapsigargin	Prostate Cancer (*in vitro, in vivo*)	↓SERCA	↓Ca^{2+} intracellularly cytochrome c release	[115]
Mipsagargin	Hepatocellular Carcinoma (Phase I)	↓SERCA	↓Ca^{2+} intracellularly	[116]

Curcumin Analogue (F36)	Colorectal Carcinoma (*in vitro*)	↓SERCA	↓Ca^{2+} intracellularly	[117]
PSA-Thapsigargin prodrug	Metastatic Prostate Cancer (*in vitro, in vivo*)	↓SERCA	↓Ca^{2+} intracellularly	[118]
Artemisin	Gallbladder Cancer (*in vitro, in vivo*)	↓ SERCA	↓ERK ↓CDK ↓Cyclin D1 ↓Ca^{2+} intracellularly	[119]
Artemisin	Colon Cancer (*in vitro*)	↓ SERCA	↓Ca^{2+} intracellularly ↓doxorubicin intracellularly ↑P-glycoprotein	[120]
Parthenolide	Colon Cancer (*in vitro*)	↓ SERCA	↓Ca^{2+} intracellularly	[120]

			↓doxorubicin intracellularly ↑P-glycoprotein	
Clerodanee ditepene casearin J.	T-cell acute Lymphoblastic Leukemia (*in vitro*)	↓ SERCA	↓Ca^{2+} intracellularly ↓Oxidative stress ↑ Notch1	[121]
Resveratrol & Piceatannol & oligomycin A	Cervical Adenocarcinoma (*in vitro*)	↓ SERCA	↓Ca^{2+} intracellularly Reverse Loss of mitochondrial membrane potential	[122]
Saikosaponin-d	Cervical Cancer & Breast Cancer	↓ SERCA	↓Ca^{2+} intracellularly ↑CaMkκβ-AMP, (AMPK), (mTOR) signaling cascade ↑ unfolded protein responses	[123]
Sch28080	Leukemia (*in vitro*)	↓HKA (α1)	↑H+ intracellularly	[124]

Pantoprazole	Gastric Cancer (*in vitro, in vivo*)	↓HKA (α)	↑H+ intracellularly	[125]
Trametenolic acid B	Gastric Cancer (*in vitro, in vivo*)	↓HKA	↑H+ intracellularly	[126]
Rabeprazole	Gastric Cancer	↓HKA	↑H+ intracellularly	[127]
Lansoprazole	Breast Cancer	↓HKA	↑H+ intracellularly	[126]
Esomeprazole	Esophageal Cancer	↓HKA	↑H+ intracellularly	[128]

Abbreviations: 5' AMP-activated protein kinase (AMPK), B-cell lymphoma-extra-large (Bcl-xL), Calcium/calmodulin-dependent protein kinase kinase 2 (CaMkκβ), Calcium ion (Ca^{2+}), c-Jun N-terminal kinases (JNK), Cyclin-dependent kinase (CDK), Fas ligand (FasL), Forkhead box O3 (F0x03a), Hypoxia-inducible factor 1-alpha ((HIF)-1α), mammalian target of rapamycin (mTOR),mitogen-activated protein kinase (MAPK), Notch homolog 1, translocation-associated (Notch-1), nuclear factor kappa-light-chain-enhancer of activated B cell (N_F-κB), PI3K-Akt Pathway (pAkt), Post exposure to drug (PETD), Potassium ion (K^+), Protein kinase RNA-like endoplasmic reticulum kinase (pERK)

Perillyl alcohol, an inhibitor of NKA, was able to promote apoptosis in glioblastoma cells by also acting on Src kinases, which in turn trigger a cascade of MAPK signalling and JNK activation [129]. In another study on NKA inhibitors, istaroxime was associated with anti-cancer abilities against prostate cancer cell lines, *in vitro* as well as *in vivo* [130]. Istaroxime has been shown to trigger activation of c-Myc oncoprotein expression and caspase-3 apoptotic mediators [130].

Differences in intracellular localization of the NKA α3 subunit have also been recorded. In normal cells, such as in the lung and colon, the α3 isoform is present close to the cytoplasmic membrane, in contrast to its peri-nuclear location in lung cancer and colon cancer. These varying intracellular localisations of the α3 isoform suggest that it can be targeted for treatment and/or serve as a biomarker, as proven with oleandrin. Oleandrin expresses anti-proliferative activity, which increases three-fold in a tumorigenic environment due to these structural characteristics [131].

Drugs known to inhibit NKA were proven to exhibit anti-cancer effects, an example being the cardiac glycosides, which are natural compounds commonly used in heart failure and cardiac arrhythmias[132]. Examples of cardiac glycosides recorded so far in targeting cancer include: bufalin in bladder and lung cancer [133,134], cinobufagin in prostate cancer [135], digoxin in leukemia [136], digitoxin in pancreatic cancer [137], lanatoside in glioblastoma [138], and neriifolin in hepatocellular carcinoma [139]. Ouabain is another cardiac glycoside known to promote hybrid cell death, apoptosis and necrosis [91]. A study assessing the migration of A549 cells, a lung cancer cell line, reported that ouabain inhibits migration via an epidermal growth factor pathway [140]. Ouabain was also found to promote glioma growth in glycoprotein non-metastatic melanoma protein B (GMB), through inhibition of migration and tumor growth, including promotion of apoptosis [141].

Gemcitabine is a chemotherapeutic drug whose effect is obstructed by chemo resistant factors, such as the nuclear factor erythroid 2-related factor 2 [142]. However, this obstruction was prevented by cardiac glycosides when tested on human pancreatic ductal adenocarcinoma [142]. Specifically, female nude mice were divided into three groups, one treated with digoxin, one

with gemcitabine, and the third group was administered both drugs simultaneously. Synergy of the drugs initiated tumor cell apoptosis more efficiently compared to each drug being administered separately [142]. In an *in vitro* study, glioblastoma cells were ceased at the G2/M phase of the cell cycle and apoptosis was increased through silencing of the NKA β subunit, while tumour growth in xenograft mice was reduced [143].

1.6.3 Sarco/endoplasmic reticulum calcium ATPase (SERCA) pump

The SERCA is a 110 kDa power-driven P-type pump that transports two Ca^{2+} ions from the cytoplasm to the sarco/endoplasmic reticulum lumen per ATP used [144]. While Ca^{2+} concentration is known to be greater extracellularly (cytosol) than intracellularly (lumen), a disordered homeostasis is indicative of pathological conditions, including cancer [144]. The SERCA pump, found in both prokaryotes and eukaryotes, is the only protein that transports, regulates, and balances the concentration of free Ca^{2+}. This action is crucial for a number of cellular processes such as gene transcription, cell proliferation and cell death [144–146]. Given that SERCA is found in fundamental structures of the cell, such as the endoplasmic reticulum, then ideally once a pump inhibitor is recognized then pro-drugs could be designed to avoid harming healthy cells and ensure cancer cells are targeted [147,148].

Three SERCA homologous genes have been identified and their presence affects the expression of each of the three SERCA isoforms ATP2A1 (SERCA1), ATP2A2 (SERCA2), and ATP2A3 (SERCA3) [149,150]. These isoforms are approximately 75% homologous and are cell-type dependent [151].

SERCA1 consists of two transcripts; 1a is mainly expressed in adult skeletal muscle whereas 1b is present in fetal skeletal muscle [152]. SERCA2 also consists of two transcripts. The 2a transcript is found in adult skeletal and cardiac muscle. SERCA 2b is abundant in all adult and fetal cardiac and skeletal muscles, but is also found in non-muscle cells, which could be used as a housekeeping gene isoform. SERCA3 is divided into three isoforms, SERCA3a–3c, all of which are expressed in non-muscle cells [153].

1.6.3.1 SERCA significance in cancer

The consequence of inhibiting SERCA has spurred interest and several studies, as a decline of Ca^{2+} concentration in mitochondria leads to the collapse of the electrochemical proton gradient, thus triggering numerous signalling pathways that may result in cell death [154]. Use of SERCA channel inhibitors in cancer has been verified through *in vitro* and *in vivo* studies; the most commonly used inhibitors being thapsigargin, artemisinin parthenolide, resveratrol and saikosaponin [155–157].

Thapsigargin is a sesquiterpene lactone isolated from *Thapsia garganica,* which represses ATPase activit. Thapsigargin has been reported to promote apoptosis in human hepatoma cells via apoptotic body formation, DNA fragmentation and chromatin condensation. All structural changes related with apoptosis were observed post thapsigargin treatment [158]. Similarly, recent clinical studies with mipsagargin, a prodrug of thapsigargin, have supported its use in hepatocellular carcinoma treatment (Table 1) [159]. Thapsigargin was also administered to nude mice xenograft models of prostate cancer over a 40-day period, resulting in a significant decrease in prostate tumor volume compared to controls [160]. Equally as effective is a second-

generation thapsigargin compound, 8-O-N-tert-butoxycarbonyl-12-aminododecanoyl derivative of 8-O-debutanoylthapsigargin, which is as equally applicable as a SERCA inhibitor plus it presented apoptotic properties [161]. The need for designing this secondary compound is due to thapsigargin not being freely soluble.

Artemisinin is a plant-derived drug proven effective in triggering a pro-apoptotic pathway in colorectal adenocarcinoma cells, but also in reducing tumor weight and volume in mice with gallbladder cancer [162]. The pathway, as has been reported, leads cancer cells to apoptosis through cell cycle arrest at G1 or G2 phase [162]. Similar observations were made in mice xenografts on prostate cancer, with limited side effects [163].

A combination of parthenolide with a product known as clerodane diterpene casearin J, was effective in initiating T-cell acute lymphoblastic leukemia cell apoptosis by inhibiting SERCA [121]. ATP2A3 experiences deep deletion in colorectal adenocarcinoma consequently supporting the need for parthenolide which also showed apoptotic patterns in colorectal cancer cells by increasing cytotoxicity (increasing cellular Ca^{2+}), while also displaying anti-angiogenetic properties [164]. Resveratrol, a polyphenol molecule, tested in both human breast cancer and human dermal fibroblast cell lines, has also proven capable of inhibiting SERCA channels and consequently promoting apoptosis [165]. Resveratrol exhibits similar inhibitory effects in lung cancer, in both *in vitro* and *in vivo* studies [156]. Resveratrol along with resveratrol derivatives proved effective in increasing Ca^{2+} concentrations within the prostate cancer endoplasmic reticulum, resulting in their cell death [166].

Another SERCA inhibitor, saikosaponin-d, promotes autophagy via Ca^{2+}/calmodulin-dependent kinase activation and was further found to be a strong cytotoxic agent in mouse apoptosis-

resistant fibroblast cells, suggesting that it could be an anti-cancer autophagic promoter targeting apoptosis-resistant cancer cells [167].

1.6.4 H/K ATPase

The H^+/ K^+ ATPase (HKA) is a heterodimer composed of two subunits, α and β, which are expressed by two separate genes (ATP4A, ATP4B) [168]. The ATP4A gene encodes for the gastric α subunit, composed of 10 transmembrane helices and housing the pump inhibitor-binding site intracellularly, known as cysteine 813. The ATP12A gene codes for a separate α subunit located outside the gastric tissue, such as the prostate and the skin [169]. The ATP4B gene encodes for the β subunit which is highly glycosylated, protecting the enzyme from the stomachs' acidic environment [170]. Its C-terminal spans the membrane once with a short N-terminus on the cytoplasmic side of the membrane and a long C-terminal on the cell surface [171]. This subunit has three-disulphide bonds that form a stable structure supporting, but also proofreading, the folding of the α subunit [172].

The HKA is a P-class family member and apart from the parietal cells of the stomach, it is also found in the distal nephrons of kidneys, prostate, skin and the placenta [173]. ATP4A and ATP4B are highly expressed in stomach and esophageal tissue which is expected given the action of HKA in maintaining pH in both organs. However, both HKA subunits are scarce in other tissues, which may explain, at least in part, why studies on this ion pump are limited.

The HKA expresses characteristic structural changes once activated, known as E1 and E2 conformations, leading to the transportation of H+ into the lumen while K+ is removed and released into the cytoplasm side of the enzyme [168,174,175]. At an almost neutral pH (~6), 2H+ and

2K+ are moved whereas in acidic conditions (pH ~3), 1H+ and 1K+ are transported. For all this to happen, energy from dephosphorylation is required, giving HKA ion pumps the ability to succour the acidic environment in organs such as the stomach [176].

1.6.4.1 H/K ATPase significance in cancer

The importance of the HKA pump was clearly visible in a study where the absence of ATP4A in mice led to hyperplasia, metaplasia and imbalance in growth factor in chronic cases suffering from hypergastrinemia and achorhydria [177]. Chemotherapy is rendered incompetent in eliminating cancerous cells due to the cells greatly acidic environment [172]. Hence, proton pump inhibitors (PPIs), such as omeprazole, pantoprazole and lansoprazole serve to restore proton movement across cellular membranes, thus restoring the pH to levels where chemotherapy drugs can be activated and express their anticancer effects [169,178–180]. One of the well-known drug metabolisers are the CYP-mediated isoforms and are known to metabolise most PPIs effectively, however they do express drug-drug interactions therefore patient history must be considered prior to administration [181].

PPIs, are drugs more commonly prescribed to patients suffering from esophageal reflux disease but given their characteristic behaviour in cancer cells they are now both biomarkers and targets for treatment. For instance, studies illustrate that ATP4B is exceedingly reduced in gastric cancer (GC) compared to its high expression in healthy gastric cells. These findings suggest ATP4B as a biomarker for GC [182]. ATP4B can be restored using 5'-aza-2'-deoxycytidine (a DNA methyltransferase inhibitor) or trichostatin A (an histone deacetylase inhibitor),

consequently restoring the β subunit which resumes HKA function of maintaining pH, hence permitting docetaxel, a chemotherapeutic drug, to operate [182].

Trametenolic acid B (TAB) is a PPI that targets HKA in human gastric carcinoma (HGC-27 cells) in a dose-dependent manner, where it promotes apoptosis of tumor cells [183]. TAB had limited to no effect on normal gastric cells, suggesting its possible use in cancer treatment [183]. In the case of rectal cancer, omeprazole improves efficacy of chemotherapy and relieves patients from chemotherapy side effects. As mentioned, these inhibitors bind to the α subunit causing conformational changes which cease ATPase action, hence the pump remains closed [170]. This favourable co-administration of PPI-chemotherapeutic drug was noticeable within a human leukemia cell line (HL60 cells), where a potent PPI inhibitor known as SCH28080, was capable of prompting cell apoptosis only when pre-administered butyrate to restore pH, by inhibiting histone deacetylase found on ATP12A [184].

Another PPI is pantoprazole, which is activated in acidic environments, such as those expressed in cancer, and has been reported to induce apoptosis in MKN-45 cells and RGM-1 cells [185]. Evaluation in a GC xenograft indicated suppressed tumor growth and promoted apoptosis, as pantoprazole covalently binds to the cysteine residues on the α subunit of HKA and manipulates the extracellular signal-regulated kinases pathway [185]. Pantoprazole also proven to reduce chemoresistance to fluorouracil (a chemotherapeutic drug) in both *in vitro* and *in vivo* studies in colorectal cancer cells [180]. Rabeprazole on the other handwas found to be effective in treating gastric cancer, mainly due to preventing ERK 1/2 phosphorylation, although simultaneously it inhibits HKA creating a less acidic environment [77].

Esophageal cancer cells express a sensitivity towards chemotherapeutics when exposed to esomeprazole (ESO), tumour survival is also reduced, and metastasis is obstructed [186]. Esophageal cancer cells lines SCC and EAC reduce metastasis of cancer cells. ESO proved to alter the expression of miRNAs involved in chemo-resistance [186] and is a proton pump inhibitor which prevents protons from entering the lumen of a cell hence intracellular pH increases to a more basic state [187]. This action has been found to sensitize human osteosarcoma cells to cisplatin, a chemotherapeutic drug [187]. ESO has also proven effective when administered along with doxorubicin. To validate the inhibitors' effect, *in vitro* experiments were performed in MDA-MB-468 plus MCF-10A breast cancer cell lines, in order to record the activity of the ATP12A protein. Doxorubicin-esomeprazole combination was significantly more effective than either drug separately [188]. This occurred as esomeprazole prevented H^+ from moving intracellularly, therefore causing a build-up of protons in the tumorigenic cells, which weakened them and favored the action of doxorubicin [188].

Efavirenz, a reverse transcriptase inhibitor, is an antiviral and anti-tumor drug whose action is impaired in acidic conditions. Lansoprazole, another PPI, is activated by the acidic environment in the cancer cells, restoring the pH via the HKA and consequently, allowing efavirenz to actively prevent reinstatement of tumor cells and decrease proliferation in human melanoma cells [189]. Lansoprazole was also proven effective in promoting apoptosis and inhibiting proliferation in breast cancer cell lines (MDA-MB-231), while inhibiting tumor growth *in vivo* [183].

Dexlansoprazole, tenatoprazole, revaprazan and vonoprazan are PPIs used for treating esophageal reflux disease, but to the reviewers knowledge they have yet to be evaluated as

potential anticancer drugs [190–193]. Even though evidence suggests these drugs present more favorable properties than some of the other PPIs in terms of inhibiting HKA reversibly and from the first dose inhibiting the acidic environment. Rohitukine on the other hand expressed both antiulcer and anticancer properties, but it is uncertain if the anticancer effects are due to HKA pump inhibition [194]. Additional studies stress the importance of treating disorders such as Helicobacter pylori, which renders HKA inactive favoring bacterial growth. If this HKA function is not restored, by any of the above mentioned PPIs, then gastric cancer may formulate [195]. This form of data pinpoints which subunit to target to ensure treatment is effective.

1.7. Clinical studies of P-class pump modulators

1.7.1 Na/K ATPase

Previous studies have shown that NKA expression is altered in various tumors, including drug-resistant tumors, marking it as a potential target by developing NKA modulators. For this reason, different NKA inhibitors, such as perillyl alcohol and cardiac glycosides, are now being used in a number of clinical trials, to assess their effect on different cancers (Supplementary Table) [197–199]. Despite their narrow therapeutic window, cardiac glycosides have exhibited acceptable tolerance, so far. In addition to their direct cytotoxic effects and anti-proliferative properties, different NKA modulators can overcome multiple mechanisms of cancer cells that often lead to failure of existing chemotherapeutic agents [196].

In particular, in one study with biochemically-relapsed prostate cancer, digoxin was well-tolerated, but was not of additional benefit compared to that observed in controls reported in

previous data (historical controls) [197]. A study of patients with BRAF-wild type metastatic melanoma, showed a better response to trametinib when administered with digoxin, compared to studies of trametinib alone [198]. Also, effects of lapatinib on digoxin were assessed in a series of patients with HER2-positive breast cancer, showing that lapatinib significantly increased the absorption of digoxin, thus underscoring the necessity for dose adjustment . No effects on the tumor were reported [199].

1.7.2 SERCA pump

As Ca^{2+} regulates different cellular functions, including proliferation and differentiation, disruption of Ca^{2+} pathways may lead to the development of anti-cancer therapies. To this end, altered function of SERCA pumps have shown to contribute to cancer development [200]. Among SERCA inhibitors, thapsigargin and its prodrug, mipsagargin, are used in different stages of clinical trials (Supplementary Table). A study of mipsagargin in patients with advanced solid tumors exhibited acceptable tolerability and safety, whereas cancer stabilization (defined as progression-free survival) was recorded, particularly in patients with hepatocellular carcinoma [159].

1.7.3 H/K ATPase

The clinical usefulness of the HKA is evident in the number of clinical trials that involve PPIs (Supplementary Table). PPIs can reduce tumor acidity, thus allowing other drugs to reach cancer cells, but also appear to exhibit direct tumor cell toxicity themselves. Additionally, by affecting the acidic environment of the tumor, they carry the ability to potentiate the pharmacokinetics of antitumor drugs [201]. For this reason, most clinical studies include PPI in combinations for

treating malignancies. Combination of high-dose PPIs and aspirin significantly improved composite end-point outcomes in patients with Barrett's esophagus [202]. High dose PPI treatment enhanced antitumor effects (translated as time to progression) of chemotherapy in patients with metastatic breast cancer [201]. Patients who received PPI during chemotherapy for colorectal cancer, had significantly lower rates of nausea and vomiting compared to patients who did not receive PPI [180]. Although pantoprazole did not affect the pharmacokinetics of intravenous doxorubicin in patients with solid tumors, esomeprazole reduced the pharmacokinetic properties of pazopanib in patients with various solid tumors, thereby suggesting decreased absorption of oral pazopanib when the gastric pH increases.

Materials and Methods

2.1 Molecular Characterization

2.1.1 Graviola leaf extraction

The powder dissolved in pure ethanol (Sigma) (1g in 30ml ethanol) and left on stirring mode for 48hr in room temperature. The sample was then centrifuged for 10 min (5000 rpm) and ethanol evaporated via vacuum rotary evaporator at 60 ◦C. The dried extract from the round bottom flask collected (re-suspended) in 2ml of pure ethanol, transferred in 3ml pre-weighted vials and evaporated by nitrogen gas in room temperature, under the hood. When dried it was weighted. The extract sample used as a stock kept in -20^{o}C until further use and the working solution stored in 4^{o}C.

2.1.3 Liquid chromatography–mass spectrometry analysis

An aliquot of the dried extract was resuspended in 20% acetonitrile, 0.1% trifluoroacetic acid solution, and purified by solid-phase extraction using an Oasis 10-mg HLB cartridge. The eluted sample was lyophilized using a centrifugal vacuum evaporator and redissolved in 35% acetonitrile and 0.1% formic acid solution prior to LC–MS analysis. Chromatographic analysis of the sample was performed on an Acquity I-Class UPLC system using an Acquity UPLC HSS T3 (2.1 × 150 mm, 1.8 mm) analytical column. Column temperature was set to 45 °C and the injection volume was 2 µL. A gradient elution with a total run time of 40 min was performed at a flow rate of 0.4 ml/min. Briefly, initial conditions of 35% of mobile phase A (0.1% formic acid in water) were kept for 5 min, followed by a linear gradient from 65 to 85% of mobile phase B (0.1% formic acid in acetonitrile) in 20 min, column wash with 99% mobile phase B for 7 min, and column equilibration to initial conditions for 8 min. Full-scan MS data from 400 to 800m/z were collected on a Waters Xevo TQD MS instrument in a positive ion mode. ESI–QTOF–MS analysis A single LC fraction (11.70–12.20 min) was collected, evaporated to dryness, redissolved in 50% methanol and 0.1% formic acid, and subjected directly to high-resolution MS analysis. The analysis was performed on a Synapt G2- Si HDMS instrument (Waters, UK) equipped with the standard z-spray electrospray ionization (ESI) source. The spectrum was acquired in an ion-positive mode. Instrument control and data processing were performed using the Waters MassLynxTM 4.1 data system. The sample was infused using a syringe pump (Harvard Syringe Pump, model 55–2222, Holliston, MA, USA) and a 100-µL Hamilton syringe (Bonaduz, Switzerland), at a flow rate of 5 µL/min.

2.1.4 Thin-layer chromatography

A standard method was used [203].The silicon membrane cut at pieces of 10cm X 20cm and spotted in a straight line to form an initial band. The developing solvent system used was HPLC grade ethanol: water (80:20 ml/ml). The spots of the extract performed in a band orientation. The developed chromatogram was observed under iodine vapor and UV light.

2.2 Anti-Cancer Effects investigation

2.2.1 Cell Culture and reagents

MCF-7, PC-3, HeLa, HEP-2 Mia PaCa2, MCF10-A and MCF12F cell lines have been provided by Barbara Ann Karmanos, Cancer Institute, Detroit, MI; and cultured as NCI-PBCF-HTB22 (ATCC® HTB-22™) and cultured in Dulbecco's medium supplemented with 10% fetal bovine serum and 1% penicillin/streptomycin (Gibco, Invitrogen). The MCF12F cell line has been cultured in DMEM medium (Gibco, Invitrogen) supplemented with 10% fetal bovine serum, EGF, Insulin, Cholera Toxin and 1% antibiotic. Cells were grown in a humidified atmosphere at 37 °C containing 5% CO_2 and were routinely tested for mycoplasma contamination. The cells media was replaced every 48h with fresh media and the total cell umber was estimated using trypan blue cell count via hemocytometer.

2.2.2 LIVE/DEAD ® Viability/Cytotoxicity Kit *for mammalian cells*

Viability Assay performed according to Molecular probes Invitrogen detection technologies (Revised: 21–December–2005). The cells were treated with the kit's reagents and incubated for 60 min. Then, cells were visualized under fluorescent microscope (Green GFP and Red Texas Red).

100–150 µL of the combined LIVE/DEAD® assay reagents was added, using optimized concentrations, to the surface of a 22 mm square coverslip, so that all cells are covered with solution. Incubations should be performed in a covered dish (e.g., 35 mm disposable petri dish) to prevent contamination or drying of the samples.

2.2.3 MTT Cell Growth Assay Kit

Cell Viability tests performed according to the manufacturer's protocol Cell Proliferation Kit I (MTT).Product No. **11465007001.**

All materials Equilibrated and all reagents prepared to room temperature prior to use. Cell Grown at varying densities (1-5 x106 cells per mL) in a clear plate were for the adherent cells, the media was carefully aspirated. After incubation, the MTT Reagent-supplemented media removed. Cells were treated with MTT reagent and incubated for 30min. Then the absorbance was measured using iMark Micro Plate reader from Bio Rad and the results of three-disting experiments transferred to excel were statistical analysis carried out. Cell viability measured as percentage of cell survival in drug-treated cells relative to untreated cells. Results are demonstrated as means from three different experiments performed in triplicate, $p < 0.05$. ANOVA.

2.3 Pathway Determination

2.3.1 Caspase-3/7 Activity Assay

The cells treated with the appropriate apoptotic inducer for the desired time. Then the CellEvent™ Caspase-3/7 Green Detection Reagent diluted into PBS with 5% FBS (Cat. Nos. 14040133 and 10082147) or complete medium to a final concentration of 2–8 µM. The media was removed from the cells and then the diluted reagent added to the cells. Finally, the cells visualized using the appropriate instrument filter sets such as those used for FITC and the Alexa Fluor™ 488 dye. The excitation/emission maxima for the CellEvent™ Caspase-3/7 Green Detection Reagent is 502/530 nm. The green staining solution was inserted to the treated and untreated cells and incubated for 40 min, followed by microscopic fluorescent visualization.

2.3.2 Western Blotting Analysis

Cells were washed twice with PBS and scraped with lysis buffer (4 % sodium dodecyl sulfate, 20 % glycerin, 20 mM Tris–HCl, 1 mM PMSF, 1 mM NaF, 200 µM Na_3VO_4). Then, they were loaded onto each lane of a 12 % SDS–polyacrylamide gel for electrophoresis and transferred onto nitrocellulose membranes. Primary antibodies (Cell Signalling Danvers, MA, USA) overnight at 1/1000 dilution. Horseradish-peroxidase conjugated secondary antibodies (DAKO, Ely, UK) were used at 1/5000 dilution. In all cases, membranes were blocked with 5 % skim milk in TBST (10 mM Tris–HCl, 0.1 M $NaCl_2$, 0.5 % Tween 20, pH 8.0) for 2hrs at room temperature. After blocking, membranes incubated for 2hrs with anti-human primary antibody at room temperature then followed by overnight incubation at 4 °C. After washing with TBST three

times, the membranes incubated with corresponding secondary antibody for 1 hr at room temperature. The protein bands detected using the Western Luminescent Detection Kit.

Finally, the Western blot images were analyzed using Chemi Doc XRS system with Actin used as the protein control.

Antibody name (anti-)	Weight (kDa)
Caspase 3	35
Caspase 8	57
Caspase 9	25
ERK	40
pERK	43
Akt	55
pAkt	50
Actin	40
a-Tubulin	55

2.4 Real Time PRC

2.4.1 RNA extraction and real-time RT–qPCR analysis

Total RNA was isolated by TRIZOL reagent (Sigma) followed by treatment with RQ1 DNase (Promega). cDNA synthesis was performed with M-MLV reverse transcriptase (invitrogen).

Quantitative qPCR assays were done in triplicate using KAPA 2G Robust HotStart PCR kit with the addition of SYBR Green (invitrogen) in conjunction with gene-specific forward and reverse primers on a LightCycler 96 (Roche) instrument. Quantification was performed with the ΔΔCt Method, as previously described (Stergiopoulos and Politis, Nat Commun, 2016), using the geometric mean of two housekeeping genes (*PPIA* and *RPL13* , as reference genes.

Primers used:

ATP1a1 fw: AATTGTGTTGAAGGCACCGC, ATP1a1 rv: CACACCCGTGATGATGTGGA

ATP1a2 fw: CTTCCAGCAGGGCATGAAGA, ATP1a2 rv: GGTGACTTTGAGCGGGTACA

ATP1a3 fw: GCATCATCGTGGCCAATGTC, ATP1a3 rv: GTGGAGCCCAGGGTTTCTAC

ATP1a4 fw: TGGAGACCCGAAACATCTGC, ATP1a4 rv: ACGTCAGGGAGGCAATTCTG

ATP1b1 fw: TGAAGATTGTGGCGATGTGC, ATP1b1 rv: TCCCAGCCATTCAAGCTTGA

ATP1b2 fw: TTCGCCCCAAGACTGAGAAC, ATP1b2 rv: TTCGTAATAGCGTCCAGGGC

ATP1b3 fw: CGTGACCAGATTCCTAGCCC, ATP1b3 rv: GCTCCATCAGGACAGACTGT

ATP1b4 fw: ACTACCCAGAGTCGGCTTCT, ATP1b4 rv: AGGCACTGCTTGGTTCTTCA

PPIA fw: TGGACCCAACACAAATGGT, PPIA rv: ATGCCTTCTTTCACTTTGCC

RPL13 fw: GCGGACCCGTGCCGAGGTTAT, RPL13 rv: CACCATCCGCTTTTTCTTGCT

2.5 Migration Assay

2.5.1 Wound-healing/ scratch assay

The wound-healing assay was performed according to Jonkman, James E. N. et al.

Cells were grow on a 6-well plate for 72h. Then a wound was created using an insulin syringe needle in the middle of the cell area. The cell growth media was replaced with serum free media contained Mitomycin –C (to stop proliferation) and monitored every 6h by measuring the width of the wound. The experiment performed in three different tests and the width used in order to determine the wound healing property (mobility) was the average of three.

2.6 P-type ATPases assay

2.6.1 Na^+, K^+-ATPase Activity.

NKA membranes were purified from pig kidney outer medulla, as previously described [38-40] . The ATPase activity assay was carried out at 37 °C in a medium consisting of 130 mM NaCl, 20 mM KCl, 4 mM $MgCl_2$, 3 mM ATP, and 20 mM histidine (pH 7.4). Enzyme was incubated with varying concentrations of the compounds for 30 min at 37 °C prior addition of ATP. Specific Na,K-ATPase activity was calculated as difference in Pi release in the absence and presence of 1 mM ouabain. The data on residual Na,K-ATPase activity are presented as function of inhibitor concentration.

2.6.2 In situ measurements of SERCA Activity

Cells were transiently transfected with the ER-targeted genetically encoded FRET Ca^{2+} sensor D1ER [41] and measured in single cells as previously described.[42, 43] During experiments, the endoplasmic reticulum was completely emptied by pre-incubation with 15 µM BHQ and 100 µM histamine in the nominal absence of extracellular Ca^{2+}. After reaching a stable minimum, the agonists and BHQ were washed and the compound to be tested was added 1 min prior re-

addition of extracellular Ca^{2+}. SERCA activity is reflected by the kinetics of ER Ca^{2+} refilling compared with controls.

2.7 Bioinformatics analysis

2.7.1 Bioinformatics

The mRNA expression of four SERCA isoforms was measured across 37 different cancer types, using data from The Cancer Genome Atlas (TCGA) platform (https://cancergenome.nih.gov/) [PMID: 24071849]. The UCSC Xena platform was used for the multiomics analysis of the GDC TCGA Pancreatic Cancer (TCGA-PAAD) dataset. [Mary Goldman, Brian Craft, Mim Hastie, Kristupas Repečka, Akhil Kamath, Fran McDade, Dave Rogers, Angela N Brooks, Jingchun Zhu, David Haussler. The UCSC Xena platform for public and private cancer genomics data visualization and interpretation. (bioRxiv 326470; doi: https://doi.org/10.1101/326470).

2.7.2 *In silico*

Chemographic Mapping with ChemGPS-NP. To describe the chemical space of annonacin and triptolide, and to predict a potential mechanism of action, a principal component analysis with ChemGPS-NP (http://chemgps.bmc.uu.se) was carried out. A database of 228 compounds was used for this task following the same procedure described therein.

Tanimoto Coefficient Similarity Search with Knime®. To compare the tanimoto coefficient of annonacin and triptolide with the database of compounds described in De Ford et al, J Nat Prod. 2015 Jun 26;78(6):1262-70 we created a data pipeline in Knime® (Zurich, Switzerland). The results were further analyzed to shed some light on the mechanism of action of both annonacin and triptolide.

Docking Calculations with GOLD 5.2.

Docking calculations were performed as previously described (Yiallouris, A et al. CDD; 2018 9:764). Briefly, the PDBs 4HYT and 3A3Y were used to dock the annonacin and triptolide with GOLD 5.2 software (CCDC, Cambridge, UK) and to study the interactions with NKA and SERCA in the high and low affinity conformations, respectively. To describe the intermolecular interactions Discovery Studio 4.0 (Accelrys Inc., San Diego, CA, USA) was used.

Bio Profiling

This method used to analyze online biological data of recently developed analytical tools for genomics, proteomics and metabolomics.[37]

TCGA-PAAD_Exemplary multiomic analysis

Genomic, epigenomic, and transcriptomic data for 32 TCGA cancer types were downloaded from the Firehose of the Broad Institute (http://gdac.broadinstitute.org/, January 2016 version).

CBio Cancer

The cBioPortal for Cancer Genomics provides **visualization**, **analysis** and **download** of large-scale cancer genomics data sets. (https://www.cbioportal.org/)

Gao et al. *Sci. Signal.* 2013 & Cerami et al. *Cancer Discov.* 2012

2.8 Animal Study

2.8.1 *In vivo* toxicity study

For the in vivo toxicity study, NOD.CB17-Prkdcscid/J mice bred (EL-42BIO/br-01, Panepistimiopolis, Larissa, Greece) were used. The mouse colony was maintained in a pathogen-free environment in type IIL cages. Female mice, 6–8-weeks old, were used in the studies described here. During the experiments, all animals were kept under specific pathogen-free conditions at the animal facility (EL42-BIO/exp- 03) and allowed ad libitum feed and water. Acute toxicity determination to find the MTD for the animals was performed following the guidelines of the NCI as described elsewhere. Extracts were administered in a 10% DMSO/5% Cremophor ELP (BASF, Ludwigshafen, Germany)/PBS carrier. An animal that received only the carrier was used as control to exclude any side effects due to the carrier. The drug was administered intraperitoneally in mice at a volume of 20 µL/1 g of weight, and the volume was adjusted for the weight of each individual mouse. For the needs of this experiment, the parameters observed and recorded were survival, weight loss, and behavioral changes for a period of 2 weeks, and two independent series of experiments were performed. Experimentation and handling of animals were performed in accordance to the Greek laws (PD 56/2013 and Circular 2215/117550/2013) and to the guidelines of the European Union (2013/63/EU). To generate xenografts, exponentially growing cultures of MIA PaCa-2 human pancreatic cancer cells were subcutaneously injected at the axillary region of 8–10-weekold female NOD.CB17Prkdcscid/J mice from our animal facility (1 × 106 cells/injection, one injection per mouse). When the tumors reached a size of about 200mm3 (advanced-stage model), the mice were arbitrarily divided into three groups and each group consisted of eight mice (n =

8/group). Subsequently, mice were treated intraperitoneally once per day for 3 weeks (15 administrations) either with vehicle (10% DMSO and 5% Cremophore in 0.9% NaCl) or Graviola extract (25 mg/kg). One group received no treatment and served as the control group. Mean tumor volume and standard deviation (SD) for all groups were calculated, and growth curves were plotted as a function of time. In order to study the in vivo effect of the extract, mean tumor volume and SD for all groups were calculated, and growth curves were plotted as a function of time. Tumor volume was calculated according to the formula [(a × b2)/2], where a = length and b = width of the tumor as measured with a vernier's caliper (measurements were performed twice a week). When tumor volume reached a size of approximately 10% of the mouse weight (2000–2200mm3), mice were euthanized. Mice were also weighed to monitor toxicity twice a week.

2.9 Statistical analysis

Statistical analysis was performed using ANOVA or Student's t-test and the GraphPad Prism version 6 software package (GraphPad Software, Inc., La Jolla, USA).

Results

Graviola/Annonacin

3.1 TLC and Mass Spectrometry

Thin-layer chromatography (TLC) was used as one of the methods of isolating/purifying annonacin (Rf=0.87) molecule out of the ethanoic GLE pill extract (data not shown). The ethanoic extract was further analyzed by liquid chromatography-mass spectrometry (LC-MS). The full MS spectrum of a chromatographic peak with a retention time (tR) of ~11.9 min, showed a main singly charged ion peak at m/z 597.63 with additional peaks at m/z 619.59, 579.64 and 561.59 Da. The main peak was in agreement with the expected protonated mass of annonacin. The additional peaks were attributed to sodium adduction (m/z 619.59) and to the loss of one and two water molecules (m/z 579.64 and 561.59 Da, respectively). The fraction eluted between 11.70 and 12.20 min was collected, re-concentrated, re-dissolved and subjected again to LC-MS analysis. The base peak intensity chromatogram of the purified sample is shown in Figure 6. The MS spectrum of the high abundant chromatographic peak at 11.68 min shows the same m/z peaks, as described above, and therefore it can be concluded that the purified sample is highly consisted of annonacin [14,15].

A)

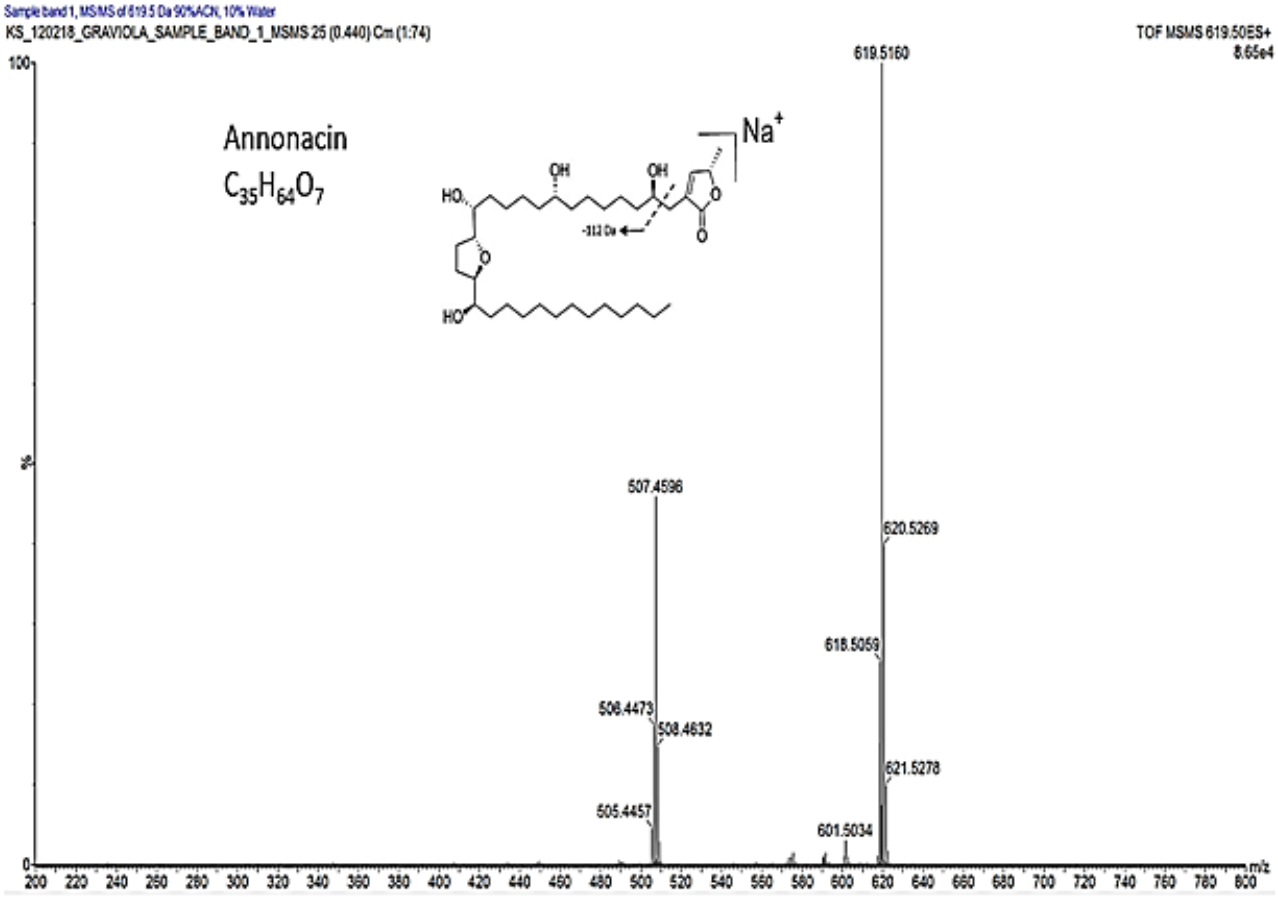

Figure 6. ESI-QTOF-MS/MS spectrum of graviola extract, indicating the annonacin as the main molecule found.

The LC purified sample obtained from the ethanoic extract of Graviola, was further analyzed using high resolution MS. The parent ion peak for the singly charged ion observed at m/z 619.4674 Da is in good agreement with the expected mass of *annonacin* (PubChem CID: 354398, monoisotopic mass: 596.465 g/mol) with a sodium adduct, similar to previous reports [1,2]. The daughter ion peak at m/z 507.4149 is generated from the loss of the lactonic ring.

3.2 In vitro cytotoxicity

The anti-proliferative and anti-tumor effects of the GLE pill was assessed in various cancer cell lines, *in vitro*. As indicated in Figure 7A, the extract induced cell death in a dose depended manner for Hep2 and Sum-159 respectively. In contrast, the extract had limited death-inducing effects in a non-transformed cell line (MCF10A). Additionally, the non-toxic effects of the extract were also observed using a clonogenic assay in non-transformed breast cell line (MCF12F) (Figure 7B). Cell migration was also investigated using a monolayer wound-healing assay. Cell movement was dramatically reduced in GLE treated pancreatic cancer cells compared to untreated cells (Figure 7C).

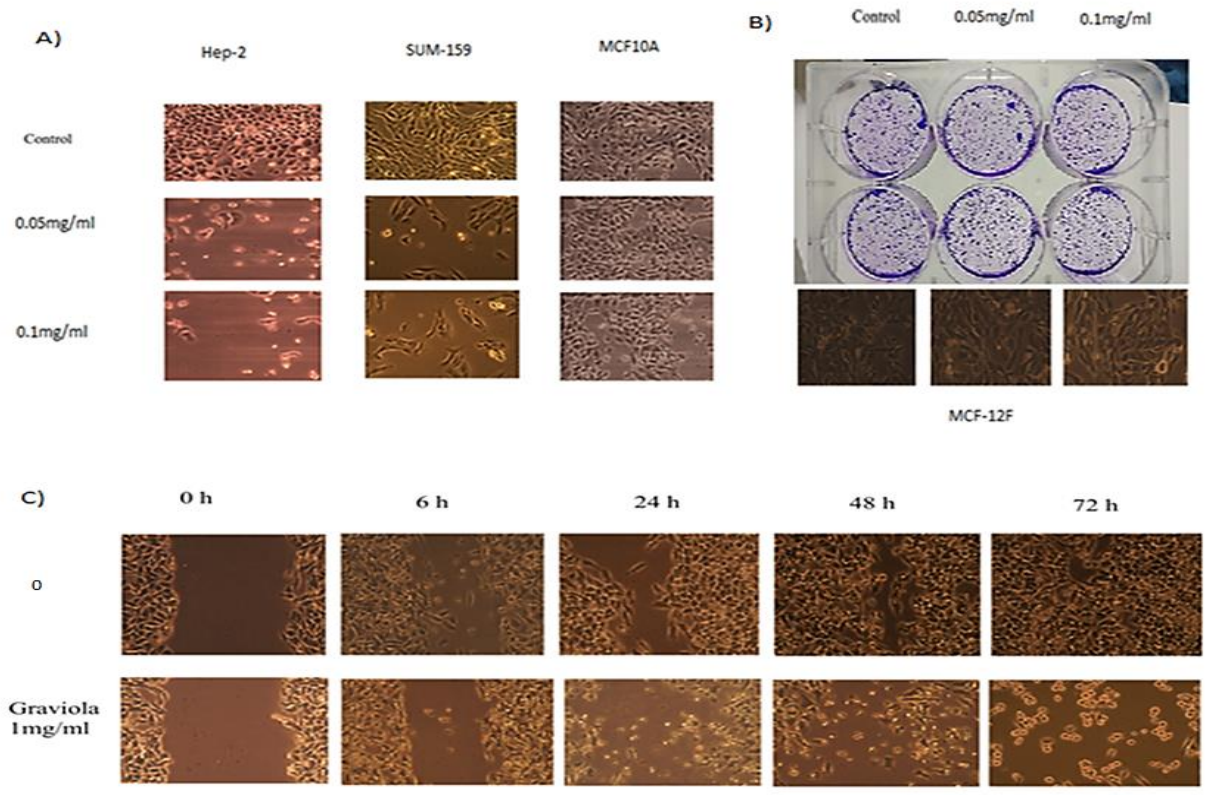

Figure 7. A. The efficacy of *annonacin* on Hep-2, SUM-159 and MCF-10A. B. The efficacy of *annonacin* on normal Vs A. cancer cell lines and its C. anti-metastatic properties.

To quantify the anti-proliferative effects of GLE, we performed the MTT (3-(4,5-dimethylthiazol-2-yl)-2,5-diphenyltetrazolium bromide) tetrazolium reduction assay. As shown in Figure 8A, GLE promoted cell death in a dose depended manner in in MCF-7, Mia Paca-2, and SUM 159 cells (IC_{50}= 0.01mg/ml). As noted, Figure 8B GLE had limited anti-proliferative effects in normal non-transformed breast cell line (MCF-12F). In contrast, the chemotherapeutic drug cisplatin, was associated with cytotoxicity effects in all cancer cell lines, as well as in normal non-transformed cells lines (Figure 8A). These findings indicate that GLE is associated with selective anti-proliferative and death inducing effects in cancer cells with limited effects on normal cells.

To determine whether the cell death effects of GLE is mediated via a caspase dependent pathway, we performed Caspase 3/7 green fluorescent assay. GLE promoted an apoptotic cell death by inducing caspase 3 and 7, respectively as indicated by the increase in fluorescent staining activity (Figure 8C). To further define the cell death pathway, the MTT assay was repeated with and without the presence of Z-VAD-FMK, a cell-permeable pan-caspase inhibitor. Z-VAD-FMK was observed to partly reduce the anti-proliferative effects of GLE (Figure 8B), suggesting that GLE death-inducing effects are partly mediated by an apoptotic pathway.

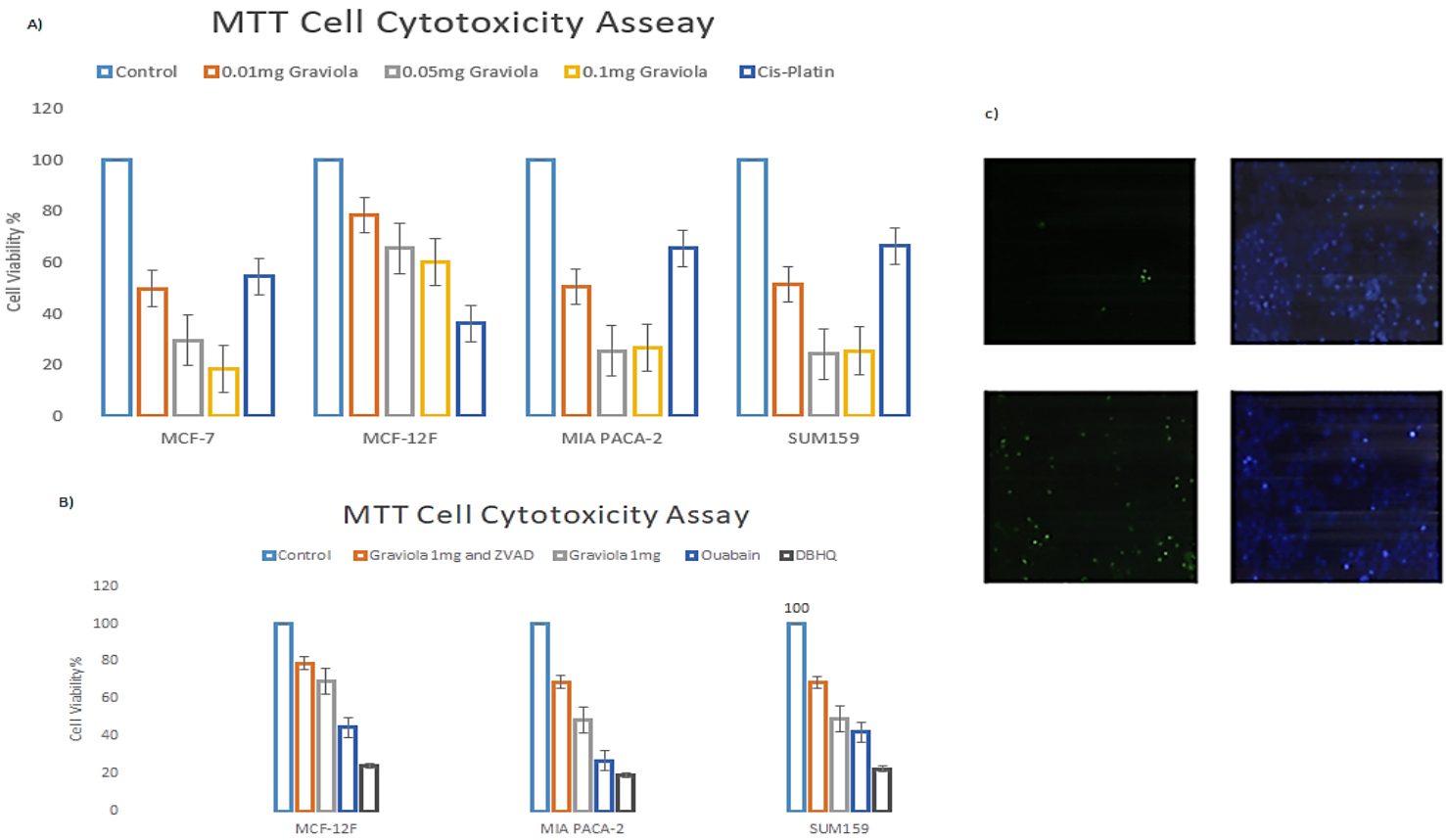

Figure 8. A. Dose-depended efficacy study of *annonacin* on cancer and normal cell viability. B. Dose-depended efficacy study of *annonacin* on cancer and normal cell viability compared with ZVAD+*annonacin*, Ouabain, DBHQ. C. Caspase 3/7 activity via fluorescent dye (GFP)

In Silico Study of GLE *and* Docking Simulations Corroborate the Predicted Targets of the Structure Similarity Analysis.

Due to the similarity of annonacin and the cardiotonic steroids (CSs) and given the fact that these compounds strongly inhibit NKA, docking experiments were performed with GOLD 5.2. The PDB 4HYT was chosen for the modeling studies since NKA was co-crystalized with ouabain in the high-affinity complex (E2P form). Before docking annonacin a validation of the results was performed by re-docking ouabain and comparing to the crystal structure. Small deviations

were observed between the predicted and crystalized ouabain with a RMSD of 0.9591 Å, including the sugar moiety (Figure 10A). Control docking experiments with the low affinity complex of NKA and ouabain (PDB ID: 3A3Y) showed a considerable reduction in the docking[16]. The docking model showed that they also bind deep in the cavity (Figure 10A). The crucial hydrogen bond with Thr797 was also predicted as well as the van der Waals interactions with Phe783 in addition to hydrogen bonds with Asp121 and Asn122, resembling the annonacin binding mode (Figure 10B). While the main interactions were observed, a conserved binding mode was not achieved among annonacin, which is attributed to the high flexibility of these compounds (Figure 10C).

To further confirm the obtained results, a data pipeline was constructed in Knime® to compare the tanimoto coefficients with the same database of cancer chemotherapeutics comprising 228 compounds. The annonacin showed similarities with both, NKA and SERCA pump inhibitors (Table 2), suggesting that they could be non-selective P-type ATPase inhibitors, such as ivermectin[17], and supporting the principal components analysis (PCA) results.

To validate our *in silico* data, we tested the effects of GLE on modulating both NKA and SERCA activity. As shown in Figure 10F, GLE inhibited NKA activity in a dose-dependent manner, whereas Amygdalin, another natural extract, served as a negative control. GLE strongly reduced SERCA activity (Fig 10E). We also compared GLE against a known SERCA inhibitor 2,5-di-t-butyl-1,4-benzohydroquinone (BHQ), and as shown in Figure 10G. These results demonstrated that GLE is a potent inhibitor of both NKA and SERCA pumps and support our *in silico* results.

Finally, we assessed whether known inhibitors of NKA and SERCA are able to promote cell death in the cancer cell lines used in this study. As seen in Figure 10D, DHBQ (a well-known NKA inhibitor) was shown to induce cell death in Mia-PACA2 pancreatic cancer cells.

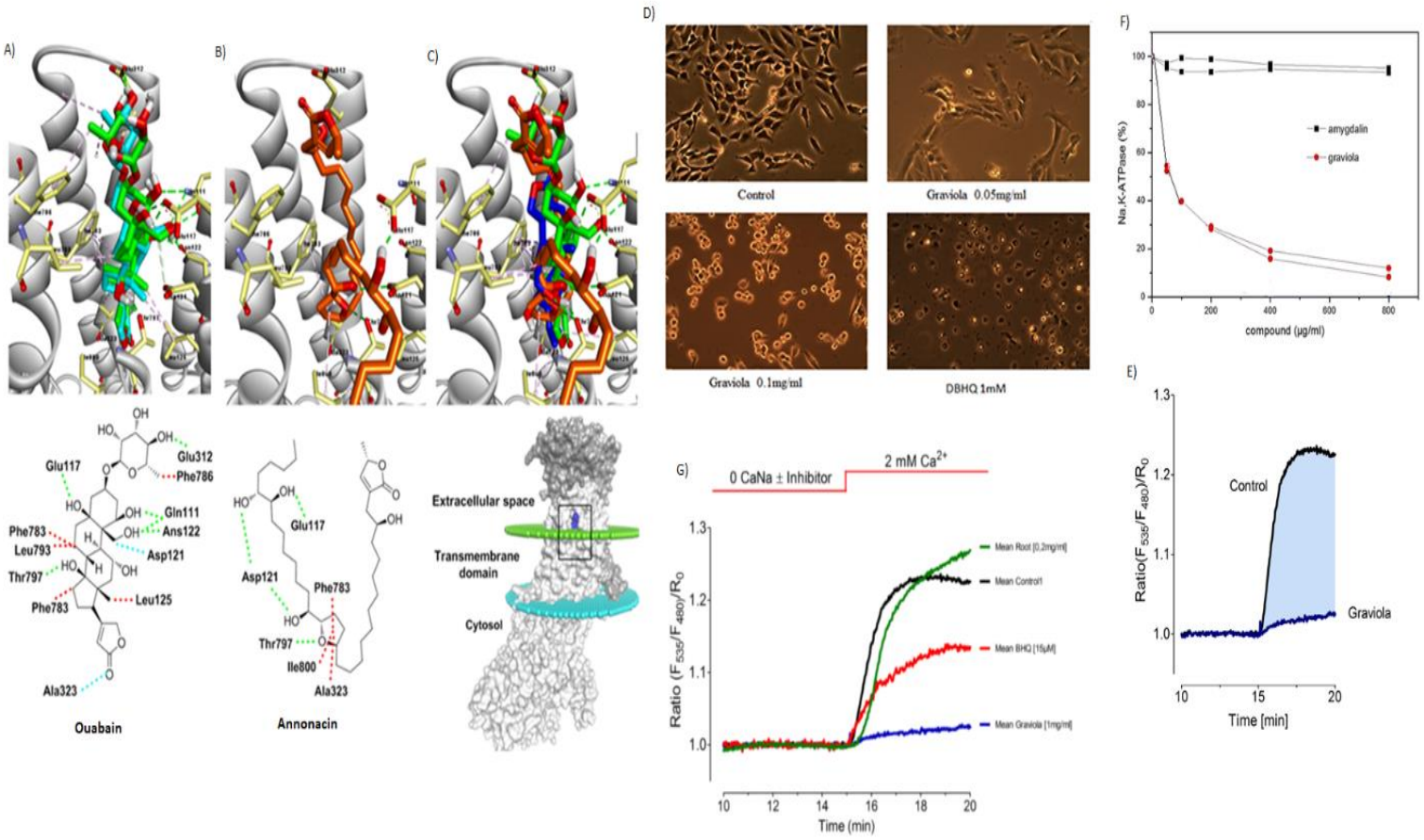

Figure 10. Docking of muricins in the transmembrane domain of Na^+ and K^+-ATPase (PDB ID: 4HYT) with GOLD 5.2

Table 2. Summary of in silico results from the PCA and docking studies

Compound	PC1	PC2	PC3	PC4	Target	Docking score[b]
Acetogenins	Very high	Non-aromatic	High	Very flexible	NKA SERCA	32.81 ± 3.97[c]
Ouabain	High	Non-aromatic	Medium	Semi-rigid	NKA	45.31 ± 0.39
Ivermectin	Very high	Non-aromatic	High	Very flexible	NKA and SERCA[a]	29.59 ± 1.51 and 29.84 ± 0.86

PC1 characterizes the size, shape, and polarizability; PC2 indicates aromaticity and conjugation; PC3 describes lipophilicity, polarity, and H-bond capacity; and PC4 describes flexibility and rigidity. *NKA* Na^+,K^+-ATPase, *SERCA* Ca^{2+}-ATPase, *n.d.* not determined

[a] According to ChemGPS-NP, CheS-Mapper, and Knime®

[b] Obtained with GOLD 5.2 using PDBs 4HYT (NKA) and 2AGV (SERCA), data represent mean ± SD

[c] Mean docking scores of the compounds that belong to this class

3.3 In vivo examination.

The *in vitro* findings suggest that GLE may have a novel role in promoting cell death in cancer cells via inhibiting NKA and SERCA dependent pathways (Figure 11). In order to further investigate the association between NKA and SERCA expression and activity with cancer, we assessed the bio-profiling and prognostic value of NKA and SERCA in low versus high-grade expression in various human cancers. As indicated in Figure 12 there was a strong correlation between increased NKA isoform and SERCA isoform expression and reduced survival rates in

various cancers including breast, colon, brain and kidney cancers. These results indicated a strong association between high expression of NKA and SERCA and survival rates.

We also examined the *in vivo* effects of GLE in a xenograft cancer mouse model. GLE was tested for toxicity in NOD.CB17-Prkdcscid/J mice at doses as high as 400mg/kg. Because of poor water solubility, a carrier based on dimethyl sulfoxide (DMSO) and Chromophore ELP was selected for the in vivo administrations. The extract was found to be toxic at doses higher than 50mg/kg (400, 200, 100, 50, 25 and 10 mg/kg tested for toxicity) as mice died soon after the adminsitration of these doses. At lower doses i.e. 25 and 10mg/kg mice survived well and showed no signs of toxicity or any other kind of side effects during the two-week observation period. Thus, we concluded that, under the experimental conditions used herein, the maximum tolerated dose (MTD) for the GLE is 25mg/kg.

The *in vivo* efficacy of GLE was further examined against MIA PaCa-2 xenografts. Experimental animals were given the MTD (25mg/kg), with mice receiving a total dose of 375mg/kg during a period of three weeks. Animals treated with GLE demonstrated a trend to delay the growth of the tumors, without however reaching a statistical significance. Mice showed no signs of toxicity throughout the experimental period (Figure 11).

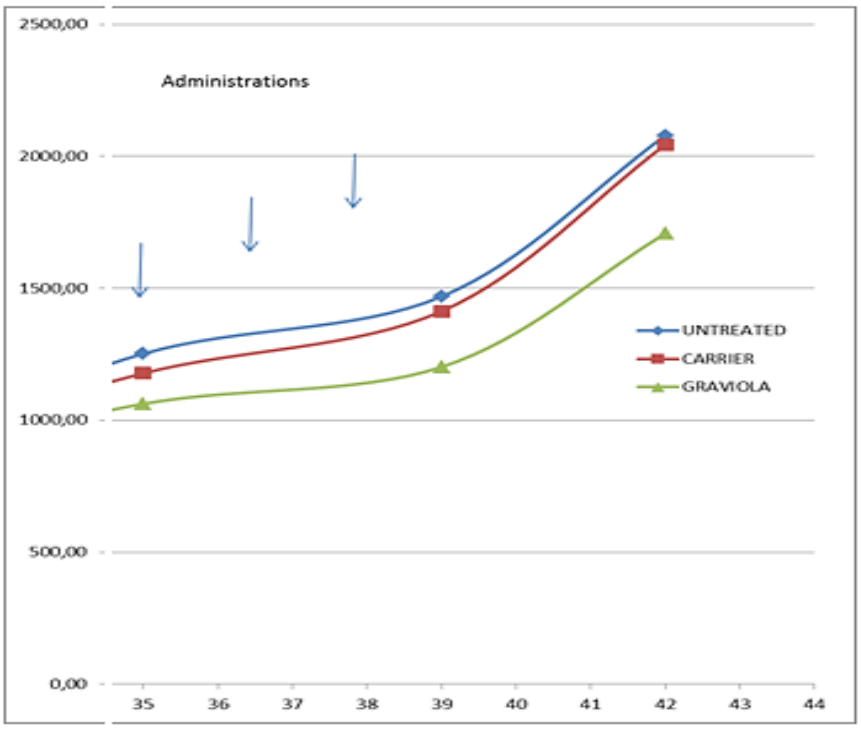

Figure 11. Effect of Graviola extract in MIA PaCa-2 xenografts.

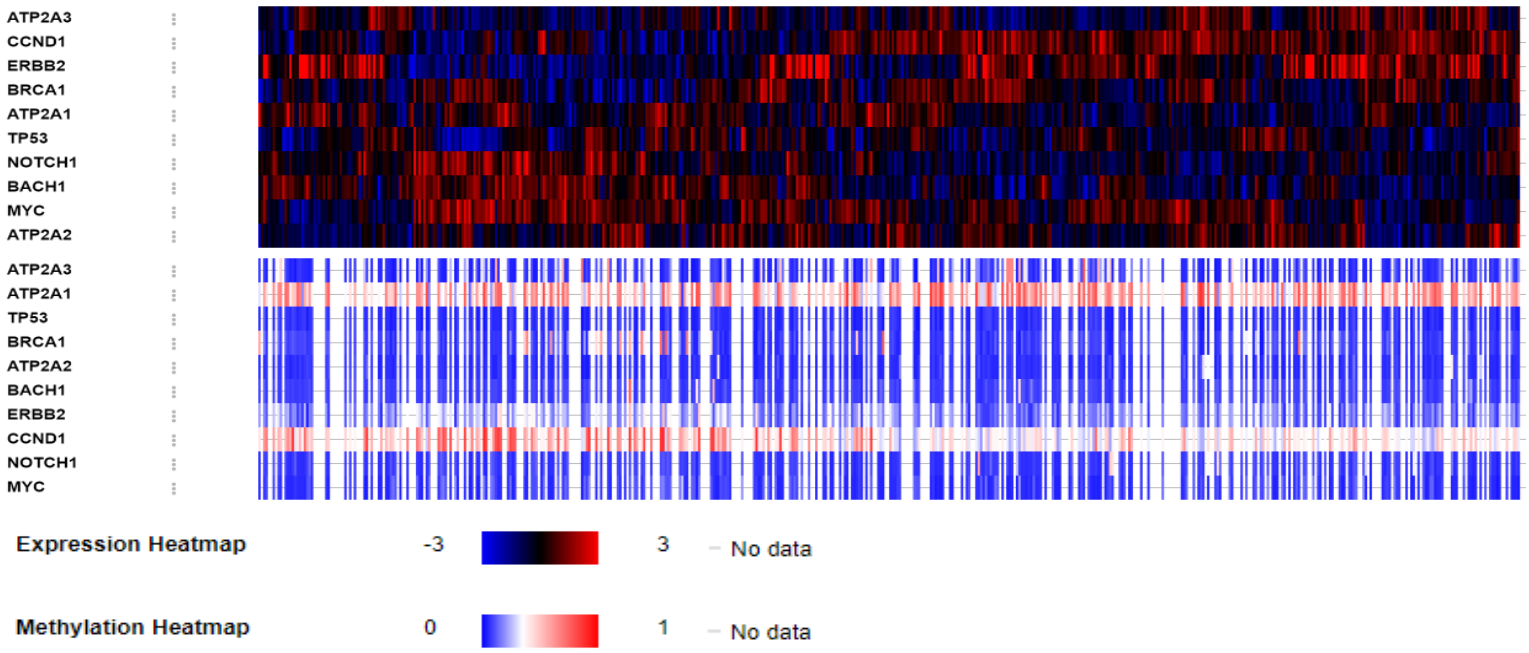

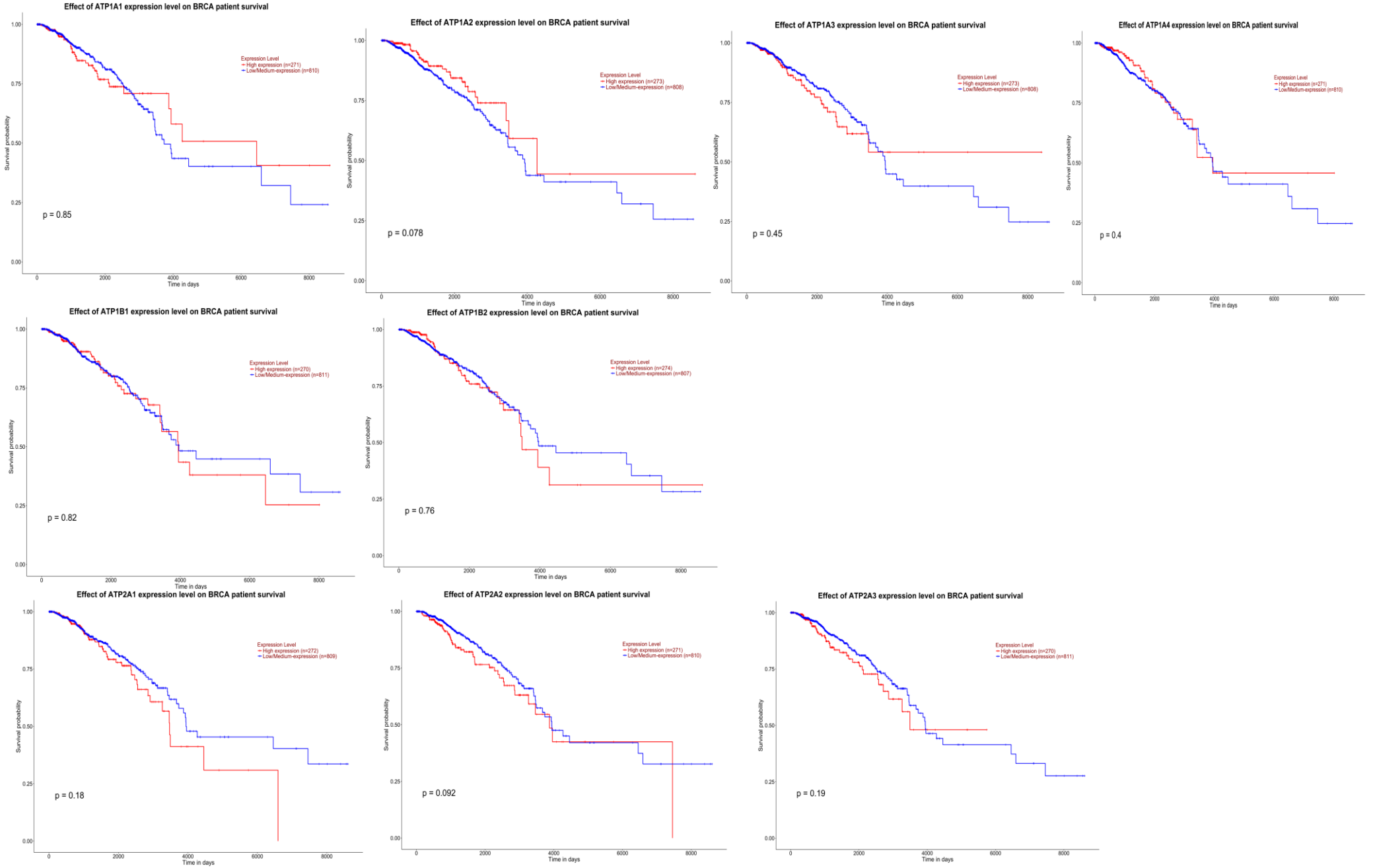

Figure 12. NKA and SERCA pump subunit expression in breast cancer survival.

3.4 NKA Expressions, implementation in cancer

First, Real-Time PCR was carried out in different cancer and normal breast cancer cell lines. From the data presented, it's obvious that specific subunits are express in cancer cell lines and shown a significant implementation in cancer. ATP1a1, ATP1a3, ATP1a4 and ATP1b2 are the ones that highly expressed in cancer cell lines compared to normal (Figure 13).

As an additional piece of confirming information, we next examined through bioinformatics databases the expression levels of NKA subunits found in different types of cancers (n=37) (Figure 13). From the data shown, it is estimated that specific subunits are high and low expressed in different cancer types compared to normal. A deeper computational analysis took place in order to further investigate the role of different NKA subunits in cancer. As an example, pancreatic cancer patient's data GDT, TCGA (PAAD) n=223 patients have been used to screen gene expressions, mutations and methylations respectively. The data shown that the subunits are not highly mutated or altered in the case of pancreatic cancer but some subunits are highly methylated which is evident tumor repression gene transcription/epigenetic alteration. More specific, ATP1a2, ATP1a1, ATP1a4 and ATP1b2 are the subunits with the most epigenetic alteration/ methylation and further tumor suppression repression. At the same time, high copy number of alterations was detected in the same subunits, which shows the cancer mortality meaning that different numbers of copies of the same gene are primed to be altered in cancer and further tumor having more copies of that gene.

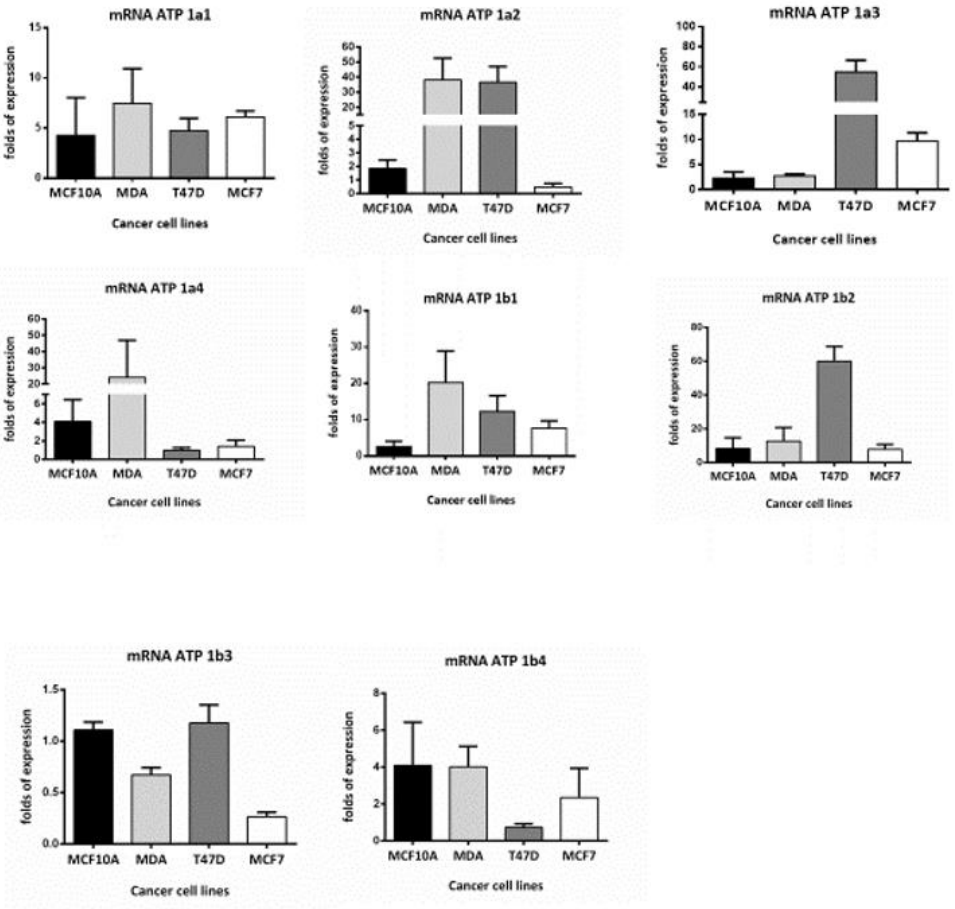

Figure 13. **NKA subunits expression in Breast cancer**

Real Time PCR of all NKA subunits on Different Breast cancer and normal Breast cell line

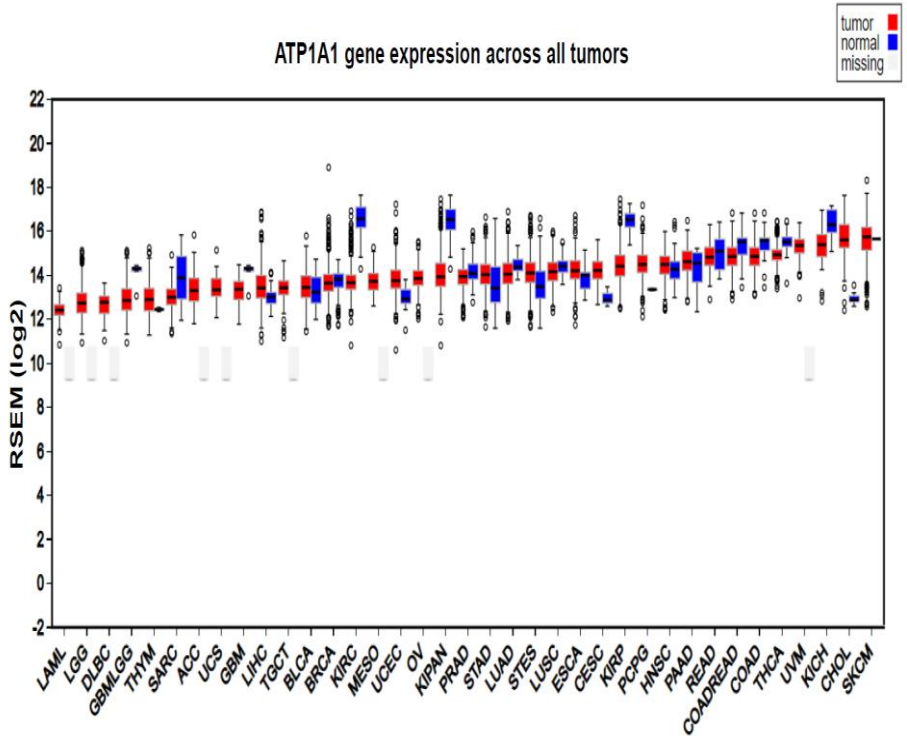
ATP1A1 gene expression across all tumors
tumor
normal
missing
RSEM (log2)
LAML LGG DLBC GBMLGG THYM SARC ACC UCS GBM LIHC TGCT BLCA BRCA KIRC MESO UCEC OV KIPAN PRAD STAD LUAD STES LUSC ESCA CESC KIRP PCPG HNSC PAAD READ COADREAD COAD THCA UVM KICH CHOL SKCM

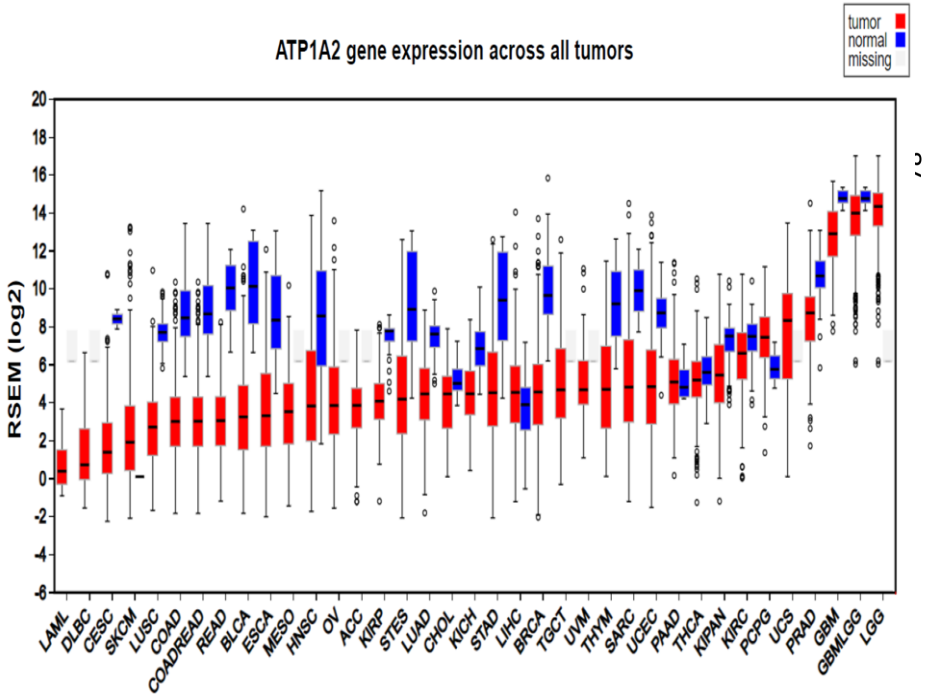
ATP1A2 gene expression across all tumors
tumor
normal
missing
RSEM (log2)
LAML DLBC CESC SKCM LUSC COAD COADREAD READ BLCA ESCA MESO HNSC OV ACC KIRP STES LUAD CHOL KICH STAD LIHC BRCA TGCT UVM THYM SARC UCEC PAAD THCA KIPAN KIRC PCPG UCS PRAD GBM GBMLGG LGG

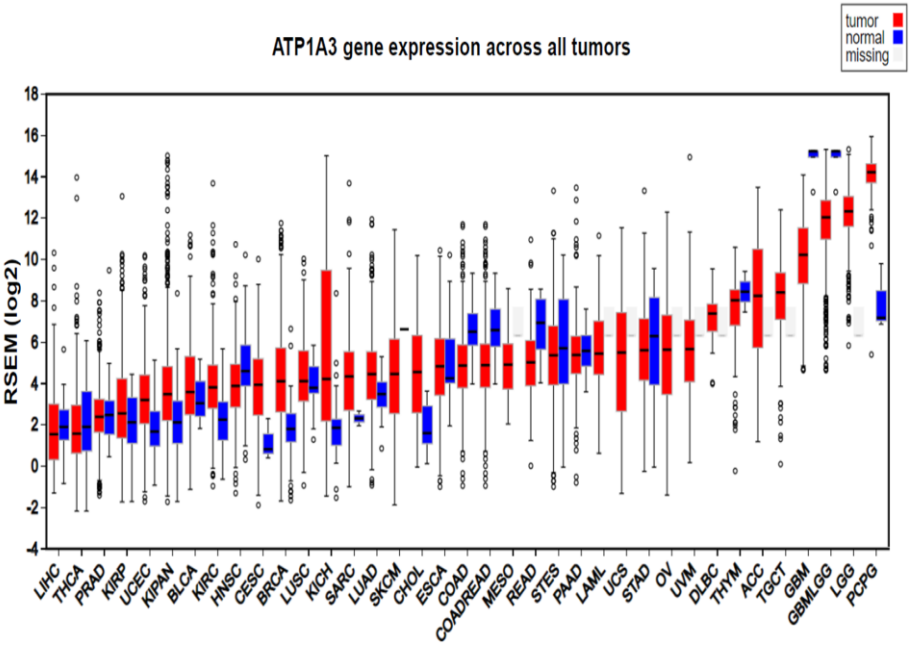
ATP1A3 gene expression across all tumors
tumor
normal
missing
RSEM (log2)
LIHC THCA PRAD KIRP UCEC KIPAN BLCA KIRC HNSC CESC BRCA LUSC KICH SARC LUAD SKCM CHOL ESCA COAD COADREAD MESO READ STES PAAD LAML UCS STAD OV UVM DLBC THYM ACC TGCT GBM GBMLGG LGG PCPG

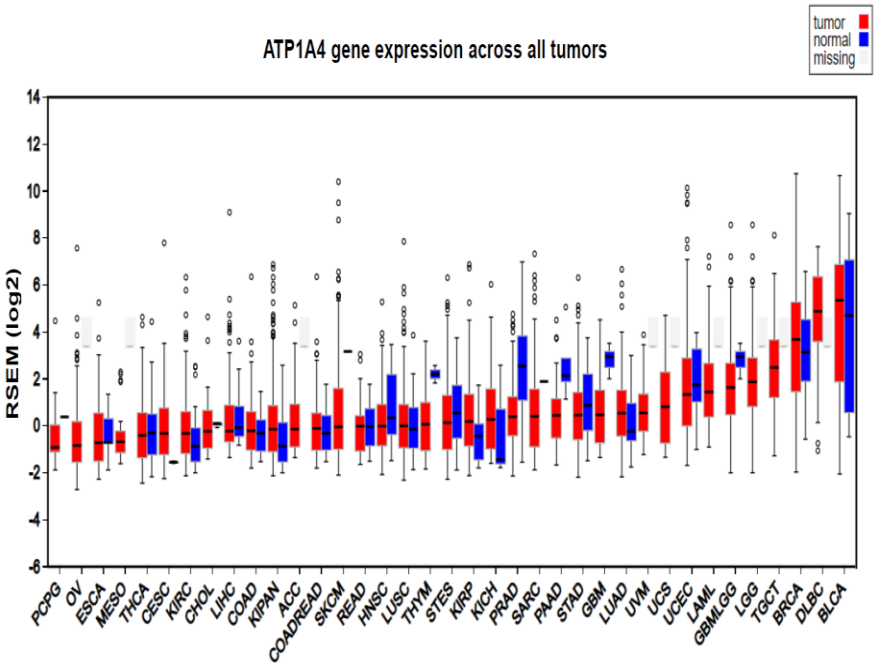
ATP1A4 gene expression across all tumors
tumor
normal
missing
RSEM (log2)
PCPG OV ESCA MESO THCA CESC KIRC CHOL LIHC COAD KIPAN ACC COADREAD SKCM READ HNSC LUSC THYM STES KIRP KICH PRAD SARC PAAD STAD GBM LUAD UVM UCS UCEC LAML GBMLGG LGG TGCT BRCA DLBC BLCA

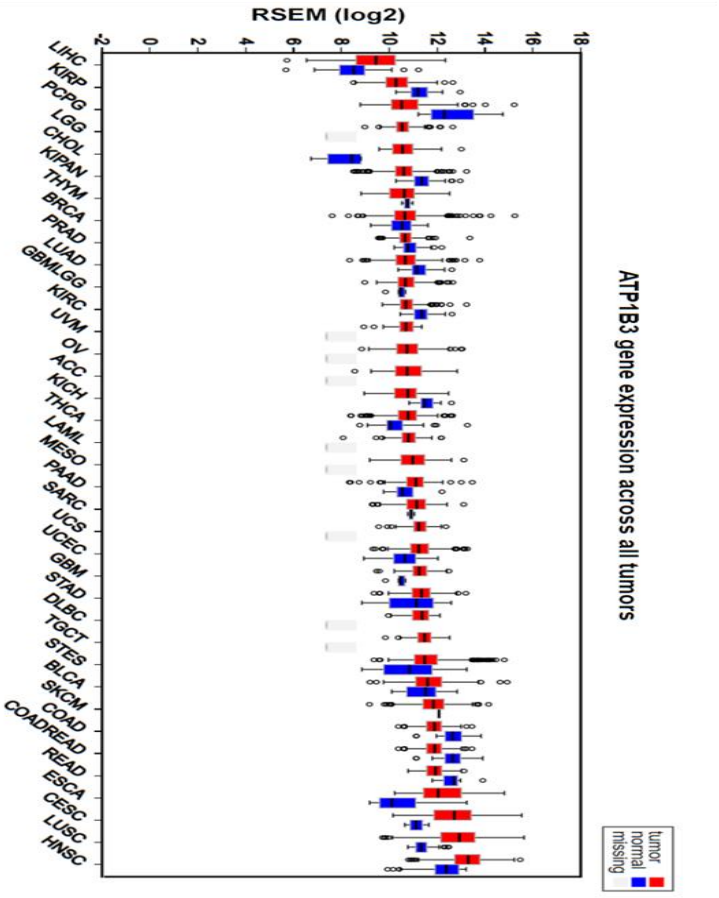
ATP1B3 gene expression across all tumors
RSEM (log2)
tumor
normal
missing

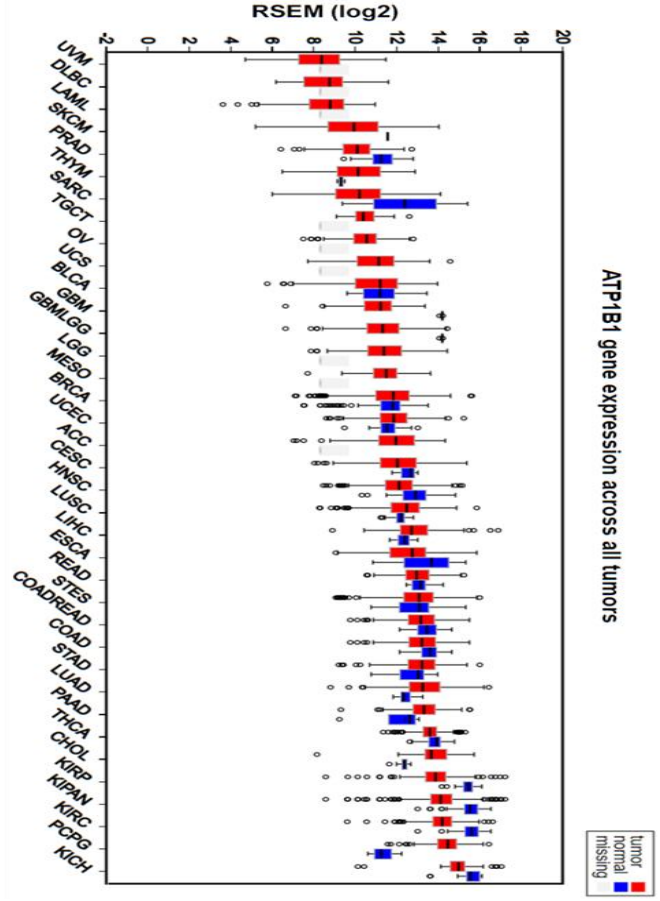
ATP1B1 gene expression across all tumors
RSEM (log2)
tumor
normal
missing

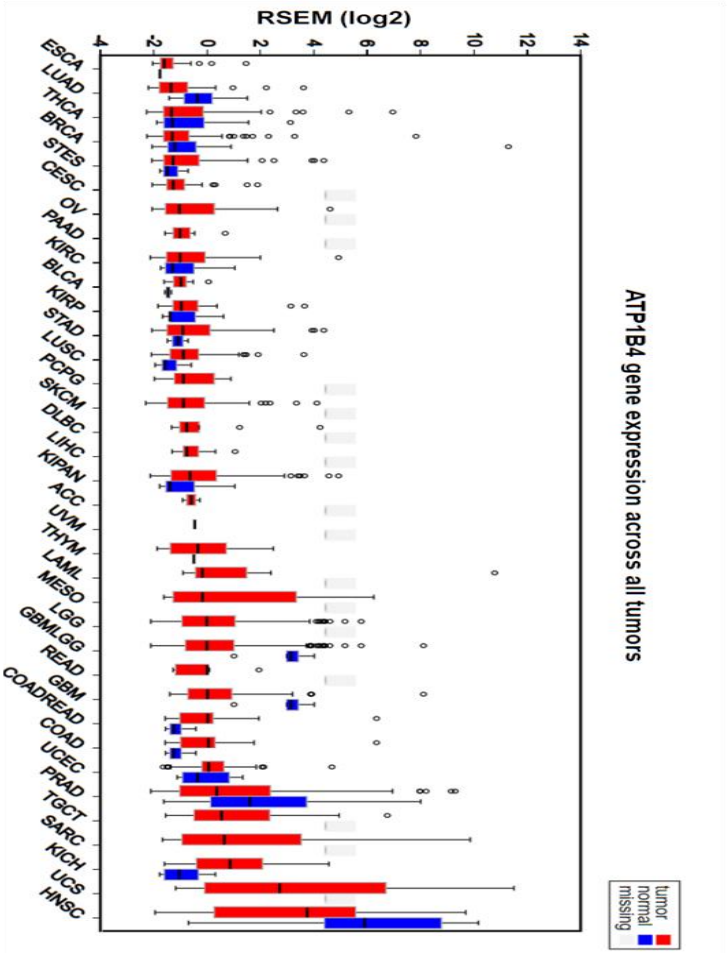
ATP1B4 gene expression across all tumors
RSEM (log2)
tumor
normal
missing

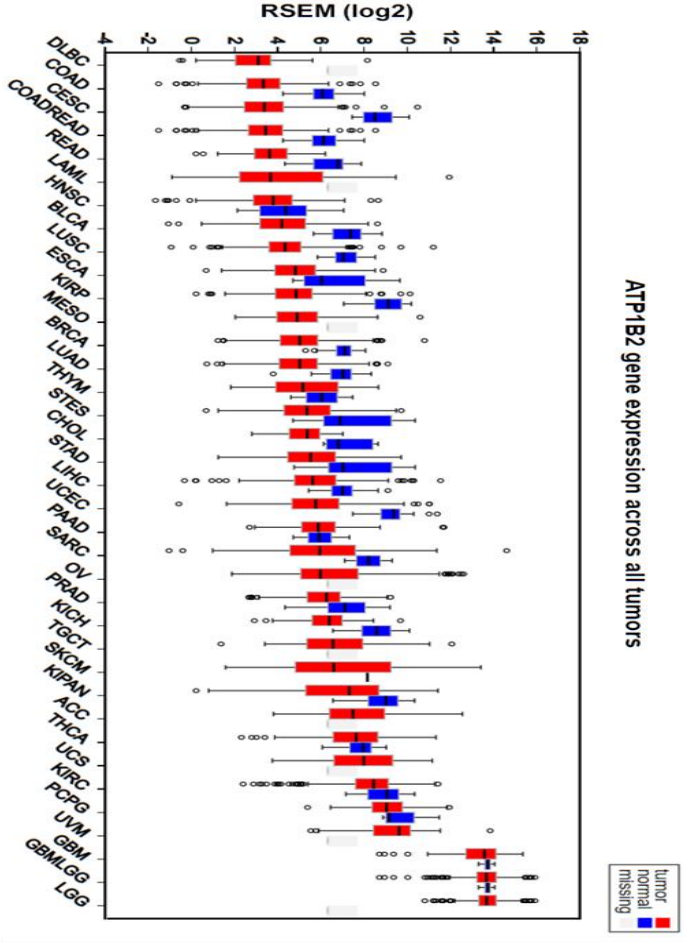
ATP1B2 gene expression across all tumors
RSEM (log2)
tumor
normal
missing

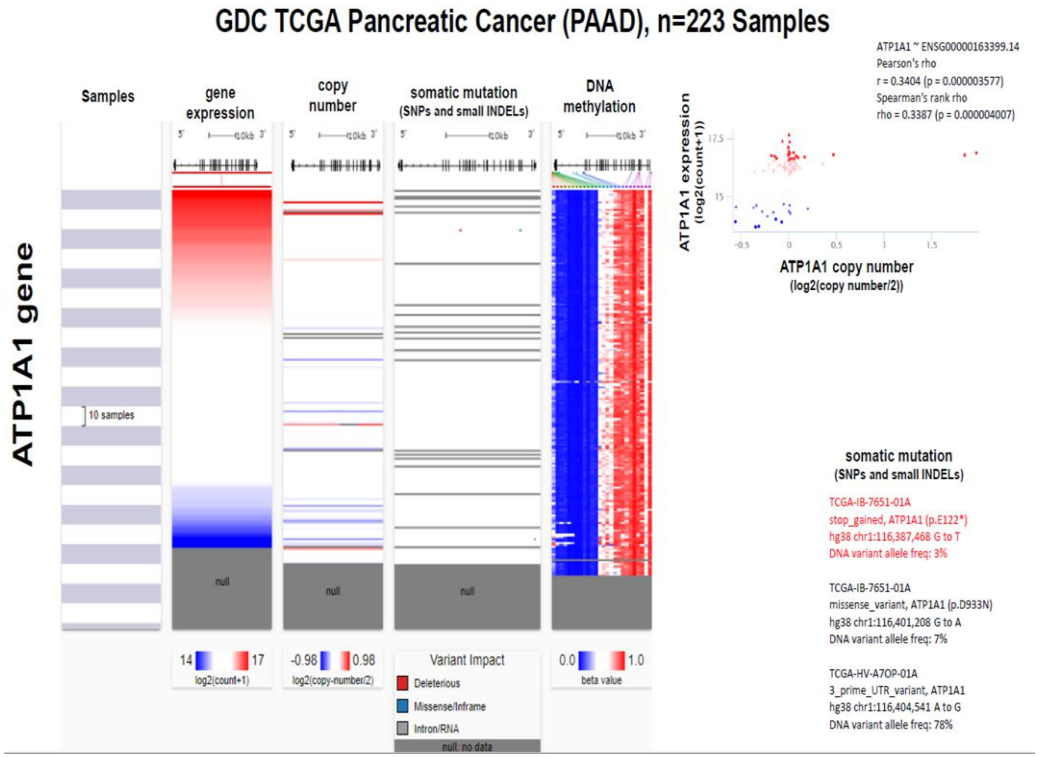
GDC TCGA Pancreatic Cancer (PAAD), n=223 Samples
ATP1A1 gene
Samples
gene expression
copy number
somatic mutation (SNPs and small INDELs)
DNA methylation
10 samples
null
14 17
log2(count+1)
-0.98 0.98
log2(copy-number/2)
Variant Impact
Deleterious
Missense/Inframe
Intron/RNA
null: no data
0.0 1.0
beta value
ATP1A1 ~ ENSG00000163399.14
Pearson's rho
r = 0.3404 (p = 0.000003577)
Spearman's rank rho
rho = 0.3387 (p = 0.000004007)
ATP1A1 expression (log2(count+1))
ATP1A1 copy number (log2(copy number/2))
somatic mutation (SNPs and small INDELs)
TCGA-IB-7651-01A
stop_gained, ATP1A1 (p.E122*)
hg38 chr1:116,387,468 G to T
DNA variant allele freq: 3%
TCGA-IB-7651-01A
missense_variant, ATP1A1 (p.D933N)
hg38 chr1:116,401,208 G to A
DNA variant allele freq: 7%
TCGA-HV-A7OP-01A
3_prime_UTR_variant, ATP1A1
hg38 chr1:116,404,541 A to G
DNA variant allele freq: 78%

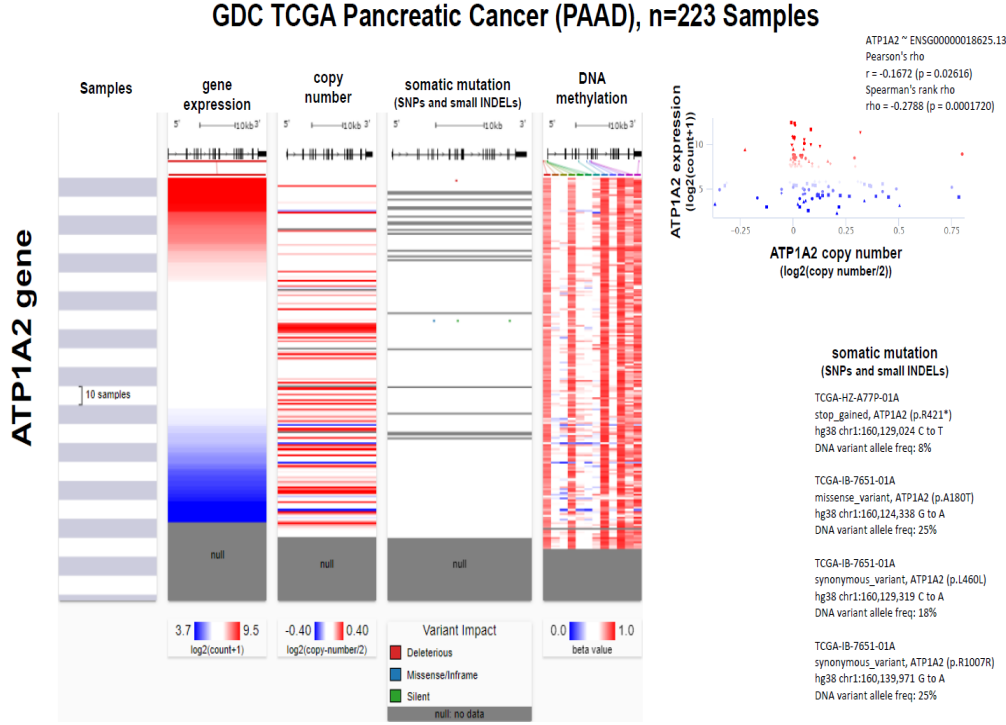
GDC TCGA Pancreatic Cancer (PAAD), n=223 Samples
ATP1A2 gene
Samples
gene expression
copy number
somatic mutation (SNPs and small INDELs)
DNA methylation
10 samples
null
3.7 9.5
log2(count+1)
-0.40 0.40
log2(copy-number/2)
Variant Impact
Deleterious
Missense/Inframe
Silent
null: no data
0.0 1.0
beta value
ATP1A2 ~ ENSG00000018625.13
Pearson's rho
r = -0.1672 (p = 0.02616)
Spearman's rank rho
rho = -0.2788 (p = 0.0001720)
ATP1A2 expression (log2(count+1))
ATP1A2 copy number (log2(copy number/2))
somatic mutation (SNPs and small INDELs)
TCGA-HZ-A77P-01A
stop_gained, ATP1A2 (p.R421*)
hg38 chr1:160,129,024 C to T
DNA variant allele freq: 8%
TCGA-IB-7651-01A
missense_variant, ATP1A2 (p.A180T)
hg38 chr1:160,124,338 G to A
DNA variant allele freq: 25%
TCGA-IB-7651-01A
synonymous_variant, ATP1A2 (p.L460L)
hg38 chr1:160,129,319 C to A
DNA variant allele freq: 18%
TCGA-IB-7651-01A
synonymous_variant, ATP1A2 (p.R1007R)
hg38 chr1:160,139,971 G to A
DNA variant allele freq: 25%

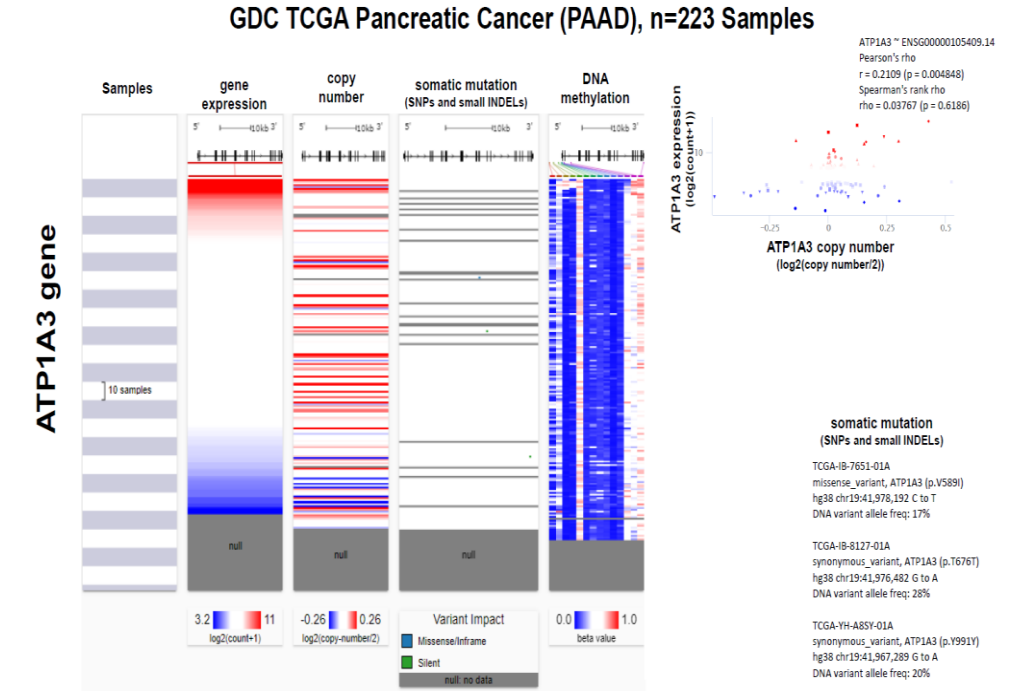
GDC TCGA Pancreatic Cancer (PAAD), n=223 Samples
ATP1A3 gene
Samples
gene expression
copy number
somatic mutation (SNPs and small INDELs)
DNA methylation
10 samples
null
3.2 11
log2(count+1)
-0.26 0.26
log2(copy-number/2)
Variant Impact
Missense/Inframe
Silent
null: no data
0.0 1.0
beta value
ATP1A3 ~ ENSG00000105409.14
Pearson's rho
r = 0.2109 (p = 0.004848)
Spearman's rank rho
rho = 0.03767 (p = 0.6186)
ATP1A3 expression (log2(count+1))
ATP1A3 copy number (log2(copy number/2))
somatic mutation (SNPs and small INDELs)
TCGA-IB-7651-01A
missense_variant, ATP1A3 (p.V589I)
hg38 chr19:41,978,192 C to T
DNA variant allele freq: 17%
TCGA-IB-8127-01A
synonymous_variant, ATP1A3 (p.T676T)
hg38 chr19:41,976,482 G to A
DNA variant allele freq: 28%
TCGA-YH-A8SY-01A
synonymous_variant, ATP1A3 (p.Y991Y)
hg38 chr19:41,967,289 G to A
DNA variant allele freq: 20%

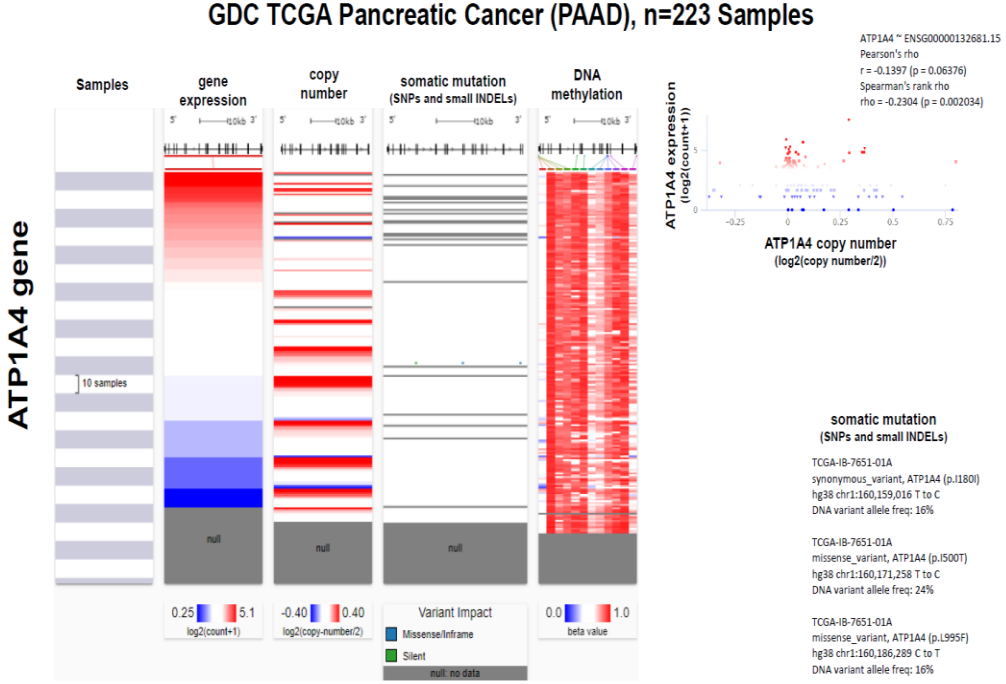
GDC TCGA Pancreatic Cancer (PAAD), n=223 Samples
ATP1A4 gene
Samples
gene expression
copy number
somatic mutation (SNPs and small INDELs)
DNA methylation
10 samples
null
0.25 5.1
log2(count+1)
-0.40 0.40
log2(copy-number/2)
Variant Impact
Missense/Inframe
Silent
null: no data
0.0 1.0
beta value
ATP1A4 ~ ENSG00000132681.15
Pearson's rho
r = -0.1397 (p = 0.06376)
Spearman's rank rho
rho = -0.2304 (p = 0.002034)
ATP1A4 expression (log2(count+1))
ATP1A4 copy number (log2(copy number/2))
somatic mutation (SNPs and small INDELs)
TCGA-IB-7651-01A
synonymous_variant, ATP1A4 (p.I180I)
hg38 chr1:160,159,016 T to C
DNA variant allele freq: 16%
TCGA-IB-7651-01A
missense_variant, ATP1A4 (p.I500T)
hg38 chr1:160,171,258 T to C
DNA variant allele freq: 24%
TCGA-IB-7651-01A
missense_variant, ATP1A4 (p.L995F)
hg38 chr1:160,186,289 C to T
DNA variant allele freq: 16%

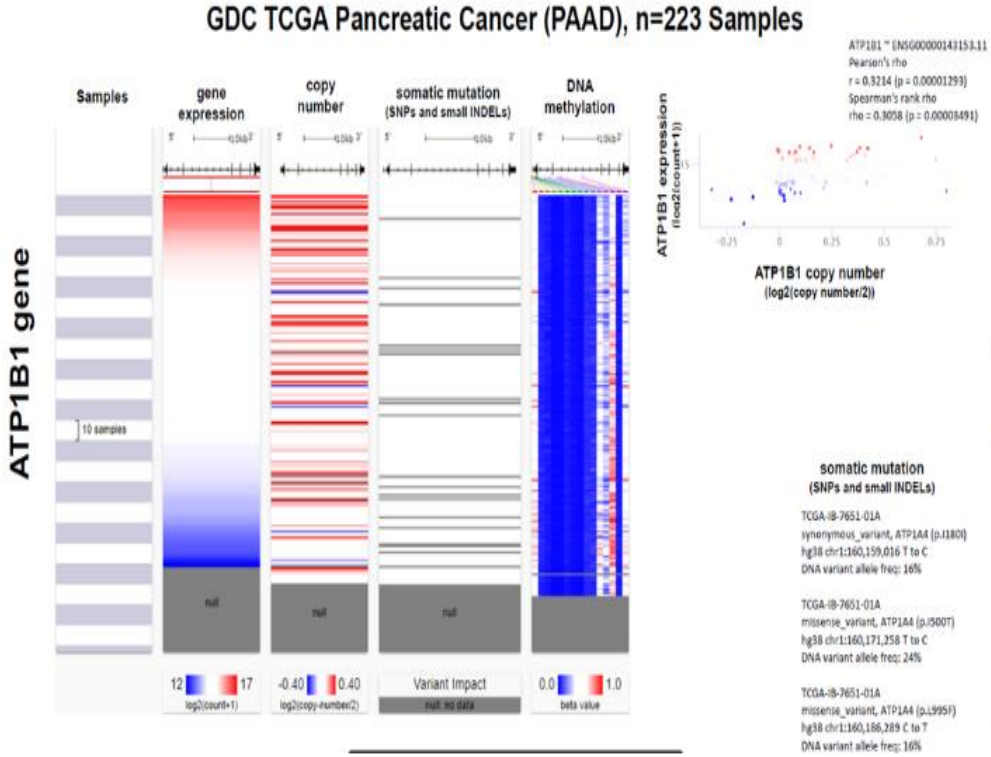
GDC TCGA Pancreatic Cancer (PAAD), n=223 Samples
ATP1B1 gene
Samples
gene expression
copy number
somatic mutation (SNPs and small INDELs)
DNA methylation
10 samples
null
12 17
log2(count+1)
-0.40 0.40
log2(copy-number/2)
Variant Impact
null: no data
0.0 1.0
beta value
ATP1B1 expression (log2(count+1))
ATP1B1 copy number (log2(copy number/2))
ATP1B1 ~ ENSG00000143153.11
Pearson's rho
r = 0.3214 (p = 0.00001293)
Spearman's rank rho
rho = 0.3058 (p = 0.00003491)
somatic mutation (SNPs and small INDELs)
TCGA-IB-7651-01A
synonymous_variant, ATP1A4 (p.I180I)
hg38 chr1:160,159,016 T to C
DNA variant allele freq: 16%
TCGA-IB-7651-01A
missense_variant, ATP1A4 (p.I500T)
hg38 chr1:160,171,258 T to C
DNA variant allele freq: 24%
TCGA-IB-7651-01A
missense_variant, ATP1A4 (p.L995F)
hg38 chr1:160,186,289 C to T
DNA variant allele freq: 16%

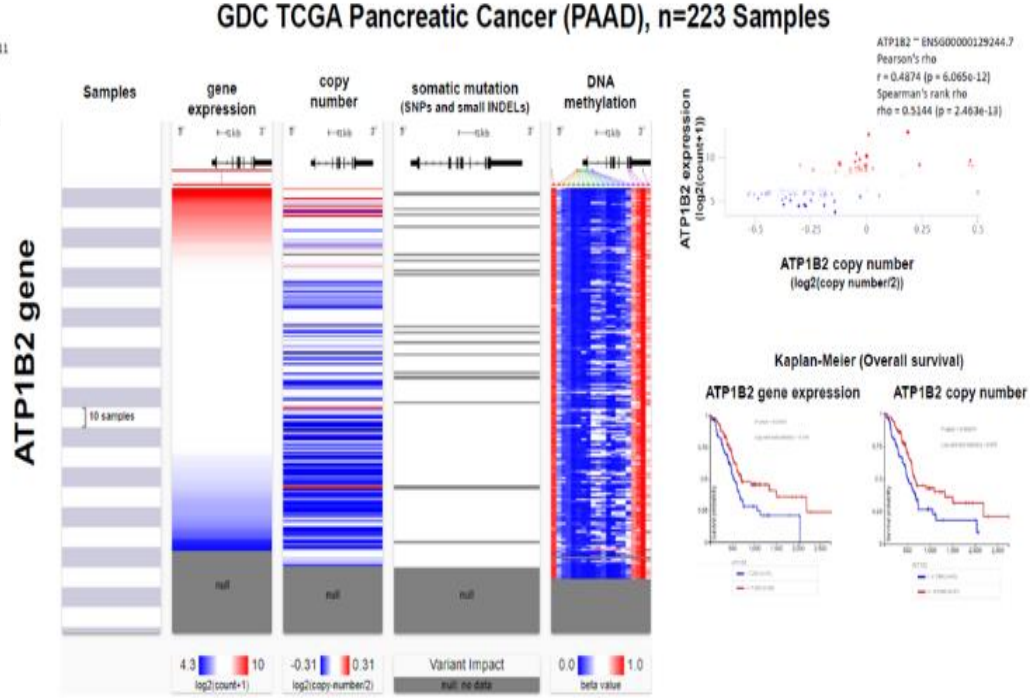
GDC TCGA Pancreatic Cancer (PAAD), n=223 Samples
ATP1B2 gene
Samples
gene expression
copy number
somatic mutation (SNPs and small INDELs)
DNA methylation
10 samples
null
4.3 10
log2(count+1)
-0.31 0.31
log2(copy-number/2)
Variant Impact
null: no data
0.0 1.0
beta value
ATP1B2 expression (log2(count+1))
ATP1B2 copy number (log2(copy number/2))
ATP1B2 ~ ENSG00000129244.7
Pearson's rho
r = 0.4874 (p = 6.065e-12)
Spearman's rank rho
rho = 0.5144 (p = 2.463e-13)
Kaplan-Meier (Overall survival)
ATP1B2 gene expression
ATP1B2 copy number

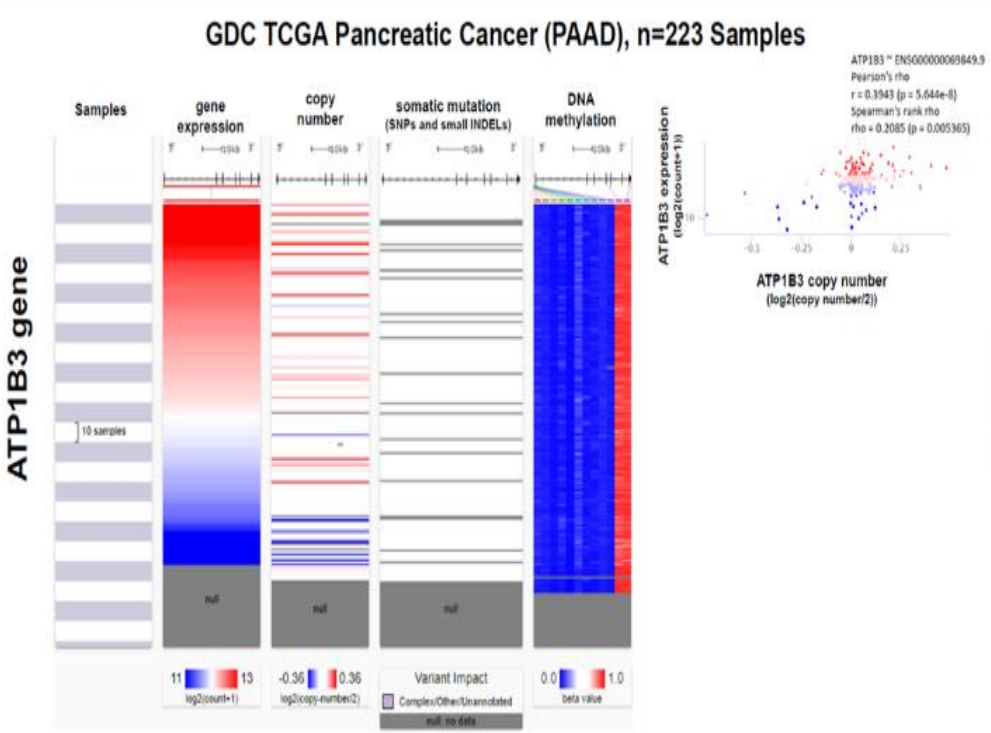
GDC TCGA Pancreatic Cancer (PAAD), n=223 Samples
ATP1B3 gene
Samples
gene expression
copy number
somatic mutation (SNPs and small INDELs)
DNA methylation
10 samples
null
11 13
log2(count+1)
-0.36 0.36
log2(copy-number/2)
Variant Impact
Complex/Other/Unannotated
null: no data
0.0 1.0
beta value
ATP1B3 expression (log2(count+1))
ATP1B3 copy number (log2(copy number/2))
ATP1B3 ~ ENSG00000069849.9
Pearson's rho
r = 0.3943 (p = 5.644e-8)
Spearman's rank rho
rho = 0.2085 (p = 0.005365)

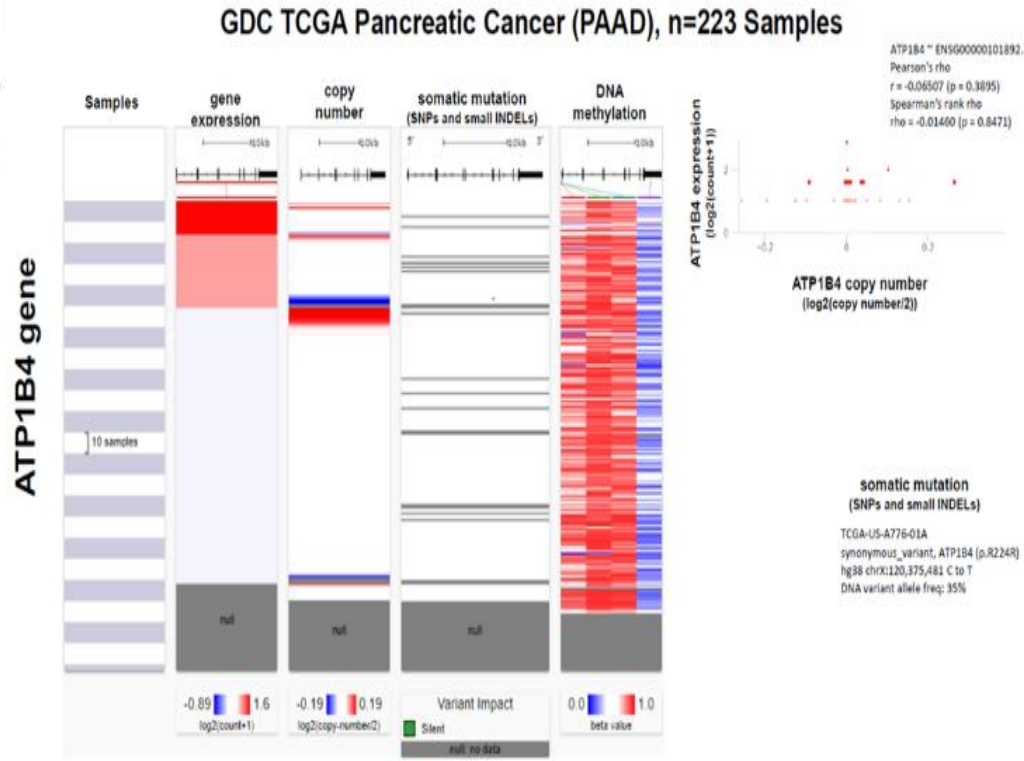
GDC TCGA Pancreatic Cancer (PAAD), n=223 Samples
ATP1B4 gene
Samples
gene expression
copy number
somatic mutation (SNPs and small INDELs)
DNA methylation
10 samples
null
-0.89 1.6
log2(count+1)
-0.19 0.19
log2(copy-number/2)
Variant Impact
Silent
null: no data
0.0 1.0
beta value
ATP1B4 expression (log2(count+1))
ATP1B4 copy number (log2(copy number/2))
ATP1B4 ~ ENSG00000101892.
Pearson's rho
r = -0.06507 (p = 0.3895)
Spearman's rank rho
rho = -0.01460 (p = 0.8471)
somatic mutation (SNPs and small INDELs)
TCGA-US-A776-01A
synonymous_variant, ATP1B4 (p.R224R)
hg38 chrX:120,375,481 C to T
DNA variant allele freq: 35%

Figure 14. NKA subunit expression across different cancer types, together with Kaplan-Mayer survival plots of NKA pump subunits in pancreatic cancer.

To determine the levels of SERCA, A1, A2 and A3 in breast cancer cells, we examined the expression profiles of MCF-7, MDA 231 and T47D and compared them to a non-transformed mammary breast cell line MCF-10A. As observed in Figure 15, SERCA-A1 expression was significantly enhanced in MCF10A compared to MDA and T47D. SERCA-A2 was significantly enhanced in MCF-7, T47D and MDA231. Whilst, SERCA-A3 was reduced in MCF-7 and T47D. These results suggested differential expression of SERCA –A1-3 in various breast cancer cell line subtypes. In addition, The involvement of SERCA subunits in new defined pathways was also investigated using KEGG pathway analysis (bioinformatics tool)/ Appendix I.

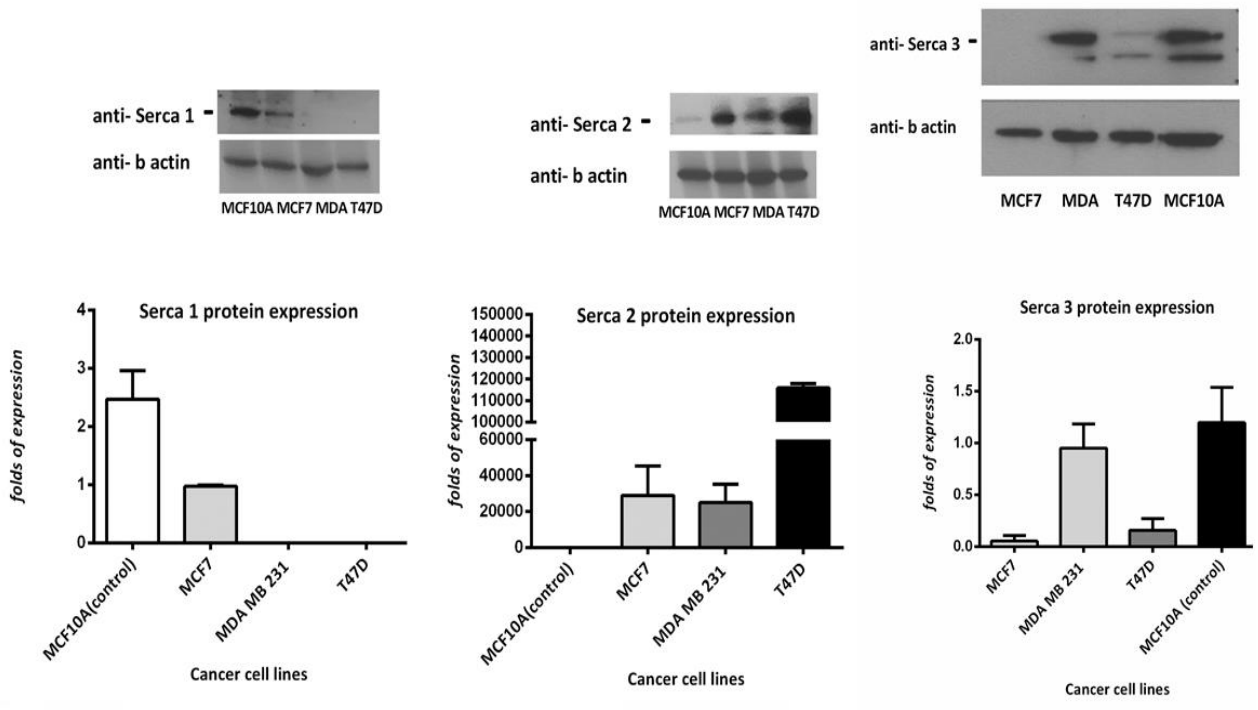

Figure 15. SERCA subunit expression across different breast cancer types.

Discussion

P-type ATPases are ion pumps belonging to a superfamily of membrane proteins that catalyze the selective active transport of different ions across biological membranes of organelles or at the plasma membrane [204,205]. Some of the most important and best studied P-type ATPase is are the NKA, SERCA pump, and the Vacuolar-H+-ATPase. Pharmacological inhibition of P-type ATPase's has been shown successful for the treatment of some pathophysiological conditions, including cancers, and are thereby attractive drug targets [204,206]

This study, addressed the mechanism of cytotoxicity of GLE and its active ingredient *annonacin* were evaluated. The data supports that *annonacin* is a potent inhibitor of the NKA. The PCA analysis showed that they were placed in-between the alkylating agents (AA) and CSs; thus confirming the reported and the new target found herein. On the other hand, the natural products from the *Annonaceae* family of plants (*annonaceous acetogenins*), are potent inhibitors of the NADH-ubiquinone reductase (complex I) activity of mammalian mitochondria[207].

Biochemical analysis showed GLE annonacin as a direct inhibitor of NKA. Nevertheless, the reported effect of partial charge distribution, and hence the long-range electrostatic interactions with Mg^{2+} observed with the carbonyl group of the lactone present in ouabain and site II[208] may be absent in the annonacin molecule presented herein. This is due to the predicted positioning of this moiety in the binding site (facing the extracellular face of NKA), which may account for the strong decrease in the inhibitory activity compared to CSs, as shown in the biochemical experiments, CSs inhibit NKA in low nanomolar range [209]. Thus, an inverted positioning of the lactone moiety of *annonacin* in the binding site (lactone facing sites I and II) would prevent the pivotal hydrogen bond with Thr797, explaining the predicted binding mode. Structural analysis of amino acid residues in the transmembrane hairpin M5-M6 of NKA have

identified Phe783 and Thr797 as determinant residues for ouabain sensitivity, thereby interactions with them play key roles in the inhibition of this ion pump, as also predicted for *annonacin* in the docking experiments (Figure 11).

The endoplasmic reticulum (ER) and calcium signaling contribute to the regulation of normal and pathological signaling that is controlled by a family of protein channel enzymes that include the sarco/endoplasmic reticulum calcium ATPase pumps (SERCAs). There are 14 different SERCA isoforms that are encoded by 3 ATP2A1-3 genes[210]. A number of studies have reported that altered expressions of SERCA isoforms are associated with cancers. Similarly, sodium/potassium ATPase pumps (NKA) that regulate the levels of sodium and potassium within cells also play a role in signaling and their activity is also altered in several pathological disorders including cancer.

In silico studies have identified for the first time *annonacin,* as a possible strong inhibitor for both NKA and SERCA pumps. We validated our *in silico* findings and proved that Graviola is able to inhibit both NKA and SERCA activity. It has been reported that *annonacins* are also potent inhibitors of the NADH-ubiquinone reductase (complex I) activity of mammalian mitochondria. Thapsigargin, a known SERCA inhibitor, disrupts Ca^{2+} homeostasis, and causes cell death in cancer cells, supporting further evidence that inhibiting SERCA activity promotes cell death[211]. Expression of different SERCA isoforms have been reported in various cancers and our bio-profiling studies show a strong correlation between high SERCA isoform expression and reduced cancer patient survival. Moreover, our in vivo xenograft pancreatic model corroborate and suggest that also reduces the growth rate of cancer which in return means that the active agent annonacin is a strong and promising candidate against cancer by acting partly on reducing SERCA activity[37].

Ouabain, a NKA inhibitor has previously been used for the treatment of atrial fibrillation and heart failure[212]. Its potential anticancer effect has also attracted great interest and it was recently shown to induce cell death in renal cancer cells. In the same study, the expression of NKA α3, but not the α1 isoform was associated with ouabain sensitivity, suggesting that isoform specificity and activity may be associated with cellular proliferation and cancer propagation[111]. Such study also substantiates our bio-profiling analysis showing strong correlation between high NKA isoform expression and reduced human kidney cancer survival. Taken together, these results suggest that GLE annonacin acts via a novel signaling pathway involving both NKA and SERCA to sensitize cell death in cancer cells without affecting normal cells that may also be dependent on the expression and specificity of NKA and SERCA isorforms in cancer[37].

Computational analysis and docking data corroborated the similarity of *annonacin* with the CSs by showing a similar binding mode in the high affinity CSs binding site, which is constituted by the transmembrane helices αM1-6 of the catalytic α-subunit forming the extracellular ion exchange pathway. The lactone of CSs is one of the most important features of these compounds, which is also present in muricins. Nevertheless, the reported effect of partial charge distribution and hence the long-range electrostatic interactions with Mg^{2+}, observed with the carbonyl group of the lactone present in ouabain and site II may be absent in the compound presented herein. This may be due to the predicted positioning of this moiety in the binding site (facing the extracellular face of NKA), which may account for the strong decrease in the inhibitory activity compared to CSs, as shown in the biochemical experiments. CSs inhibit NKA in low nanomolar range. Thus, an inverted positioning of the lactone moiety of *annonacin* in the binding site (lactone facing sites II and I) would prevent the pivotal hydrogen bond with Thr797, explaining the predicted binding mode. Structural analysis of amino acid residues in the

transmembrane hairpin M5-M6 of NKA have identified Phe783 and Thr797 as determinant residues for ouabain sensitivity, thereby interactions with them play key roles in the inhibition of this ion pump, as also predicted for *annonacin* in the present docking experiments.

Moreover, the *in vitro* data additionally show that the cell death inducing-effects of annonacin may be partly mediated via an apoptotic pathway as indicated by the increase expression of both active caspase-9 and caspase-3[53]. The inhibition of SERCA pump by Graviola may provoke mitochondrial activity and induce generation of mitochondrial ROS and trigger cytochrome C- caspase-9 –caspase-3 intrinsic pathways. However, we cannot rule out other cell death pathways that may be mediated by GLE annonacin such as necroptosis and autophagic-induced cell death. The NKA inhibitor, ouabain has been shown to induce apoptosis and autophagy in Burkit lymphoma and lung cancer cells. Similarly, SERCA inhibitors have also been reported to induce both apoptosis and autophagic cell death[213]. Despite the differences in cell death pathways, it has been suggested that apoptosis, necroptosis and autophagy may be intimately connected and modulated by similar regulators. Further work is required to determine whether GLE annonacin can possibly act by mediating multiple cell death pathways. This study has highlighted and identified a novel pathway mediated by GLE annonacin as an inhibitor of both NKA and SERCA pumps. We propose that GLE annonacin could be targeting NKA and SERCA activity in cancer sensitizing them to cell death and therefore be a novel promising approach towards treating cancer.

Concluding remarks and future studies

Evidence suggests that abnormal ion homeostasis may result in unwanted pathophysiological mechanisms leading to a number of disorders, including cancer, while on the

contrary manipulation of ion pumps can aid in treating cancer. Consequently, the functional roles of NKA, SERCA reviewed for their potential role as biomarkers and their mode of action in cancer genesis and progression. Managing these pumps proved effective against cellular proliferation and angiogenesis in various cancer types, primarily by selectively inducing apoptosis of cancer cells. Manipulating pumps also reinstates ion homeostasis intracellularly, which favors the action of anticancer drugs.

NKA α1 is abundant in the body and expresses a lower affinity to drugs than the α2 and α3 subunits [214]. Anti-cancer drugs need to be tissue-type specific and subunit-selective to have maximum possible effect. Despite the infrequent presence of FXYD as an element of NKA, its effectiveness on α and β subunits is noteworthy, however further studies are required to understand its relationship to cancer.

Gene expression profiling and gene analysis of NKA and SERCA, indicated altered expression levels and presence of mutations of various P-class pumps isoforms in cancer samples, compared to healthy cells. Through bioinformatics, both NKA and SERCA expression in liver cells are characteristic and yet, no studies were found to date evaluating their clinical outcome. Also ATP2A1 is significantly downregulated in head and neck squamous cell carcinoma, whereas ATP1B3 is significantly upregulated in the same cancer cells. Whether either of these findings are significant is still unknown but it is important to understand that expression either may be over- or under- expressed in pathological conditions. Recognizing specific mutated loci present only in cancer cells is crucial, as their reversal may be therapeutic. Silencing genes of each subunit separately may also help to understand the exact effect they express on healthy cells.

P-type pump expression is altered in tumor cells, triggering several modifications on cellular pathways, involved in cell cycle, apoptosis, angiogenesis and metastasis; activation of MAPK, Caspase 3, ERK phosphorylation, downregulation/inhibition of IL-8, TNF- α/NF- κB,f and Bcl-2

[100,101,215,216,216–219]. Already existing p-pump drugs have a primary function involved in other disorders were further evaluation may determine the exact cellular pathways p-class pumps affect and hence determine whether they can potentially contribute to novel cancer treatment [124,220]. Additionally, according to the U.S National Library of Medicine (https://clinicaltrials.gov/ct2/home), no clinical trials are currently running, evaluating the effects of drugs that have shown anticancer effects *in vivo*, such as ouabain (NKA) and artemisinin (SERCA).

Of note, reference to toxicity was scarce throughout the literature, as the majority of reported studies were performed *in vitro*. Despite the aforementioned effectiveness of PPIs, it is crucial to consider drug toxicity to determine possible effects of short and long-term administration of PPIs as, despite being inconclusive, there have been reports of development of gastric cancer after long-term PPI treatment [221–223].

In overall, manipulation of P–class ion pumps expresses anticancer effects, with the potential to act as additive treatment, by altering the internal environment where chemotherapeutic drugs can perform. Environmental alterations however can also affect alternative chemical pathways, setting off a cascade of events that can result in apoptosis of cancer cells and inhibit proliferation and migration.

In addition, two new inhibitors are placed in the list, where annonacin is a considered a strong NKA and SERCA inhibitor and TWHFE as a selective NKA, were both are considered strong anti-cancer agents.

Further studies needed to elucidate the safety and clinical impact of the above findings as well as identify key isoforms/subunits responsible for targeting proliferation, migration and survival. Finally, the involvement of P-class pumps in other diseases could be a new area of investigation i.e. Alzheimer's and diabetes.

References

1. Cooper, G. M. The Development and Causes of Cancer. *The Cell: A Molecular Approach. 2nd edition* (2000).
2. Comprehensive Cancer Information. *National Cancer Institute* https://www.cancer.gov/ (1980).
3. NCI Dictionary of Cancer Terms. *National Cancer Institute* https://www.cancer.gov/publications/dictionaries/cancer-terms (2011).
4. Tumor Grade Fact Sheet. *National Cancer Institute* https://www.cancer.gov/about-cancer/diagnosis-staging/prognosis/tumor-grade-fact-sheet (2013).
5. Worldwide cancer data. *World Cancer Research Fund* https://www.wcrf.org/dietandcancer/cancer-trends/worldwide-cancer-data (2018).
6. Drug repurposing: progress, challenges and recommendations | Nature Reviews Drug Discovery. https://www.nature.com/articles/nrd.2018.168.
7. Xue, H., Li, J., Xie, H. & Wang, Y. Review of Drug Repositioning Approaches and Resources. *Int J Biol Sci* **14**, 1232–1244 (2018).
8. Corsello, S. M. *et al.* The Drug Repurposing Hub: a next-generation drug library and information resource. *Nat Med* **23**, 405–408 (2017).
9. Olgen, S. & Kotra, L. Drug Repurposing in the Development of Anticancer Agents. *Curr. Med. Chem.* (2018) doi:10.2174/0929867325666180713155702.
10. Tiriveedhi, V. Impact of Precision Medicine on Drug Repositioning and Pricing: A Too Small to Thrive Crisis. *J Pers Med* **8**, (2018).
11. Drug Repositioning - an overview | ScienceDirect Topics. https://www.sciencedirect.com/topics/nursing-and-health-professions/drug-repositioning.
12. Mullard, A. Low-cost non-profit drug repurposing. *Nature Reviews Drug Discovery* **18**, 7 (2018).

13. Herranz-López, M., Losada-Echeberría, M. & Barrajón-Catalán, E. The Multitarget Activity of Natural Extracts on Cancer: Synergy and Xenohormesis. *Medicines (Basel)* **6**, (2018).

14. Howitz, K. T. & Sinclair, D. A. Xenohormesis: Sensing the Chemical Cues of Other Species. *Cell* **133**, 387–391 (2008).

15. Xenohormetic and anti-aging activity of secoiridoid polyphenols present in extra virgin olive oil: A new family of gerosuppressant agents: Cell Cycle: Vol 12, No 4. https://www.tandfonline.com/doi/full/10.4161/cc.23756.

16. Ruiz-Torres, V. *et al.* An Updated Review on Marine Anticancer Compounds: The Use of Virtual Screening for the Discovery of Small-Molecule Cancer Drugs. *Molecules* **22**, 1037 (2017).

17. Grochowski, D. M. *et al.* A comprehensive review of agrimoniin. *Annals of the New York Academy of Sciences* **1401**, 166–180 (2017).

18. A Review on the Dietary Flavonoid Tiliroside - Grochowski - 2018 - Comprehensive Reviews in Food Science and Food Safety - Wiley Online Library. https://onlinelibrary.wiley.com/doi/full/10.1111/1541-4337.12389.

19. Barrajon, E. *Natural Compounds as New Cancer Treatments*. (MDPI, 2019).

20. In Silico Approaches for Drug Discovery and Development | Bentham Science. https://www.eurekaselect.com/150353/chapter/in-silico-approaches-for-drug-discovery-and-developmen.

21. In Silico Approaches for Drug Discovery and Development. *http://www.eurekaselect.com* http://www.eurekaselect.com/150353/chapter.

22. Ignacimuthu, S., Ayyanar, M. & Sivaraman K, S. Ethnobotanical investigations among tribes in Madurai District of Tamil Nadu (India). *J Ethnobiol Ethnomed* **2**, 25 (2006).

23. Prakash, O., Kumar, A., Kumar, P. & Ajeet, A. Anticancer Potential of Plants and Natural Products: A Review. *AJPS* **1**, 104–115 (2013).

24. Ioannis, P., Anastasis, S. & Andreas, Y. Graviola: A Systematic Review on Its Anticancer Properties. *American Journal of Cancer Prevention* **3**, 128–131 (2016).

25. Dai, Y. *et al.* Selective growth inhibition of human breast cancer cells by graviola fruit extract in vitro and in vivo involving downregulation of EGFR expression. *Nutr Cancer* **63**, 795–801 (2011).

26. Torres, M. P. *et al.* Graviola: a novel promising natural-derived drug that inhibits tumorigenicity and metastasis of pancreatic cancer cells in vitro and in vivo through altering cell metabolism. *Cancer Lett.* **323**, 29–40 (2012).

27. Rady, I. *et al.* Anticancer Properties of Graviola (Annona muricata): A Comprehensive Mechanistic Review. *Oxid Med Cell Longev* **2018**, (2018).

28. Graviola (soursop) | Complementary and alternative therapy | Cancer Research UK. https://www.cancerresearchuk.org/about-cancer/cancer-in-general/treatment/complementary-alternative-therapies/individual-therapies/graviola.

29. UPLC–QTOF–MS and NMR analyses of graviola (Annona muricata) leaves. http://www.scielo.br/scielo.php?script=sci_arttext&pid=S0102-695X2016000200174.

30. Qazi, A. K. *et al.* Emerging therapeutic potential of graviola and its constituents in cancers. *Carcinogenesis* **39**, 522–533 (2018).

31. Paul, J., Gnanam, R., Jayadeepa, R. M. & Arul, L. Anti cancer activity on Graviola, an exciting medicinal plant extract vs various cancer cell lines and a detailed computational study on its potent anti-cancerous leads. *Curr Top Med Chem* **13**, 1666–1673 (2013).

32. Moghadamtousi, S. Z. *et al.* Annona muricata (Annonaceae): A Review of Its Traditional Uses, Isolated Acetogenins and Biological Activities. *Int J Mol Sci* **16**, 15625–15658 (2015).

33. Abd El-Kareem, S. A. Biochemical and biophysical study of chemopreventive and chemotherapeutic anti-tumor potential of some Egyptian plant extracts. *Biochem Biophys Rep* **18**, (2019).

34. Yajid, A. I., Ab Rahman, H. S., Wong, M. P. K. & Wan Zain, W. Z. Potential Benefits of Annona muricata in Combating Cancer: A Review. *Malays J Med Sci* **25**, 5–15 (2018).

35. Zeweil, M. M., Sadek, K. M., Taha, N. M., El-Sayed, Y. & Menshawy, S. Graviola attenuates DMBA-induced breast cancer possibly through augmenting apoptosis and antioxidant pathway and downregulating estrogen receptors. *Environ Sci Pollut Res* **26**, 15209–15217 (2019).

36. Deep, G. *et al.* Graviola inhibits hypoxia-induced NADPH oxidase activity in prostate cancer cells reducing their proliferation and clonogenicity. *Sci Rep* **6**, (2016).

37. Yiallouris, A. *et al.* Annonacin promotes selective cancer cell death via NKA-dependent and SERCA-dependent pathways. *Cell Death Dis* **9**, 764 (2018).

38. Agu, K. C. & Okolie, P. N. Proximate composition, phytochemical analysis, and in vitro antioxidant potentials of extracts of Annona muricata (Soursop). *Food Sci Nutr* **5**, 1029–1036 (2017).

39. Frontiers | Exploring the Leaves of Annona muricata L. as a Source of Potential Anti-inflammatory and Anticancer Agents | Pharmacology. https://www.frontiersin.org/articles/10.3389/fphar.2018.00661/full.

40. Yang, C. *et al.* Synergistic interactions among flavonoids and acetogenins in Graviola (Annona muricata) leaves confer protection against prostate cancer. *Carcinogenesis* **36**, 656–665 (2015).

41. Ishola, I. O., Awodele, O., Olusayero, A. M. & Ochieng, C. O. Mechanisms of Analgesic and Anti-Inflammatory Properties of Annona muricata Linn. (Annonaceae) Fruit Extract in Rodents. *J Med Food* **17**, 1375–1382 (2014).

42. Alali, F. Q., Liu, X. X. & McLaughlin, J. L. Annonaceous acetogenins: recent progress. *J. Nat. Prod.* **62**, 504–540 (1999).

43. Chang, F. R. & Wu, Y. C. Novel cytotoxic annonaceous acetogenins from Annona muricata. *J. Nat. Prod.* **64**, 925–931 (2001).

44. Wu, F. E. *et al.* Two new cytotoxic monotetrahydrofuran Annonaceous acetogenins, annomuricins A and B, from the leaves of Annona muricata. *J. Nat. Prod.* **58**, 830–836 (1995).

45. Ko, Y.-M. *et al.* Annonacin induces cell cycle-dependent growth arrest and apoptosis in estrogen receptor-α-related pathways in MCF-7 cells. *J Ethnopharmacol* **137**, 1283–1290 (2011).

46. Pieme, C. A. *et al.* Antiproliferative activity and induction of apoptosis by Annona muricata (Annonaceae) extract on human cancer cells. *BMC Complement Altern Med* **14**, 516 (2014).

47. Kumar, M., Kaur, V., Kumar, S. & Kaur, S. Phytoconstituents as apoptosis inducing agents: strategy to combat cancer. *Cytotechnology* **68**, 531–563 (2016).

48. Coller, H. A. & Desai, A. Cell cycle, cell division, and cell death. *Mol Biol Cell* **28**, 693–694 (2017).

49. Cell death by mitotic catastrophe: a molecular definition | Oncogene. https://www.nature.com/articles/1207528.

50. Cell Death - an overview | ScienceDirect Topics. https://www.sciencedirect.com/topics/neuroscience/cell-death.

51. Galluzzi, L. *et al.* Molecular mechanisms of cell death: recommendations of the Nomenclature Committee on Cell Death 2018. *Cell Death & Differentiation* **25**, 486–541 (2018).

52. Wu, J. Apoptosis and angiogenesis: two promising tumor markers in breast cancer (review). *Anticancer Res.* **16**, 2233–2239 (1996).

53. Elmore, S. Apoptosis: A Review of Programmed Cell Death. *Toxicol Pathol* **35**, 495–516 (2007).

54. Alberts, B. *et al.* Programmed Cell Death (Apoptosis). *Molecular Biology of the Cell. 4th edition* (2002).

55. BCL-2 family isoforms in apoptosis and cancer | Cell Death & Disease. https://www.nature.com/articles/s41419-019-1407-6.

56. Porter, A. G. & Jänicke, R. U. Emerging roles of caspase-3 in apoptosis. *Cell Death Differ* **6**, 99–104 (1999).

57. Fulda, S. & Debatin, K.-M. Extrinsic versus intrinsic apoptosis pathways in anticancer chemotherapy. *Oncogene* **25**, 4798–4811 (2006).

58. Glick, D., Barth, S. & Macleod, K. F. Autophagy: cellular and molecular mechanisms. *J Pathol* **221**, 3–12 (2010).

59. Autophagy: process and function. http://genesdev.cshlp.org/content/21/22/2861.full.html.

60. Li, W., Li, J. & Bao, J. Microautophagy: lesser-known self-eating. *Cell. Mol. Life Sci.* **69**, 1125–1136 (2012).

61. Tanida, I. Autophagosome formation and molecular mechanism of autophagy. *Antioxid. Redox Signal.* **14**, 2201–2214 (2011).

62. Necrosis as Programmed Cell Death | IntechOpen. https://www.intechopen.com/books/cell-death-autophagy-apoptosis-and-necrosis/necrosis-as-programmed-cell-death.

63. Necrosis - an overview | ScienceDirect Topics. https://www.sciencedirect.com/topics/neuroscience/necrosis.

64. Necroptosis - Latest research and news | Nature. https://www.nature.com/subjects/necroptosis.

65. Choi, M. E., Price, D. R., Ryter, S. W. & Choi, A. M. K. Necroptosis: a crucial pathogenic mediator of human disease. *JCI Insight* **4**,.

66. RIP1/RIP3-regulated necroptosis as a target for multifaceted disease therapy (Review). https://www.spandidos-publications.com/10.3892/ijmm.2019.4244.

67. Mou, Y. *et al.* Ferroptosis, a new form of cell death: opportunities and challenges in cancer. *J Hematol Oncol* **12**, (2019).

68. Lei, P., Bai, T. & Sun, Y. Mechanisms of Ferroptosis and Relations With Regulated Cell Death: A Review. *Front. Physiol.* **10**, (2019).

69. The Hallmarks of Ferroptosis | Annual Review of Cancer Biology. https://www.annualreviews.org/doi/abs/10.1146/annurev-cancerbio-030518-055844.

70. Miao, E. A., Rajan, J. V. & Aderem, A. Caspase-1-induced pyroptotic cell death. *Immunol. Rev.* **243**, 206–214 (2011).

71. Pyroptosis - an overview | ScienceDirect Topics. https://www.sciencedirect.com/topics/medicine-and-dentistry/pyroptosis.

72. Montell, D. Anastasis, a new mechanism driving cell survival and evolution.

73. Cell Survival by Anastasis | Denise Montell Lab | UC Santa Barbara. https://labs.mcdb.ucsb.edu/montell/denise/research/cell-survival-anastasis.

74. Pedersen, P. L. Transport ATPases into the year 2008: a brief overview related to types, structures, functions and roles in health and disease. *J. Bioenerg. Biomembr.* **39**, 349–355 (2007).

75. Apell, H.-J. Structure-function relationship in P-type ATPases--a biophysical approach. *Rev. Physiol. Biochem. Pharmacol.* **150**, 1–35 (2003).

76. Palmgren, M. G. & Axelsen, K. B. Evolution of P-type ATPases. *Biochim. Biophys. Acta* **1365**, 37–45 (1998).

77. Gu, M. *et al.* Rabeprazole exhibits antiproliferative effects on human gastric cancer cell lines. *Oncol Lett* **8**, 1739–1744 (2014).

78. De Milito, A. & Fais, S. Tumor acidity, chemoresistance and proton pump inhibitors. *Future Oncol* **1**, 779–786 (2005).

79. Forrest, M. D. The sodium-potassium pump is an information processing element in brain computation. *Frontiers in Physiology* **5**, (2014).

80. Castillo, J. P. *et al.* Mechanism of potassium ion uptake by the Na+/K+-ATPase. *Nature Communications* **6**, (2015).

81. Yiallouris, A., Stephanou, A. & Patrikios, I. Anticancer properties of Na<sup>+/K<sup>+-ATPase: a mini review. *Asian Journal of Science and Technology* **7**, 2864–2868 (2016).

82. Li, Z. *et al.* Na/K-ATPase Mimetic pNaKtide Peptide Inhibits the Growth of Human Cancer Cells. *J Biol Chem* **286**, 32394–32403 (2011).

83. Sweadner, K. J. Isozymes of the Na<sup>+/K<sup>+-ATPase. *Biochimica Et Biophysica Acta* **988**, 185–220 (1989).

84. Lingrel, J. B. & Kuntzweiler, T. Na+,K(+)-ATPase. *J. Biol. Chem.* **269**, 19659–19662 (1994).

85. Kaplan, J. H. Biochemistry of Na,K-ATPase. *Annual Review of Biochemistry* **71**, 511–535 (2002).

86. Martin-Vasallo, P., Dackowski, W., Emanuel, J. R. & Levenson, R. Identification of a putative isoform of the Na,K-ATPase beta subunit. Primary structure and tissue-specific expression. *J. Biol. Chem.* **264**, 4613–4618 (1989).

87. Shyjan, A. W., Gottardi, C. & Levenson, R. The Na, K-ATPase beta 2 subunit is expressed in rat brain and copurifies with Na, K-ATPase activity. *Journal of Biological Chemistry* **265**, 5166–5169 (1990).

88. Sundaram, S. M. *et al.* Differential expression patterns of sodium potassium ATPase alpha and beta subunit isoforms in mouse brain during postnatal development. *Neurochem. Int.* **128**, 163–174 (2019).

89. Malik, N., Canfield, V. A., Beckers, M.-C., Gros, P. & Levenson, R. Identification of the Mammalian Na,K-ATPase β3 Subunit. *J Biol Chem* **271**, 22754–22758 (1996).

90. Good, P. J., Richter, K. & Dawid, I. B. A Nervous System-Specific Isotype of the |beta Subunit of Na<sup>+ ,K<sup>+ - ATPase Expressed During Early Development of Xenopus Laevis. *Proc Natl Acad Sci USA* **87**, 9088–9092 (1990).

91. Rajasekaran, S. A. *et al.* Na,K-ATPase Subunits as Markers for Epithelial-Mesenchymal Transition in Cancer and Fibrosis. *Molecular Cancer Therapeutics* **9**, 1515–1524 (2010).

92. Arcangeli, A. *et al.* Targeting ion channels in cancer: a novel frontier in antineoplastic therapy. *Curr. Med. Chem.* **16**, 66–93 (2009).

93. Baker Bechmann, M. *et al.* Na,K-ATPase Isozymes in Colorectal Cancer and Liver Metastases. *Frontiers in Physiology* **7**, (2016).

94. Chandrashekar, D. S. *et al.* UALCAN: A Portal for Facilitating Tumor Subgroup Gene Expression and Survival Analyses. *Neoplasia* **19**, 649–658 (2017).

95. Mobasheri, A. *et al.* Epithelial Na, K-ATPase expression is down-regulated in canine prostate cancer; a possible consequence of metabolic transformation in the process of prostate malignancy. *Cancer Cell Int.* **3**, 8 (2003).

96. Yang, P. *et al.* Cellular Location and Expression of Na+,K+-ATPase Subunits Affect the Anti-Proliferative Activity of Oleandrin. *Molecular Carcinogenesis 53:253-263 (2014)* 253–263 (2014) doi:DOI 10.1002/mc.21968.

97. McConkey, D. J., Lin, Y., Nutt, L. K., Ozel, H. Z. & Newman, R. A. Cardiac Glycosides Stimulate Ca2⁺ Increases and Apoptosis in Androgen- independent, Metastatic Human Prostate Adenocarcinoma Cells. 7.

98. Newman, R. A. *et al.* Autophagic Cell Death of Human Pancreatic Tumor Cells Mediated by Oleandrin, a Lipid-Soluble Cardiac Glycoside. *Integr Cancer Ther* **6**, 354–364 (2007).

99. Li, Z. *et al.* Na/K-ATPase Mimetic pNaKtide Peptide Inhibits the Growth of Human Cancer Cells. *J. Biol. Chem.* **286**, 32394–32403 (2011).

100. Garcia, D. G. *et al.* Na/K-ATPase as a target for anticancer drugs: studies with perillyl alcohol. *Mol Cancer* **14**, 105 (2015).

101. Alevizopoulos, K. *et al.* Functional characterization and anti-cancer action of the clinical phase II cardiac Na^+/K^+ ATPase inhibitor istaroxime: *in vitro* and *in vivo* properties and cross talk with the membrane androgen receptor. *Oncotarget* **7**, (2016).

102. Meng. Na+/K+-ATPase α3 mediates sensitivity of hepatocellular carcinoma cells to bufalin. *Oncol Rep* **25**, (2011).

103. Numazawa, S., Shinoki, M.-A., Ito, H., Yoshida, T. & Kuroiwa, Y. Involvement of Na+, K+-ATPase inhibition in K562 cell differentiation induced by bufalin. *J. Cell. Physiol.* **160**, 113–120 (1994).

104. Sun, X. *et al.* Bufalin, a Traditional Chinese Medicine Compound, Prevents Tumor Formation in Two Murine Models of Colorectal Cancer. *Cancer Prev Res* **12**, 653–666 (2019).

105. Yu, C.-H., Kan, S.-F., Pu, H.-F., Jea Chien, E. & Wang, P. S. Apoptotic signaling in bufalin- and cinobufagin-treated androgen-dependent and -independent human prostate cancer cells. *Cancer Science* **99**, 2467–2476 (2008).

106. Ihenetu, K., Qazzaz, H. M., Crespo, F., Fernandez-Botran, R. & Valdes, R. Digoxin-Like Immunoreactive Factors Induce Apoptosis in Human Acute T-Cell Lymphoblastic Leukemia. *Clinical Chemistry* **53**, 1315–1322 (2007).

107. Prassas, I. *et al.* Digitoxin-Induced Cytotoxicity in Cancer Cells Is Mediated through Distinct Kinase and Interferon Signaling Networks. *Molecular Cancer Therapeutics* **10**, 2083–2093 (2011).

108. Hsu, I.-L. *et al.* Targeting FXYD2 by cardiac glycosides potently blocks tumor growth in ovarian clear cell carcinoma. *Oncotarget* **7**, (2016).

109. Kang, M. A. *et al.* Lanatoside C suppressed colorectal cancer cell growth by inducing mitochondrial dysfunction and increased radiation sensitivity by impairing DNA damage repair. *Oncotarget* **7**, (2016).

110. Liu, N. *et al.* Inhibition of cell migration by ouabain in the A549 human lung cancer cell line. *Oncology Letters* **6**, 475–479 (2013).

111. Huang, Y.-T., Chueh, S.-C., Teng, C.-M. & Guh, J.-H. Investigation of ouabain-induced anticancer effect in human androgen-independent prostate cancer PC-3 cells. *Biochemical Pharmacology 67 (2004) 727–733* **67**, 727–733 (2004).

112. Ono, Y. *et al.* Glycoprotein nonmetastatic melanoma protein B (GPNMB) promotes the progression of brain glioblastoma via Na+/K+-ATPase. *Biochemical and Biophysical Research Communications* **481**, 7–12 (2016).

113. Li, S. *et al.* Targeting β2 subunit of Na+/K+-ATPase induces glioblastoma cell apoptosis through elevation of intracellular Ca2+. 19.

114. Rocha, S. C. *et al.* 21-Benzylidene Digoxin: A Proapoptotic Cardenolide of Cancer Cells That Up-Regulates Na,K-ATPase and Epithelial Tight Junctions. *PLoS ONE* **9**, e108776 (2014).

115. Denmeade, S. R. & Isaacs, J. T. The SERCA pump as a therapeutic target: Making a "smart bomb" for prostate cancer. *Cancer Biology & Therapy* **4**, 21–29 (2005).

116. Mahalingam, D. *et al.* Mipsagargin, a novel thapsigargin-based PSMA-activated prodrug: results of a first-in-man phase I clinical trial in patients with refractory, advanced or metastatic solid tumours. *Br J Cancer* **114**, 986–994 (2016).

117. Fan, L. *et al.* Novel role of Sarco/endoplasmic reticulum calcium ATPase 2 in development of colorectal cancer and its regulation by F36, a curcumin analog. *Biomedicine & Pharmacotherapy* **68**, 1141–1148 (2014).

118. Denmeade, S. R. *et al.* Prostate-Specific Antigen-Activated Thapsigargin Prodrug as Targeted Therapy for Prostate Cancer. *JNCI Journal of the National Cancer Institute* **95**, 990–1000 (2003).

119. Jia, J. *et al.* Artemisinin inhibits gallbladder cancer cell lines through triggering cell cycle arrest and apoptosis. *Molecular Medicine Reports* **13**, 4461–4468 (2016).

120. Riganti, C. *et al.* Artemisinin induces doxorubicin resistance in human colon cancer cells via calcium-dependent activation of HIF-1a and P-glycoprotein overexpression. *British Journal of Pharmacology* 13 (2009).

121. De Ford, C. *et al.* The clerodane diterpene casearin J induces apoptosis of T-ALL cells through SERCA inhibition, oxidative stress, and interference with Notch1 signaling. *Cell Death Dis* **7**, e2070 (2016).

122. Madreiter-Sokolowski, C. T. *et al.* Resveratrol Specifically Kills Cancer Cells by a Devastating Increase in the Ca^{2+} Coupling Between the Greatly Tethered Endoplasmic Reticulum and Mitochondria. *Cell Physiol Biochem* **39**, 1404–1420 (2016).

123. Wong, V. K. *et al.* Saikosaponin-d, a novel SERCA inhibitor, induces autophagic cell death in apoptosis-defective cells. *Cell Death Dis* **4**, e720–e720 (2013).

124. Jakab, M. *et al.* The Putative Role of the Non-Gastric H^+/K^+-ATPase ATP12A (ATP1AL1) as Anti-Apoptotic Ion Transporter: Effect of the H^+/K^+ ATPase Inhibitor SCH28080 on Butyrate-Stimulated Myelomonocytic HL-60 Cells. *Cell Physiol Biochem* **34**, 1507–1526 (2014).

125. Yeo, M. Selective Induction of Apoptosis with Proton Pump Inhibitor in Gastric Cancer Cells. *Clinical Cancer Research* **10**, 8687–8696 (2004).

126. Zhang, Q. *et al.* The H+/K+-ATPase inhibitory activities of Trametenolic acid B from Trametes lactinea (Berk.) Pat, and its effects on gastric cancer cells. *Fitoterapia* **89**, 210–217 (2013).

127. Gu, M. *et al.* Rabeprazole exhibits antiproliferative effects on human gastric cancer cell lines. *Oncology Letters* **8**, 1739–1744 (2014).

128. Lindner, K. *et al.* Proton pump inhibitors (PPIs) impact on tumour cell survival, metastatic potential and chemotherapy resistance, and affect expression of resistance-relevant miRNAs in esophageal cancer. *Clinical Cancer Research* 12 (2014).

129. Garcia, D. G. *et al.* Na/K-ATPase as a target for anticancer drugs: studies with perillyl alcohol. *Molecular Cancer* **14**, (2015).

130. Alevizopoulos, K. *et al.* Functional characterization and anti-cancer action of the clinical phase II cardiac Na+/K+ ATPase inhibitor istaroxime: in vitro and in vivo properties and cross talk with the membrane androgen receptor. *Oncotarget* **7**, 24415 (2016).

131. Yang, P. *et al.* Cellular location and expression of Na^+, K^+-ATPase α subunits affect the anti-proliferative activity of oleandrin: Cellular distribution of Na^+, K^+-ATPase. *Molecular Carcinogenesis* **53**, 253–263 (2014).

132. Prassas, I. & Diamandis, E. P. Novel therapeutic applications of cardiac glycosides. *Nature Reviews Drug Discovery* **7**, 926–935 (2008).

133. Huang, W.-W. *et al.* Bufalin induces G0/G1 phase arrest through inhibiting the levels of cyclin D, cyclin E, CDK2 and CDK4, and triggers apoptosis via mitochondrial signaling pathway in T24 human bladder cancer cells. *Mutat. Res.* **732**, 26–33 (2012).

134. Zhu, Z. *et al.* Bufalin Induces Lung Cancer Cell Apoptosis via the Inhibition of PI3K/Akt Pathway. *International Journal of Molecular Sciences* **13**, 2025–2035 (2012).

135. Yu, C.-H., Kan, S.-F., Pu, H.-F., Jea Chien, E. & Wang, P. S. Apoptotic signaling in bufalin- and cinobufagin-treated androgen-dependent and -independent human prostate cancer cells. *Cancer Sci.* **99**, 2467–2476 (2008).

136. Ihenetu, K., Qazzaz, H. M., Crespo, F., Fernandez-Botran, R. & Valdes, R. Digoxin-Like Immunoreactive Factors Induce Apoptosis in Human Acute T-Cell Lymphoblastic Leukemia. *Clinical Chemistry* **53**, 1315–1322 (2007).

137. Prassas, I. *et al.* Digitoxin-Induced Cytotoxicity in Cancer Cells Is Mediated through Distinct Kinase and Interferon Signaling Networks. *Molecular Cancer Therapeutics* **10**, 2083–2093 (2011).

138. Badr, C. E. *et al.* Lanatoside C sensitizes glioblastoma cells to tumor necrosis factor–related apoptosis-inducing ligand and induces an alternative cell death pathway. *Neuro-Oncology* **13**, 1213–1224 (2011).

139. Zhao, Q. *et al.* Neriifolin from seeds of Cerbera manghas L. induces cell cycle arrest and apoptosis in human hepatocellular carcinoma HepG2 cells. *Fitoterapia* **82**, 735–741 (2011).

140. Liu, N. *et al.* Inhibition of cell migration by ouabain in the A549 human lung cancer cell line. *Oncology Letters* **6**, 475–479 (2013).

141. Ono, Y. *et al.* Glycoprotein nonmetastatic melanoma protein B (GPNMB) promotes the progression of brain glioblastoma via Na+/K+-ATPase. *Biochemical and Biophysical Research Communications* **481**, 7–12 (2016).

142. Zhou, Y. *et al.* Digoxin sensitizes gemcitabine-resistant pancreatic cancer cells to gemcitabine via inhibiting Nrf2 signaling pathway. *Redox Biology* **22**, 101131 (2019).

143. Li, S. *et al.* Targeting β2 subunit of Na+/K+-ATPase induces glioblastoma cell apoptosis through elevation of intracellular Ca2. *Am J Cancer Res* **9**, 1293–1308 (2019).

144. Casemore, D. & Xing, C. SERCA as a target for cancer therapies. *Integr Cancer Sci Therap* **2**, (2015).

145. Sacchetto, R. *et al.* Crystal structure of sarcoplasmic reticulum Ca2+-ATPase (SERCA) from bovine muscle. *Journal of Structural Biology* **178**, 38–44 (2012).

146. Stewart, T. A., Yapa, K. T. D. S. & Monteith, G. R. Altered calcium signaling in cancer cells. *Biochimica et Biophysica Acta (BBA) - Biomembranes* **1848**, 2502–2511 (2015).

147. Denmeade, S. R. & Isaacs, J. T. The SERCA pump as a therapeutic target: making a 'smart bomb' for prostate cancer. *Cancer Biol. Ther.* **4**, 14–22 (2005).

148. Doan, N. T. Q. *et al.* Targeting thapsigargin towards tumors. *Steroids* **97**, 2–7 (2015).

149. Chemaly, E. R., Bobe, R., Adnot, S., Hajjar, R. J. & Lipskaia, L. Sarco (Endo) Plasmic Reticulum Calcium Atpases (SERCA) Isoforms in the Normal and Diseased Cardiac, Vascular and Skeletal Muscle. *Journal of Cardiovascular Diseases & Diagnosis* **01**, (2013).

150. Arbabian, A. *et al.* Endoplasmic reticulum calcium pumps and cancer. *BioFactors* **37**, 139–149 (2011).

151. Wootton, L. L. & Michelangeli, F. The Effects of the Phenylalanine 256 to Valine Mutation on the Sensitivity of Sarcoplasmic/Endoplasmic Reticulum Ca^{2+} ATPase (SERCA) Ca^{2+} Pump Isoforms 1, 2, and 3 to Thapsigargin and Other Inhibitors. *Journal of Biological Chemistry* **281**, 6970–6976 (2006).

152. Brandl, C. J., deLeon, S., Martin, D. R. & MacLennan, D. H. Adult forms of the Ca2+ATPase of sarcoplasmic reticulum. Expression in developing skeletal muscle. *J. Biol. Chem.* **262**, 3768–3774 (1987).

153. Martin, V. *et al.* Three novel sarco/endoplasmic reticulum Ca2+-ATPase (SERCA) 3 isoforms. Expression, regulation, and function of the membranes of the SERCA3 family. *J. Biol. Chem.* **277**, 24442–24452 (2002).

154. Celsi, F. *et al.* Mitochondria, calcium and cell death: A deadly triad in neurodegeneration. *Biochimica et Biophysica Acta (BBA) - Bioenergetics* **1787**, 335–344 (2009).

155. Riganti, C. *et al.* Artemisinin induces doxorubicin resistance in human colon cancer cells via calcium-dependent activation of HIF-1α and P-glycoprotein overexpression. *British journal of pharmacology* **156**, 1054–1066 (2009).

156. Yousef, M., Vlachogiannis, I. & Tsiani, E. Effects of Resveratrol against Lung Cancer: In Vitro and In Vivo Studies. *Nutrients* **9**, 1231 (2017).

157. Wong, V. K. *et al.* Saikosaponin-d, a novel SERCA inhibitor, induces autophagic cell death in apoptosis-defective cells. *Cell Death & Disease* **4**, e720–e720 (2013).

158. Gu, J., Liu, H., Fu, T. & Xu, Y. Thapsigargin increases apoptotic cell death in human hepatoma BEL-7404 cells*. *Cell Research* **5**, 59–65 (1995).

159. Mahalingam, D. *et al.* Mipsagargin, a novel thapsigargin-based PSMA-activated prodrug: results of a first-in-man phase I clinical trial in patients with refractory, advanced or metastatic solid tumours. *British Journal of Cancer* **114**, 986–994 (2016).

160. Denmeade, S. R. *et al.* Prostate-specific antigen-activated thapsigargin prodrug as targeted therapy for prostate cancer. *Journal of the National Cancer Institute* **95**, 990–1000 (2003).

161. Søhoel, H. *et al.* Natural products as starting materials for development of second-generation SERCA inhibitors targeted towards prostate cancer cells. *Bioorg. Med. Chem.* **14**, 2810–2815 (2006).

162. Jia, J. *et al.* Artemisinin inhibits gallbladder cancer cell lines through triggering cell cycle arrest and apoptosis. *Molecular Medicine Reports* **13**, 4461–4468 (2016).

163. Willoughby, J. A. *et al.* Artemisinin Blocks Prostate Cancer Growth and Cell Cycle Progression by Disrupting Sp1 Interactions with the Cyclin-dependent Kinase-4 (CDK4) Promoter and Inhibiting CDK4 Gene Expression. *Journal of Biological Chemistry* **284**, 2203–2213 (2009).

164. Kim, S.-L. *et al.* Synergistic antitumor effect of 5-fluorouracil in combination with parthenolide in human colorectal cancer. *Cancer Lett.* **335**, 479–486 (2013).

165. Peterson, J. A., Oblad, R. V., Mecham, J. C. & Kenealey, J. D. Resveratrol inhibits plasma membrane Ca 2+ -ATPase inducing an increase in cytoplasmic calcium. *Biochemistry and Biophysics Reports* **7**, 253–258 (2016).

166. Peterson, J. A., Crowther, C. M., Andrus, M. B. & Kenealey, J. D. Resveratrol derivatives increase cytosolic calcium by inhibiting plasma membrane ATPase and inducing calcium release from the endoplasmic reticulum in prostate cancer cells. *Biochem Biophys Rep* **19**, 100667 (2019).

167. Wong, V. K. W. *et al.* Saikosaponin-d, a novel SERCA inhibitor, induces autophagic cell death in apoptosis-defective cells. *Cell Death Dis* **4**, e720 (2013).

168. Vander Stricht, D., Raussens, V., Oberg, K. A., Ruysschaert, J.-M. & Goormaghtigh, E. Difference between the E1 and E2 conformations of gastric H+/K+-ATPase in a multilamellar lipid film system.

169. Streif, D. *et al.* Expression of the non-gastric H+/K+ ATPase ATP12A in normal and pathological human prostate tissue. *Cellular Physiology and Biochemistry* **28**, 1287–1294 (2011).

170. Chow, D. C. & Forte, J. G. Functional significance of the beta-subunit for heterodimeric P-type ATPases. *Journal of Experimental Biology* **198**, 1–17 (1995).

171. Abe, K., Tani, K., Nishizawa, T. & Fujiyoshi, Y. Inter-subunit interaction of gastric a H<sup>+, K<sup>+-ATPase prevents reverse reaction of the transport cycle. *The EMBO Journal* **28**, 1637–1643 (2009).

172. Yan, D., Hu, Y., Li, S. & Cheng, M. A model of 3D structure of H<sup>+, K<sup>+-ATPase catalytic subunit derived by homology modeling. *Acta Pharmacol Sin* **25**, 474–479 (2004).

173. Sachs, G. *et al.* The gastric H,K ATPase as a drug target: past, present, and future. *Journal of Clinical Gastroenterology* **41**, S226–S242 (2007).

174. Koenderink, J. B., Swarts, H. G. P., Willems, P. H. G. M., Krieger, E. & De Pont, J. J. H. H. M. A Conformation-specific Interhelical Salt Bridge in the K^+ Binding Site of Gastric H,K-ATPase. *Journal of Biological Chemistry* **279**, 16417–16424 (2004).

175. Bindu, P. H., Sastry, G. M., Murty, U. S. & Sastry, G. N. Structural and conformational changes concomitant with the E1–E2 transition in H+K+-ATPase: a comparative protein modeling study. *Biochemical and Biophysical Research Communications* **319**, 312–320 (2004).

176. Shin, J. M., Munson, K., Vagin, O. & Sachs, G. The gastric HK-ATPase: structure, function, and inhibition. *Pflugers Arch.* **457**, 609–622 (2009).

177. Judd, L. M. *et al.* Gastric achlorhydria in H/K-ATPase-deficient (Atp4a(-/-)) mice causes severe hyperplasia, mucocystic metaplasia and upregulation of growth factors. *J. Gastroenterol. Hepatol.* **20**, 1266–1278 (2005).

178. Schubert, M. L. & Peura, D. A. Control of Gastric Acid Secretion in Health and Disease. *Gastroenterology* **134**, 1842–1860 (2008).

179. Wu, J. Apoptosis and angiogenesis: two promising tumor markers in breast cancer (review). *Anticancer Res.* **16**, 2233–2239 (1996).

180. Wang, X. *et al.* Proton pump inhibitors increase the chemosensitivity of patients with advanced colorectal cancer. *Oncotarget* **8**, 58801–58808 (2017).

181. Roche, V. F. The chemically elegant proton pump inhibitors. *Am J Pharm Educ* **70**, 101 (2006).

182. Lin, S. *et al.* Silencing of ATP4B of ATPase H+/K+ Transporting Beta Subunit by Intragenic Epigenetic Alteration in Human Gastric Cancer Cells. *Oncol. Res.* **25**, 317–329 (2017).

183. Zhang, Q. *et al.* The H+/K+-ATPase inhibitory activities of Trametenolic acid B from Trametes lactinea (Berk.) Pat, and its effects on gastric cancer cells. *Fitoterapia* **89**, 210–217 (2013).

184. Jakab, M. *et al.* The putative role of the non-gastric H^+/K^+-ATPase ATP12A (ATP1AL1) as anti-apoptotic ion transporter: effect of the H^+/K^+ ATPase inhibitor SCH28080 on butyrate-stimulated myelomonocytic HL-60 cells. *Cell. Physiol. Biochem.* **34**, 1507–1526 (2014).

185. Yeo, M. *et al.* Selective induction of apoptosis with proton pump inhibitor in gastric cancer cells. *Clinical Cancer Research* **10**, 8687–8696 (2004).

186. Lindner, K. *et al.* Proton pump inhibitors (PPIs) impact on tumour cell survival, metastatic potential and chemotherapy resistance, and affect expression of resistance-relevant miRNAs in esophageal cancer. *J. Exp. Clin. Cancer Res.* **33**, 73 (2014).

187. Ferrari, S. *et al.* Proton pump inhibitor chemosensitization in human osteosarcoma: from the bench to the patients' bed. *J Transl Med* **11**, 268 (2013).

188. Goh, W., Sleptsova-Freidrich, I. & Petrovic, N. Use of proton pump inhibitors as adjunct treatment for triple-negative breast cancers. An introductory study. *Journal of Pharmacy & Pharmaceutical Sciences* **17**, 439–446 (2014).

189. Lugini, L. *et al.* Antitumor effect of combination of the inhibitors of two new oncotargets: proton pumps and reverse transcriptase. *Oncotarget* **8**, 4147–4155 (2017).

190. Galmiche, J. P. *et al.* Tenatoprazole, a novel proton pump inhibitor with a prolonged plasma half-life: effects on intragastric pH and comparison with esomeprazole in healthy volunteers. *Aliment. Pharmacol. Ther.* **19**, 655–662 (2004).

191. Wu, D.-C. *et al.* A Pilot Randomized Controlled Study of Dexlansoprazole MR-Based Triple Therapy for Helicobacter Pylori Infection. *Medicine (Baltimore)* **95**, e2698 (2016).

192. Otake, K. *et al.* Characteristics of the Novel Potassium-Competitive Acid Blocker Vonoprazan Fumarate (TAK-438). *Adv Ther* **33**, 1140–1157 (2016).

193. Inatomi, N., Matsukawa, J., Sakurai, Y. & Otake, K. Potassium-competitive acid blockers: Advanced therapeutic option for acid-related diseases. *Pharmacol. Ther.* **168**, 12–22 (2016).

194. Singh, N. *et al.* Gastroprotective effect of anti-cancer compound rohitukine: possible role of gastrin antagonism and H(+) K (+)-ATPase inhibition. *Naunyn Schmiedebergs Arch. Pharmacol.* **385**, 277–286 (2012).

195. Yao, X. & Smolka, A. J. Gastric Parietal Cell Physiology and Helicobacter pylori-Induced Disease. *Gastroenterology* **156**, 2158–2173 (2019).

196. Mijatovic, T., Dufrasne, F. & Kiss, R. Cardiotonic Steroids-Mediated Targeting of the Na<sup>+/K<sup>+-ATPase to Combat Chemoresistant Cancers. *Current Medicinal Chemistry* **19**, 627–646 (2012).

197. Lin, J. *et al.* A pilot phase II Study of digoxin in patients with recurrent prostate cancer as evident by a rising PSA. *Am J Cancer Ther Pharmacol* **2**, 21–32 (2014).

198. Frankel, A. E. *et al.* Digoxin Plus Trametinib Therapy Achieves Disease Control in BRAF Wild-Type Metastatic Melanoma Patients. *Neoplasia* **19**, 255–260 (2017).

199. Koch, K. M. *et al.* Effect of lapatinib on oral digoxin absorption in patients: Clinical Pharmacology in Drug Development. *Clinical Pharmacology in Drug Development* **4**, 449–453 (2015).

200. Chemaly, E. R., Troncone, L. & Lebeche, D. SERCA control of cell death and survival. *Cell Calcium* **69**, 46–61 (2018).

201. Wang, B.-Y. *et al.* Intermittent high dose proton pump inhibitor enhances the antitumor effects of chemotherapy in metastatic breast cancer. *Journal of Experimental & Clinical Cancer Research* **34**, (2015).

202. Jankowski, J. A. Z. *et al.* Esomeprazole and aspirin in Barrett's oesophagus (AspECT): a randomised factorial trial. *Lancet* **392**, 400–408 (2018).

203. Thin-Layer Chromatography - an overview | ScienceDirect Topics. https://www.sciencedirect.com/topics/engineering/thin-layer-chromatography.

204. Yatime, L. *et al.* P-type ATPases as drug targets: Tools for medicine and science. *Biochimica et Biophysica Acta (BBA) - Bioenergetics* **1787**, 207–220 (2009).

205. Lodish, H. *et al.* Active Transport by ATP-Powered Pumps. *Molecular Cell Biology. 4th edition* (2000).

206. Bublitz, M., Morth, J. P. & Nissen, P. P-type ATPases at a glance. *Journal of cell science* **124**, 2515–2519 (2011).

207. The mitochondrial complex I inhibitor annonacin is toxic to mesencephalic dopaminergic neurons by impairment of energy metabolism. - PubMed - NCBI. https://www.ncbi.nlm.nih.gov/pubmed/14521988.

208. Laursen, M., Yatime, L., Nissen, P. & Fedosova, N. U. Crystal structure of the high-affinity Na+K+-ATPase-ouabain complex with Mg2+ bound in the cation binding site. *Proceedings of the National Academy of Sciences of the United States of America* vol. 110 10958–10963 (2013).

209. Kepp, O. *et al.* Anticancer activity of cardiac glycosides. *Oncoimmunology* **1**, 1640–1642 (2012).

210. Dang, D. & Rao, R. Calcium-ATPases: Gene Disorders and Dysregulation in Cancer. *Biochim Biophys Acta* **1863**, 1344–1350 (2016).

211. Huang, F., Wang, P. & Wang, X. Thapsigargin induces apoptosis of prostate cancer through cofilin-1 and paxillin. *Oncol Lett* **16**, 1975–1980 (2018).

212. Ouabain - an overview | ScienceDirect Topics. https://www.sciencedirect.com/topics/medicine-and-dentistry/ouabain.

213. McDonnell, S. J., Spiller, D. G., White, M. R. H., Prior, I. A. & Paraoan, L. ER stress-linked autophagy stabilizes apoptosis effector PERP and triggers its co-localization with SERCA2b at ER–plasma membrane junctions. *Cell Death Discovery* **5**, 1–12 (2019).

214. Juhaszova, M. & Blaustein, M. P. Na+ pump low and high ouabain affinity subunit isoforms are differently distributed in cells. *Proceedings of the National Academy of Sciences* **94**, 1800–1805 (1997).

215. Rajasekaran, S. A. *et al.* Na,K-ATPase Subunits as Markers for Epithelial-Mesenchymal Transition in Cancer and Fibrosis. *Molecular Cancer Therapeutics* **9**, 1515–1524 (2010).

216. Slingerland, M., Cerella, C., Guchelaar, H. J., Diederich, M. & Gelderblom, H. Cardiac glycosides in cancer therapy: from preclinical investigations towards clinical trials. *Invest New Drugs* **31**, 1087–1094 (2013).

217. Inge, L. J. *et al.* Evidence for a potential tumor suppressor role for the Na,K- ATPase ß1-subunit. 16 (2009).

218. Park, K. C. *et al.* Survival of Cancer Stem-Like Cells Under Metabolic Stress via CaMK2α-mediated Upregulation of Sarco/Endoplasmic Reticulum Calcium ATPase Expression. *Clin Cancer Res* **24**, 1677–1690 (2018).

219. Chow, D. C. & Forte, J. G. FUNCTIONAL SIGNIFICANCE OF THE -SUBUNIT FOR HETERODIMERIC. 17.

220. Peterson, J. A., Oblad, R. V., Mecham, J. C. & Kenealey, J. D. Resveratrol inhibits plasma membrane Ca 2+ -ATPase inducing an increase in cytoplasmic calcium. *Biochemistry and Biophysics Reports* **7**, 253–258 (2016).

221. Cheung, K. S. & Leung, W. K. Long-term use of proton-pump inhibitors and risk of gastric cancer: a review of the current evidence. *Therap Adv Gastroenterol* **12**, 175628481983451 (2019).

222. Hammadi, M. Dysregulation of gastric H,K-ATPase by cigarette smoke extract. *WJG* **15**, 4016 (2009).

223. Robertson, D. J. *et al.* Proton Pump Inhibitor Use and Risk of Colorectal Cancer: A Population-Based, Case–Control Study. *Gastroenterology* **133**, 755–760 (2007).

Appendix I.

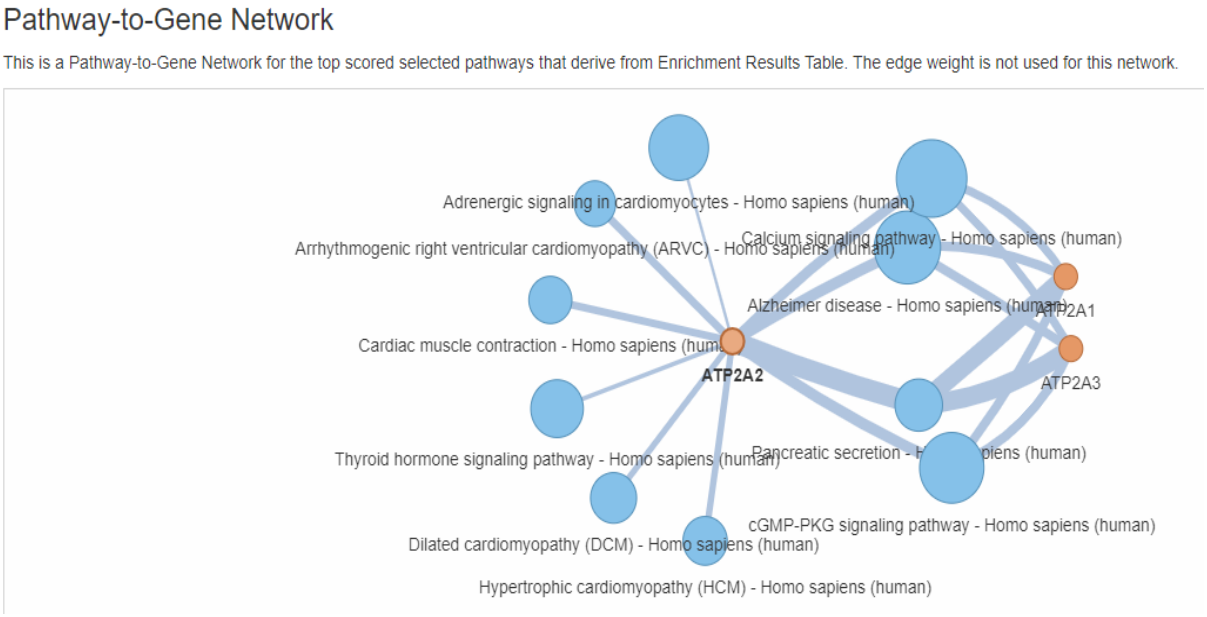

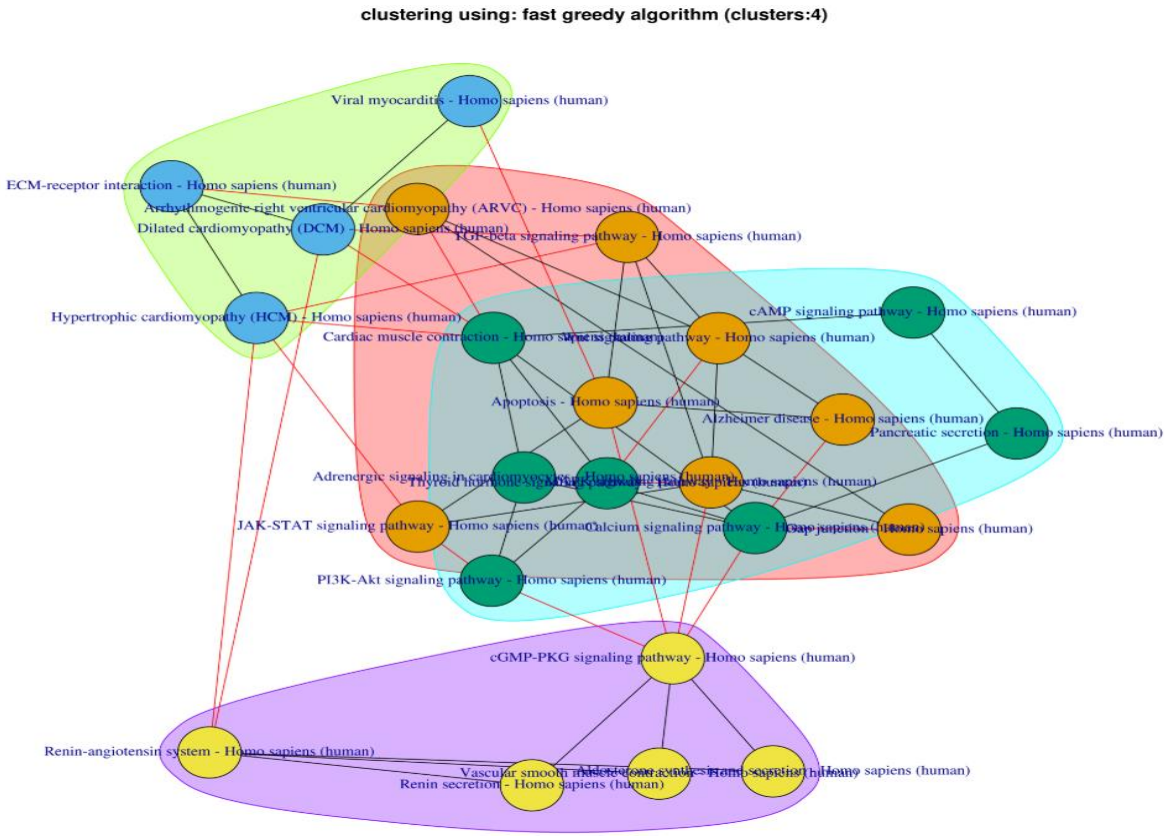

Supplementary Figure 1. NKA and SERCA subunit expression involvement in new defined pathways.

List of Publications:

1. Yiallouris, A., Patrikios, I., Johnson, E. *et al.* Annonacin promotes selective cancer cell death via NKA-dependent and SERCA-dependent pathways. *Cell Death Dis* **9,** 764 (2018). https://doi.org/10.1038/s41419-018-0772.

2. Yiallouris A, Tsioutis C, Agapidaki E, Zafeiri M, Agouridis AP, Ntourakis D, Johnson EO. Adrenal Aging and Its Implications on Stress Responsiveness in Humans. Front Endocrinol (Lausanne). 2019 Feb 7;10:54. doi: 10.3389/fendo.2019.00054. eCollection 2019

3. ''Tripterygium wilfordii Promotes Selective Cancer Cell death through Na+/K+ ATPase (NKA) Pathway'' (Submitted PLOS ONE)

4. ''Altered SERCA gene Expression in Breast Cancer'' (Submitted BMC Medical Genomics)

5. "Clinical Significance of P-Class Pumps in Cancer", (Submitted Cancer Biology and Therapy)